Second-principles simulations of counter-rotating vortices pairs in $PbTiO_3/SrTiO_3$ superlattices

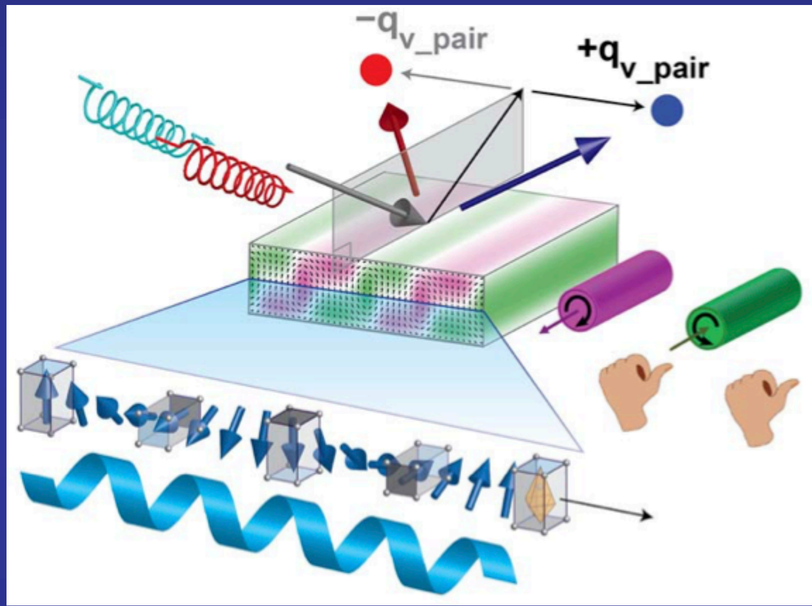

Javier Junquera

UNIVERSIDAD DE CANTABRIA

CITIMAC

Collaborators

Pablo García-Fernández

UC UNIVERSIDAD DE CANTABRIA

CITIMAC

Fernando Gómez

Jorge Íñiguez

LUXEMBOURG INSTITUTE OF SCIENCE AND TECHNOLOGY LIST

Mauro Gonçalves

Pablo Aguado-Puente

Queen's University Belfast

…Plus all the experimental group of Prof. Ramesh at UC Berkeley

Spin Textures in Magnets with D-M Interactions
Skyrmions, Merons, Anti-merons,…

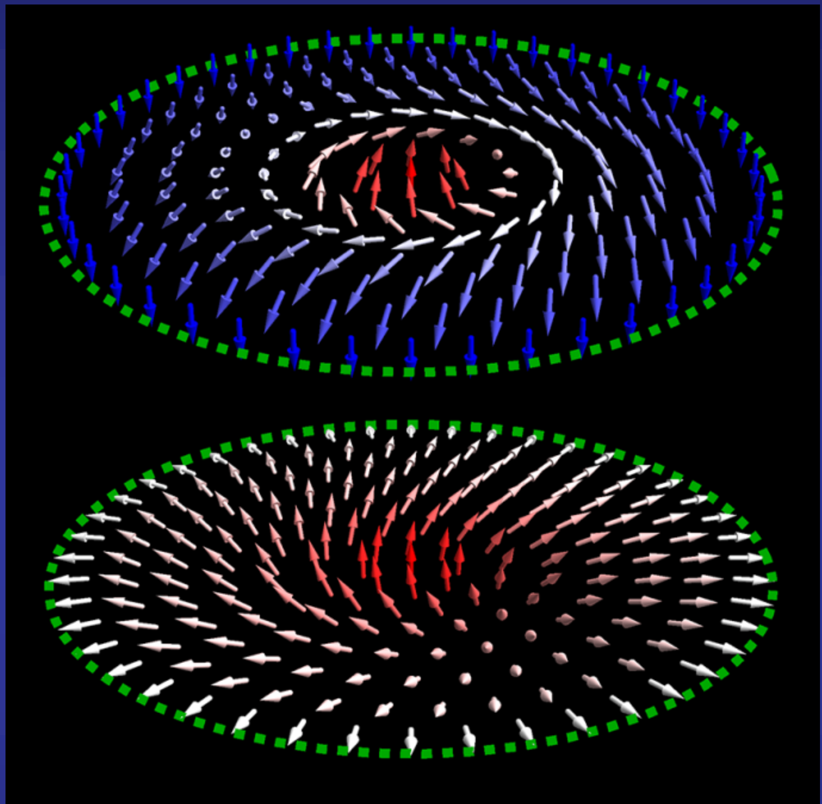

Rich physics
Key role of D-M interactions
Chirality

$$f = Am^2 \sum_{i,j} (\partial_i n_j)^2 + \eta A (\nabla m)^2 + f_{\mathrm{D}}(\mathbf{m}) + f_0(m)$$

Magnetic Stiffness

Gradient term

D-M Interactions

Free energy

Can we do the same in ferroelectrics?
Are there fundamental differences between the spin and dipole moment..
Lot of debate on this

U. K. Rößler, A. N. Bogdanov, and C. Pfleiderer, Nature 442, 797 (2006)

Spin Textures in Magnets with D-M Interactions Skyrmions, Merons, Anti-merons,…

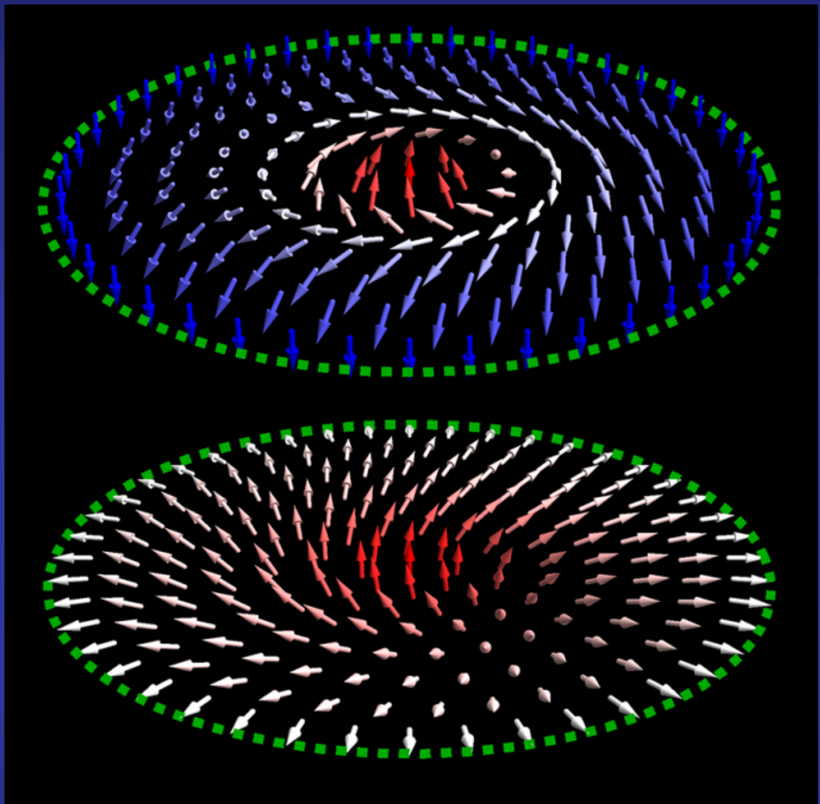

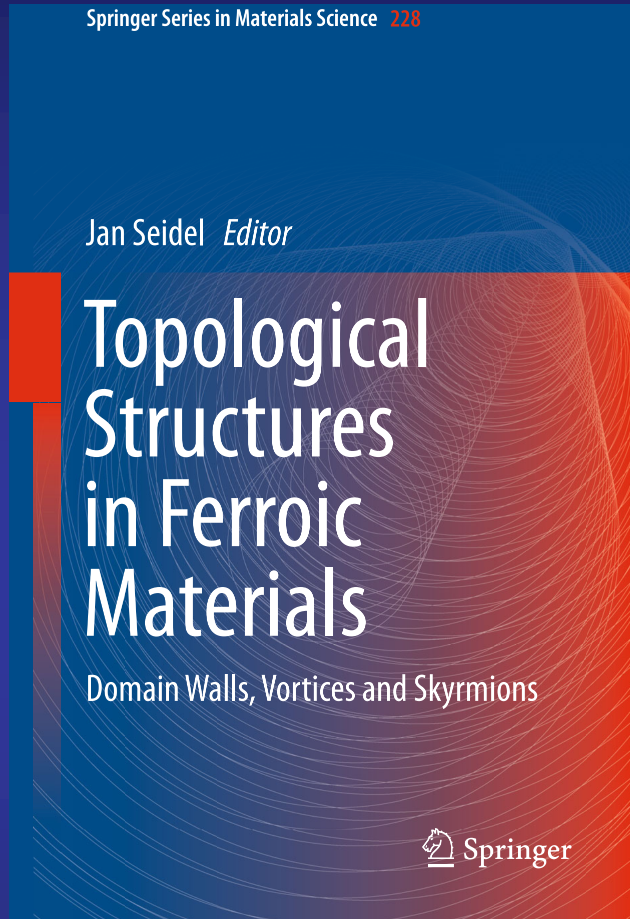

Can we do the same in ferroelectrics?
Are there fundamental differences between the spin and dipole moment..
Lot of debate on this

U. K. Rößler, A. N. Bogdanov, and C. Pfleiderer, Nature 442, 797 (2006)

Complex domain arrangements in nanoscale FE has triggered the search for exotic topologies

Néel-like domain wall in $Pb(Zr_{0.40}Ti_{0.60})O_3$

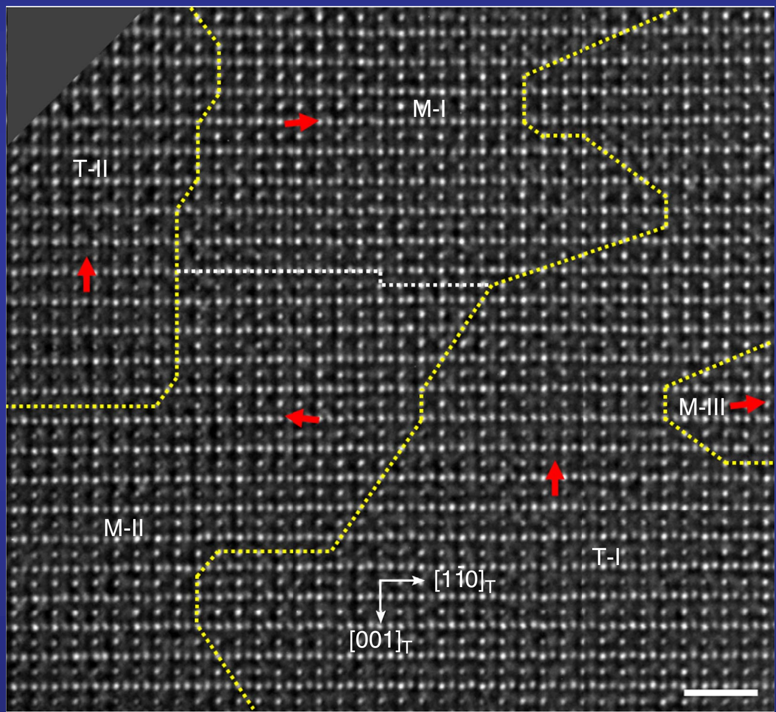

X.-K. Wei *et al.*
Nat. Commun. 7, 12385 (2016)

Kittel-like domain wall in $Co/PbTiO_3/(La,Sr)MnO_3$

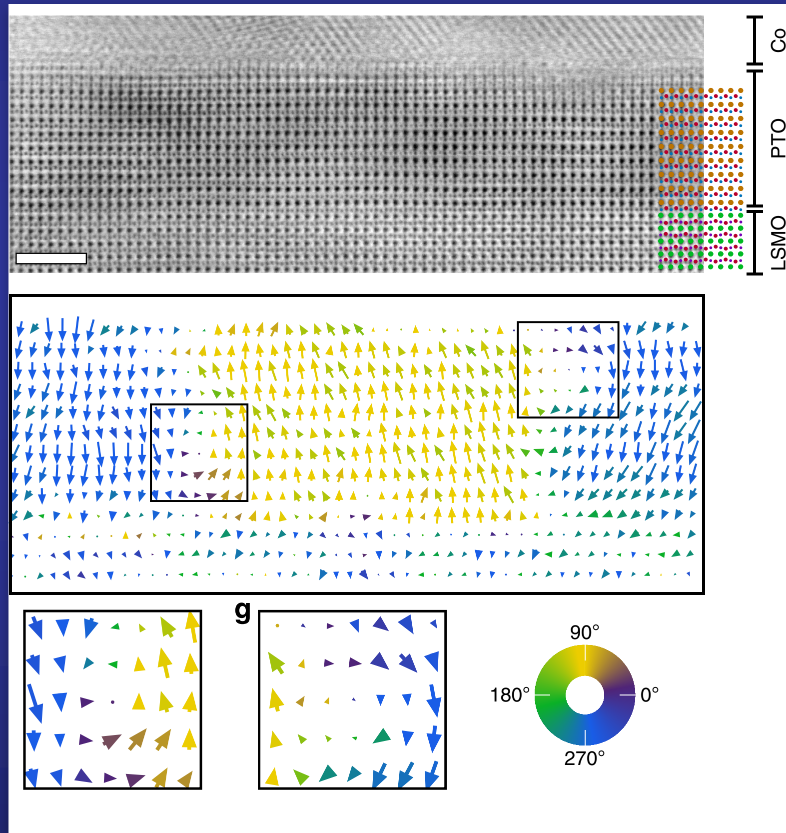

J. J. P. Peters *et al.*
Nat. Commun. 7, 13484 (2016)

Requirements: both in-plane and out-of-plane P; interface must show polarization rotation

The balance of elastic, electrostatic, and gradient energies yield a very complex phase diagram

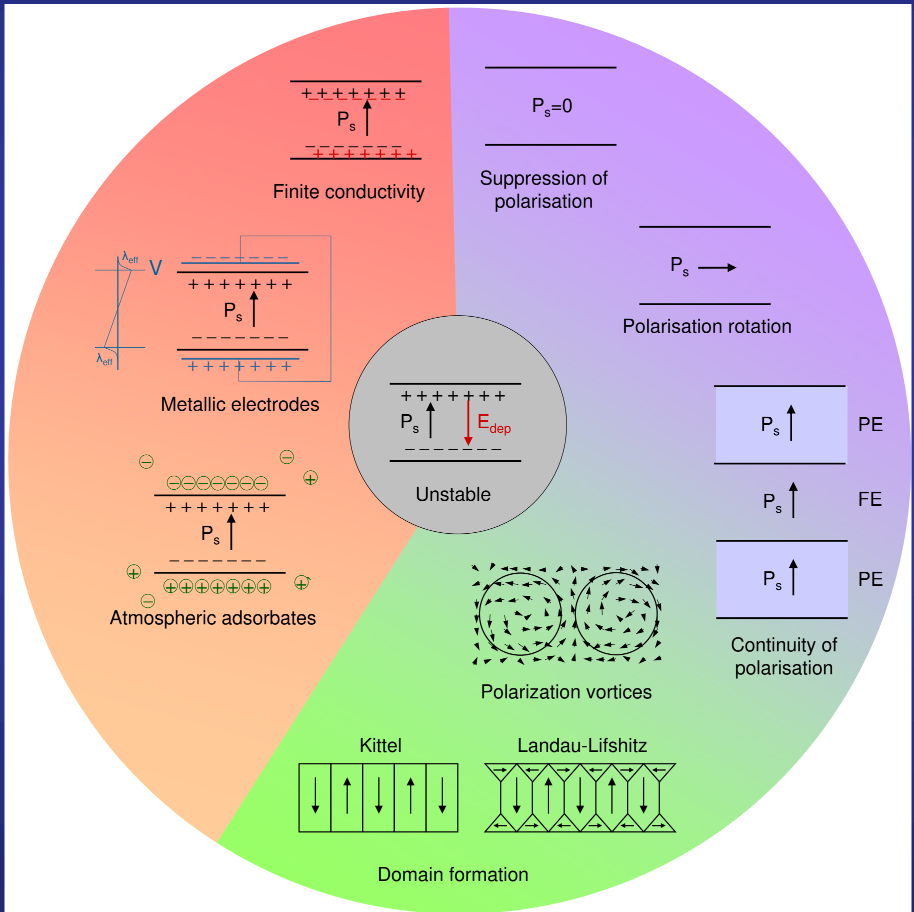

C. Lichtensteiger *et al.*, Chapter 12 in Oxide Ultrathin Films, Science and Technology, Wiley (2011).

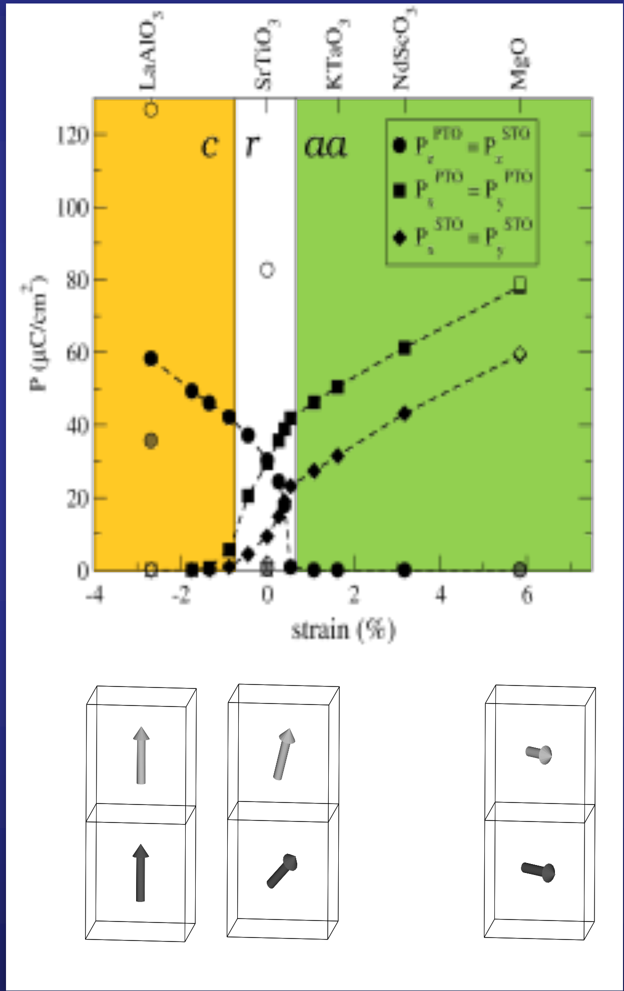

P. Aguado-Puente *et al.* Phys. Rev. Lett. 107, 217601 (2017)

Short-period $PbTiO_3/SrTiO_3$ superlattices: the GS involves trilinear coupling between two AFD modes and a polar FE mode

Hybrid improper ferroelectricity

E. Bousquet *et al.*, Nature 452, 732 (2008)

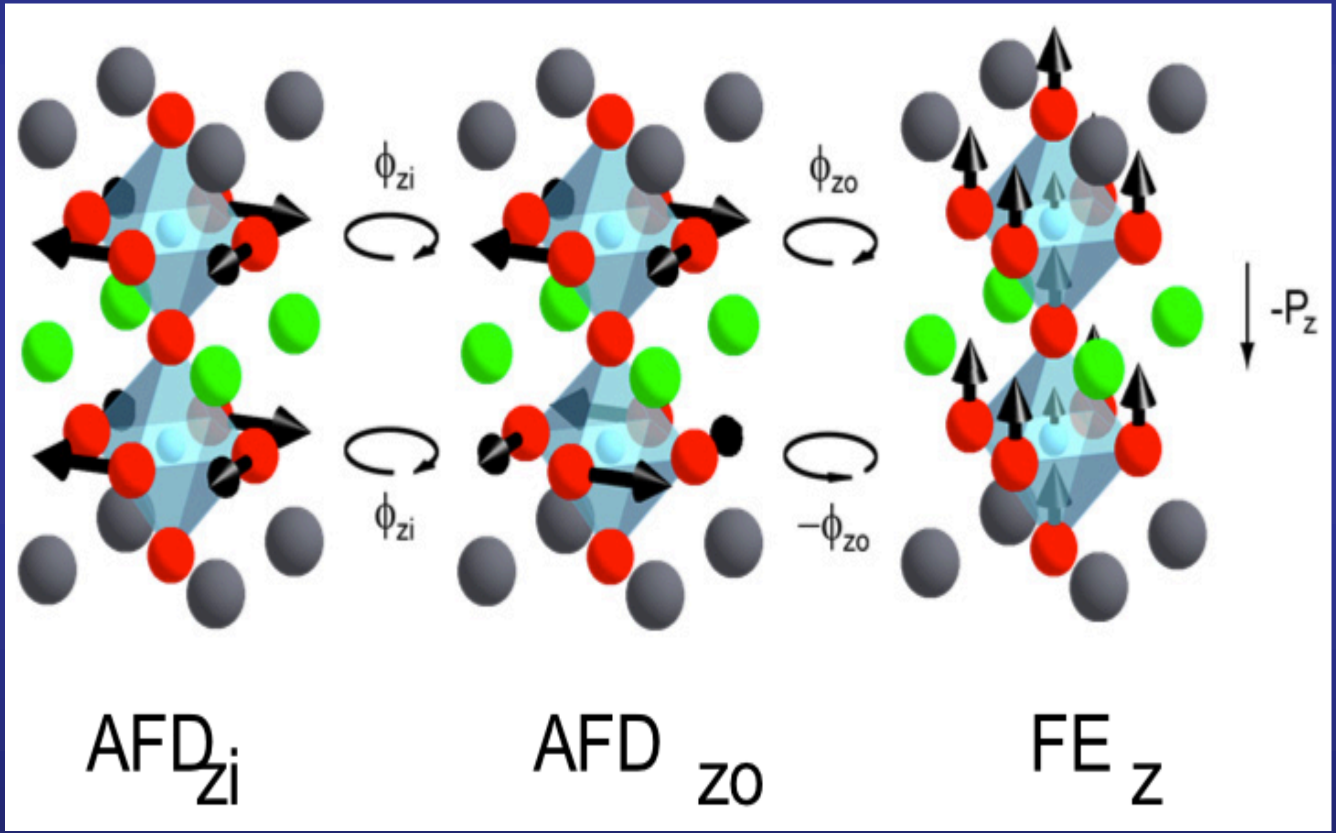

In-phase AFD rotations of O octahedra	Out-of-phase AFD rotations of O octahedra	Ferroelectric mode

Evolution of the interlayer coupling with periodicity in $(PbTiO_3)_n/(SrTiO_3)_n$ superlattices

Transition between strong interlayer coupling (monodomain) to weak interlayer coupling (polydomain) electrostatic regime

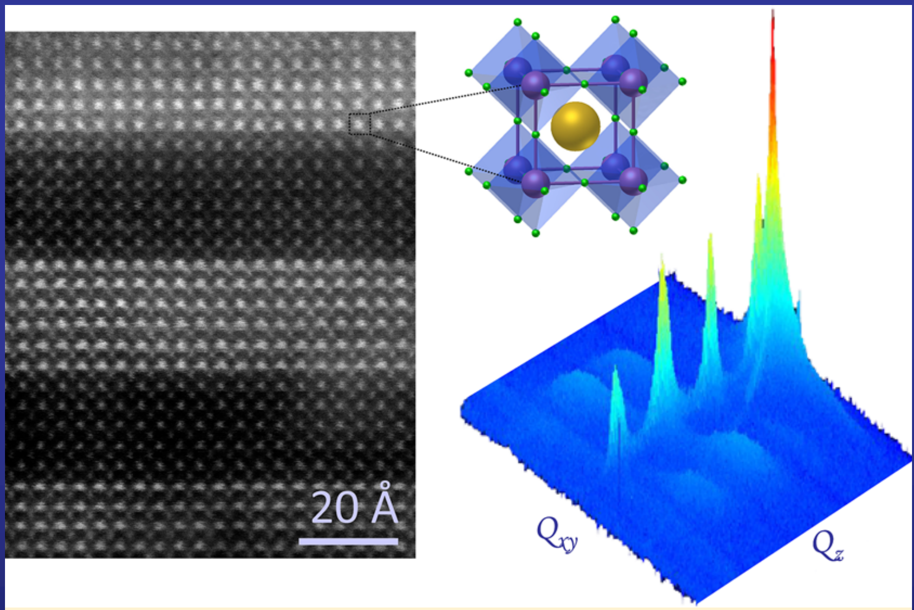

P. Zubko *et al*. Nano Letters 12, 2846 (2012)

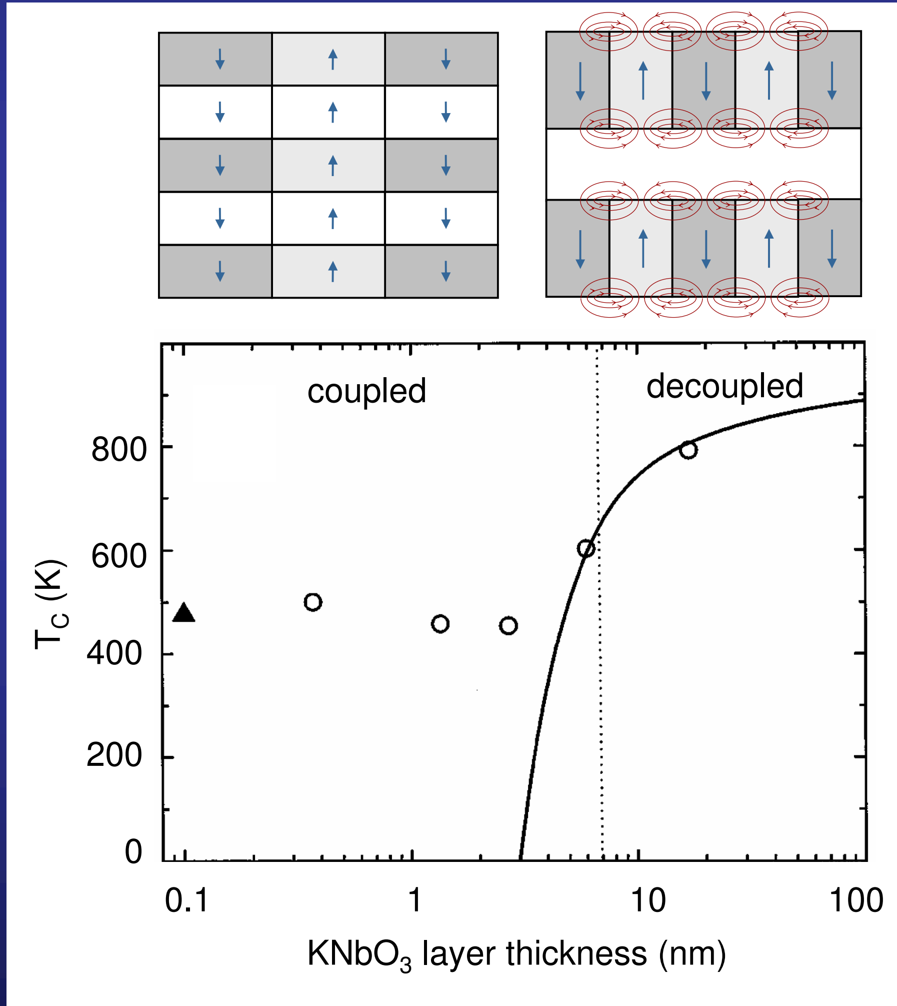

Transition between strong interlayer coupling (monodomain) to weak interlayer coupling (polydomain) electrostatic regime

P. Aguado-Puente and J. Junquera
Phys. Rev. B 85, 184105 (2012)

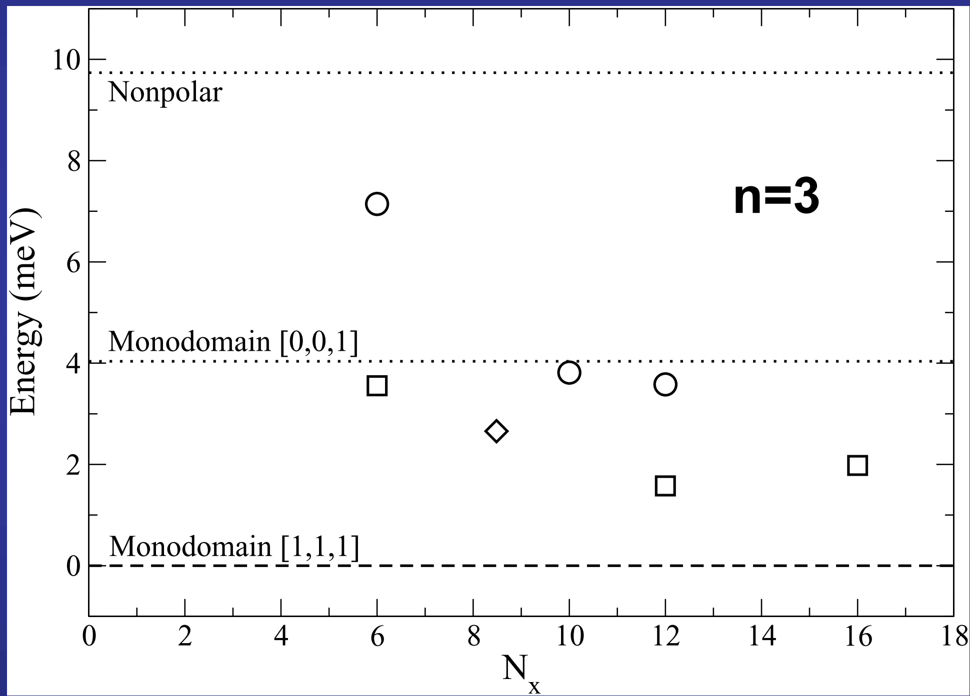

- AFD not allowed
- AFD allowed
- Domain walls along [110]

Domains in $PbTiO_3/SrTiO_3$ superlattices: adopt the closure-domain structure with vortices

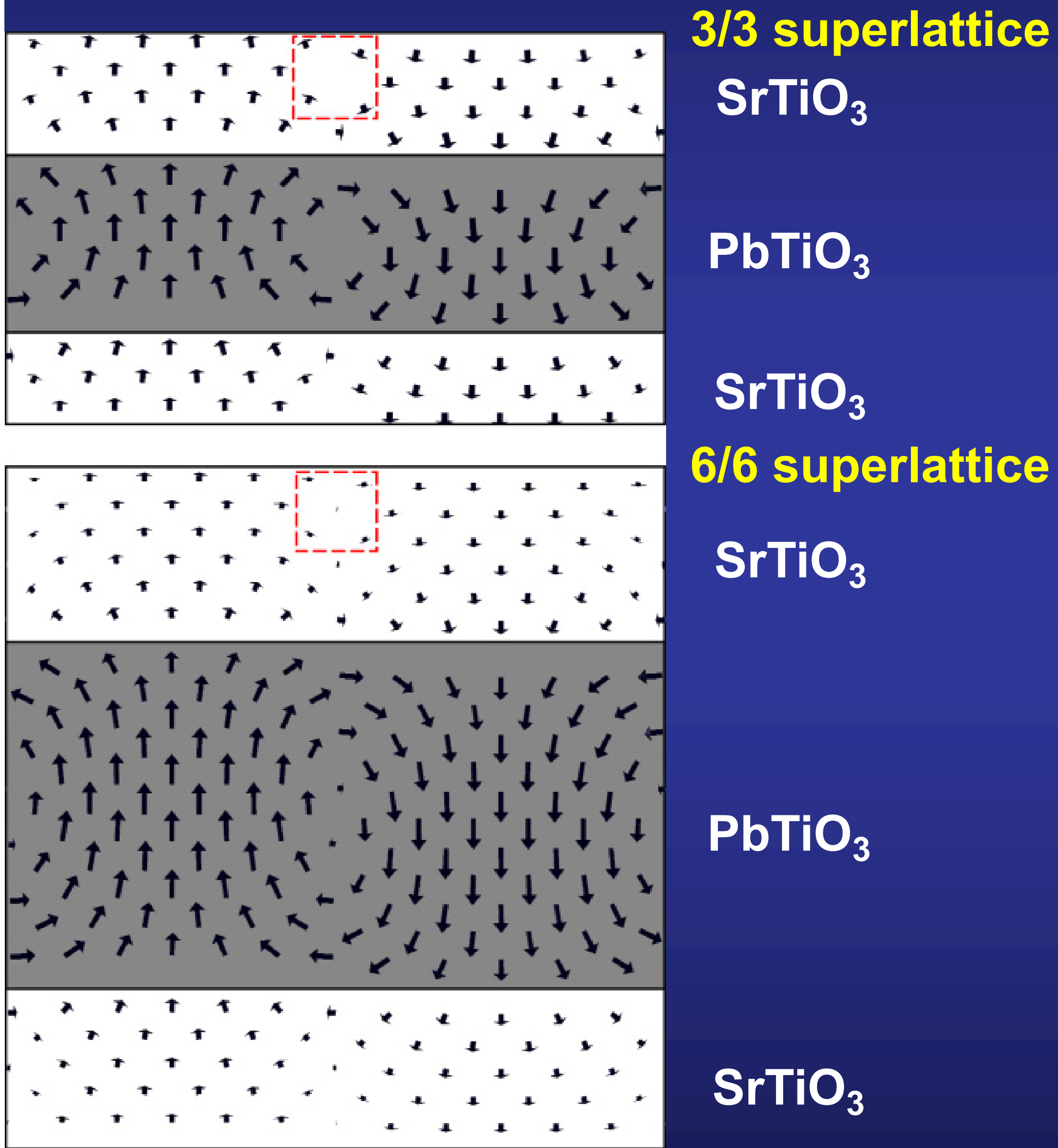

Near the DWs the local polarization pattern displays a continuous polarization rotation within 3 u.c. around the DW, connecting two 180° domains

P. Aguado-Puente and J. Junquera Phys. Rev. B 85, 184105 (2012)

Observation of Polar Vortices: $(PbTiO_3)_n/(SrTiO_3)_n$ superlattices on $DyScO_3$ substrate

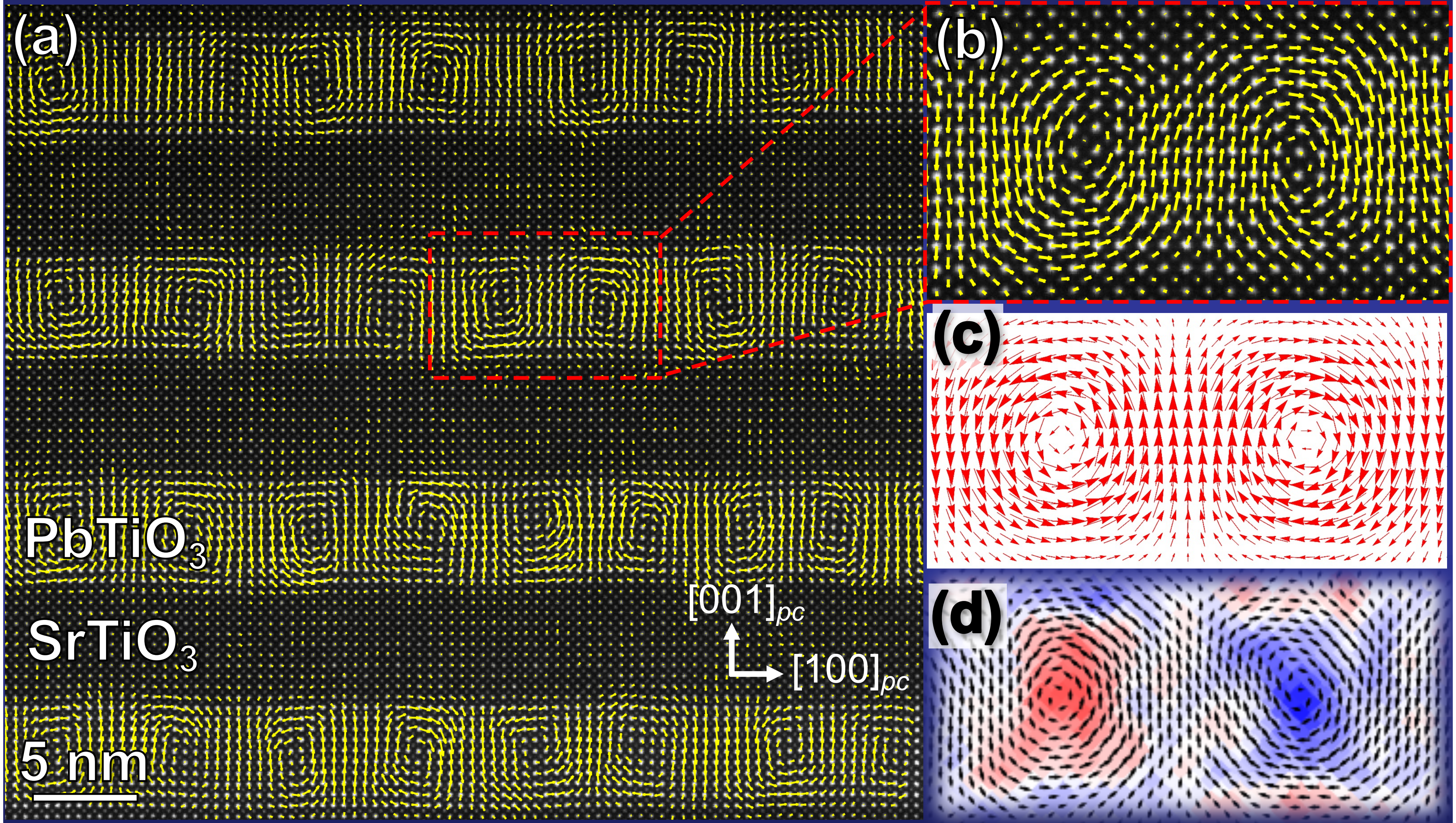

Yadav *et al*, Nature 530, 198 (2016)

Complex polarization textures in ferroelectric nanostructures

Both a vortex and a polarization aligned along the normal of the plane containing the vortex

$BaTiO_3$ nanowires embedded in a $SrTiO_3$ matrix

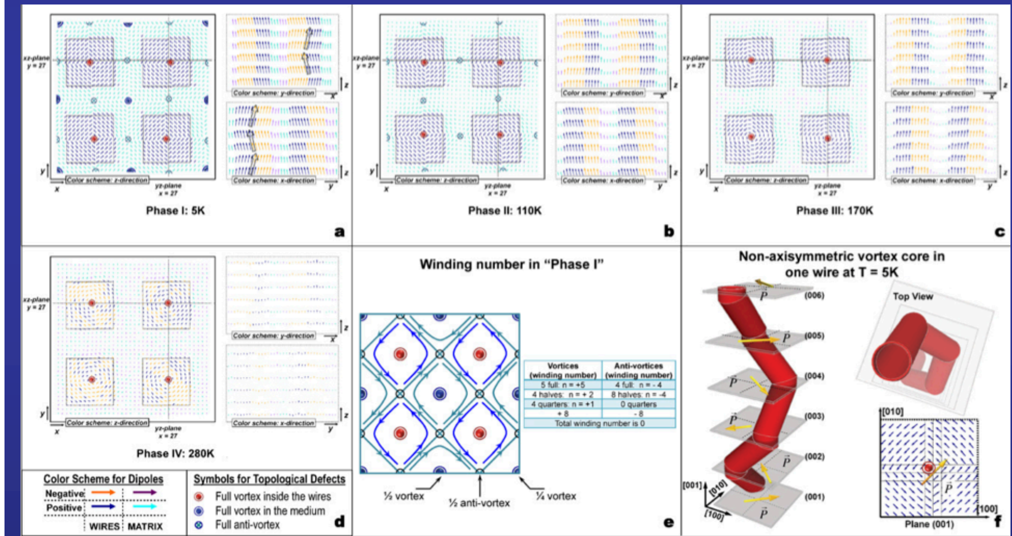

The whole system is chiral

L. Louis *et al.*
J. Phys.: Condens. Matter 24, 402201 (2012)

Occurrence of natural optical activity

$BaTiO_3$ nanowires embedded in a $SrTiO_3$ matrix

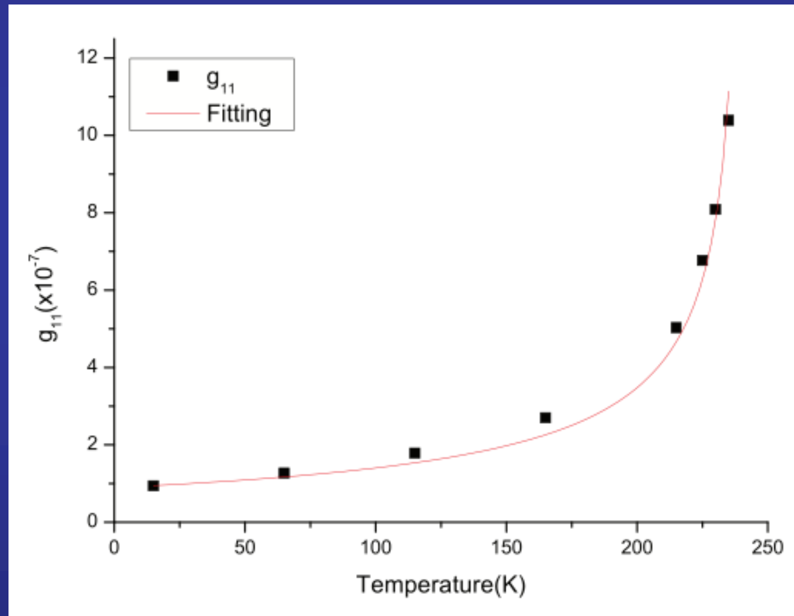

Large gyrotropic coefficient. Sense of rotation can be reversed by an external electric field

S. Prosandeev *et al.*
Phys. Rev. B 87, 195111 (2013)

Complex polarization textures in ferroelectric nanostructures

Both a vortex and a polarization aligned along the normal of the plane containing the vortex

$BaTiO_3$ nanowires embedded in a $SrTiO_3$ matrix

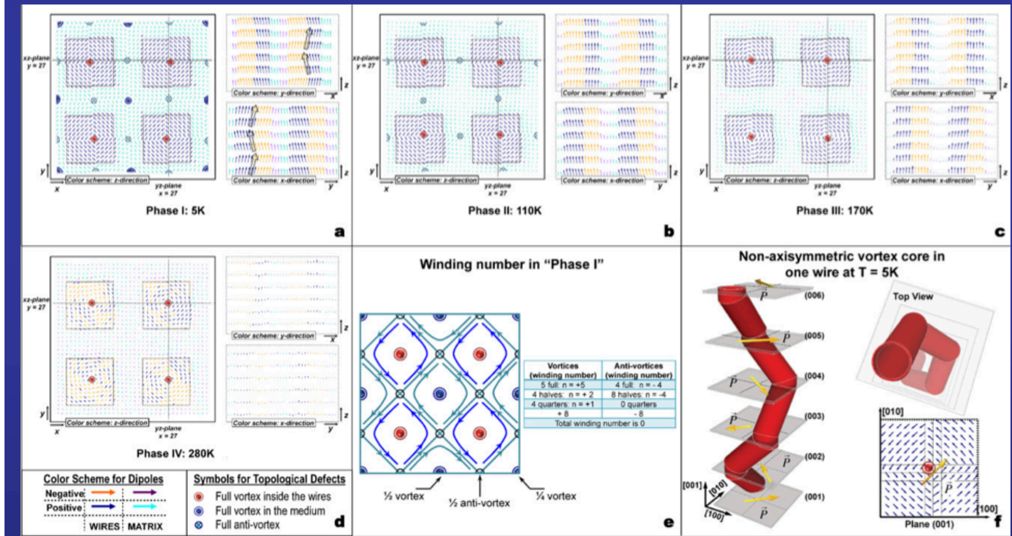

The whole system is chiral

L. Louis *et al.*
J. Phys.: Condens. Matter 24, 402201 (2012)

Discovery of stable skyrmion states in ferroelectric nanocomposites

$BaTiO_3$ nanowires embedded in a $SrTiO_3$ matrix

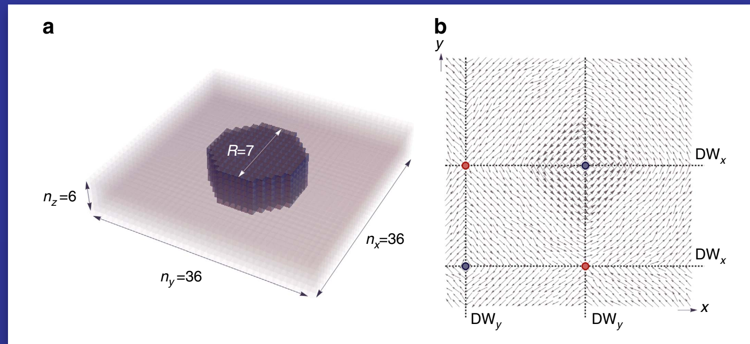

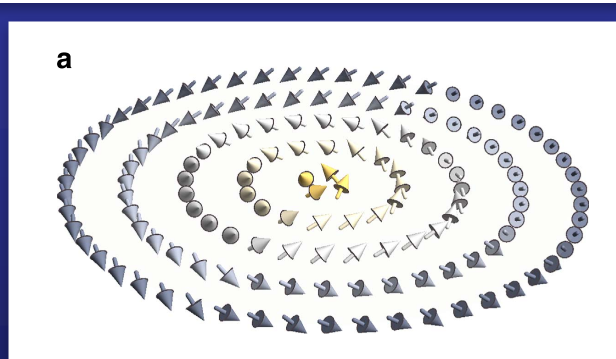

Y. Nahas *et al.*
Nat. Commun. 6, 8542 (2015)

Second-principles method including the relevant electron and lattice degrees of freedom

PHYSICAL REVIEW B **93**, 195137 (2016)

Second-principles method for materials simulations including electron and lattice degrees of freedom

Pablo García-Fernández,[1] Jacek C. Wojdeł,[2] Jorge Íñiguez,[2,3] and Javier Junquera[1]

Goal:

- Simulate both atomic and electronic degrees of freedom of very large systems (over 10^4 atoms) on the same footing
- With arbitrary high accuracy
- At a modest computational cost
- At operating conditions (finite-T, time-dependent fields, …)

SCALE UP
An implementation of SPDFT

SCALE-UP:
Second-principles Computational Approach for Lattice and Electrons
https://www.secondprinciples.unican.es

SCALE-UP:
Second-principles Computational Approach for Lattice and Electrons
https://www.secondprinciples.unican.es

PHYSICAL REVIEW B **93**, 195137 (2016)

Second-principles method for materials simulations including electron and lattice degrees of freedom

Pablo García-Fernández,[1] Jacek C. Wojdeł,[2] Jorge Íñiguez,[2,3] and Javier Junquera[1]

Accurate model potential to describe the lattice-dynamical properties

+

A tight-binding like approach to describe the relevant electronic degrees of freedom

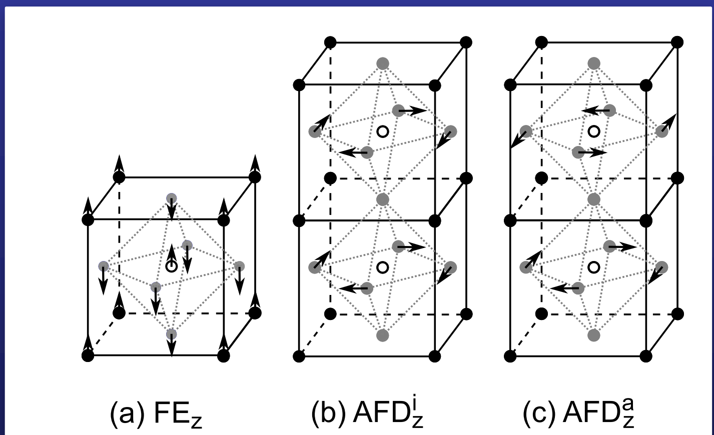

J. Wojdel *et al.*
J. Phys.: Condens. Matter 25, 305401 (2013)

Electron-phonon interactions

Parameters fitted from first-principles simulations on small systems

Emergent topological properties at $PbTiO_3/SrTiO_3$ superlattices

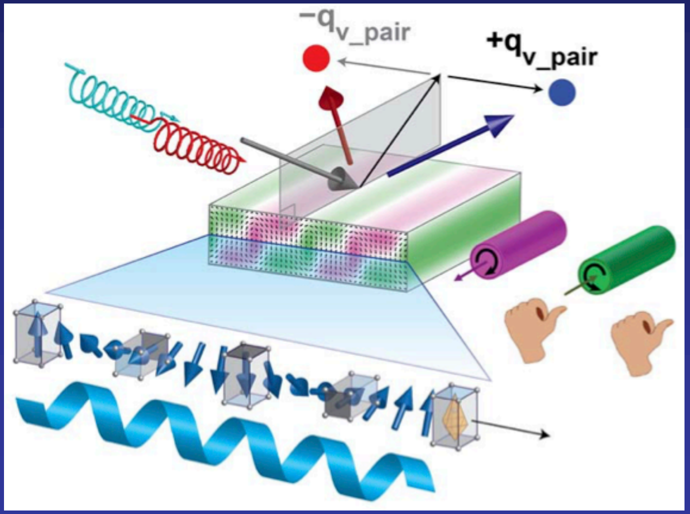

Emerging chirality in polar vortex superlattices

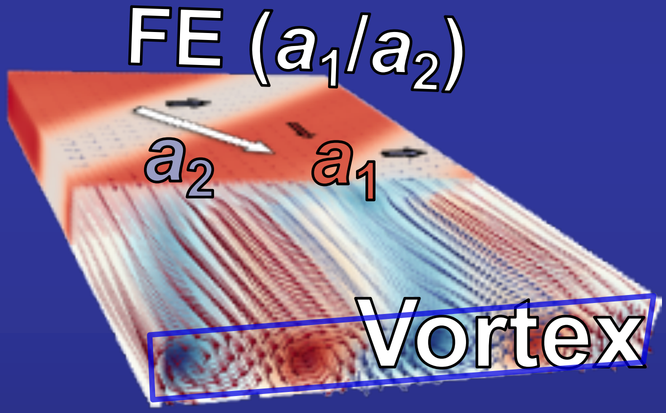

Coexistence of phases

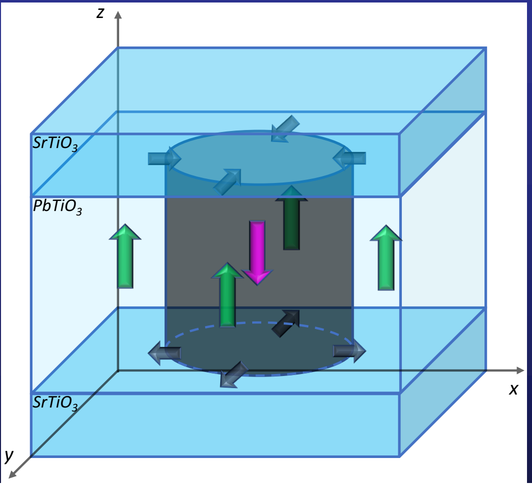

Bubble skyrmions

Second-principles simulations of $(PbTiO_3)_n/(SrTiO_3)_n$ superlattices (n=10)

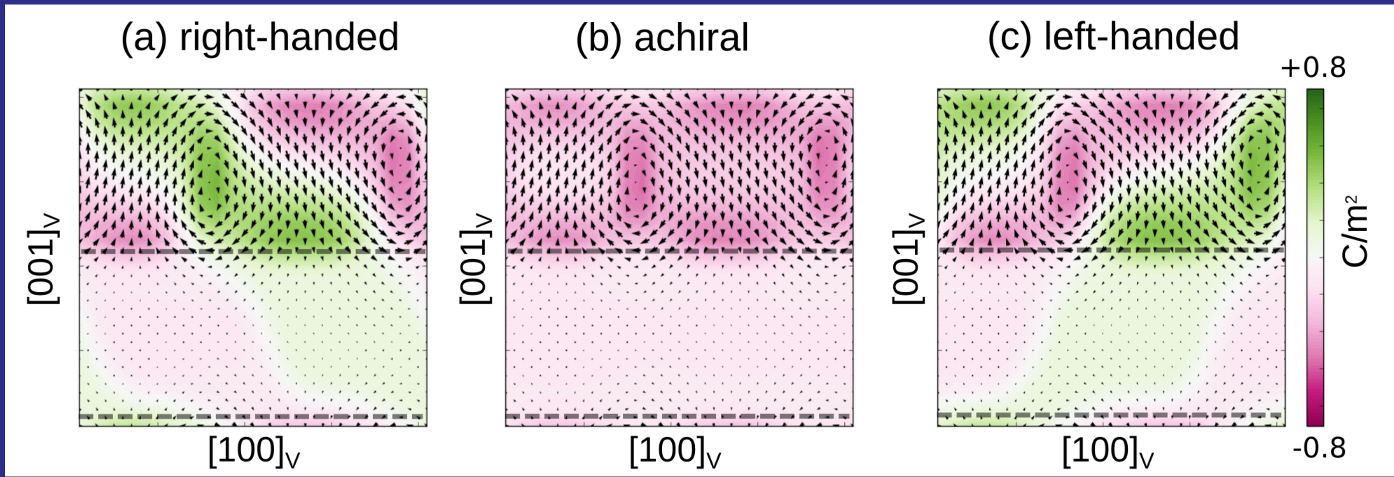

Different atomic geometries very close in energy

Continuous rotation of the local dipoles with pairs of clock-wise and counter-clock-wise rotation patterns along $[100]_V$

Superimposed to the vortices: a polarization component along the axial direction of the vortices $[010]_V$

P. Shafer, P. García-Fernández *et al*. submitted

In plane polarization in FE domains

The domain walls might be ferroelectric themselves

PRL **112,** 247603 (2014) PHYSICAL REVIEW LETTERS week ending 20 JUNE 2014

Ferroelectric Transitions at Ferroelectric Domain Walls Found from First Principles

Jacek C. Wojdeł and Jorge Íñiguez

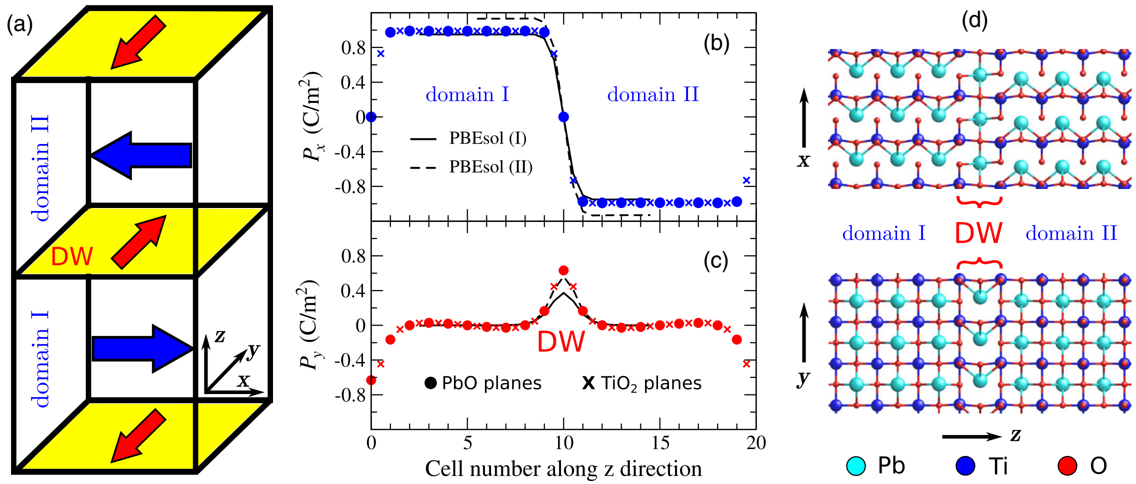

In plane polarization in FE domains

Rich structure predicted in (111) $BaTiO_3$ domain walls

PHYSICAL REVIEW B **92**, 094106 (2015)

Ising lines: Natural topological defects within ferroelectric Bloch walls

V. Stepkova, P. Marton, and J. Hlinka*

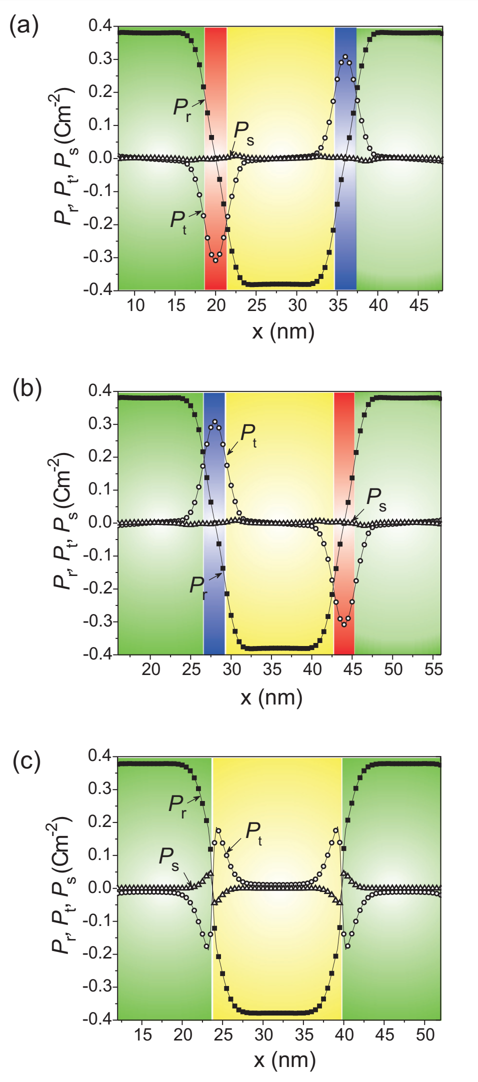

Plus many works by E. Salkje

Second-principles simulations of $(PbTiO_3)_n/(SrTiO_3)_n$ superlattices (n=10)

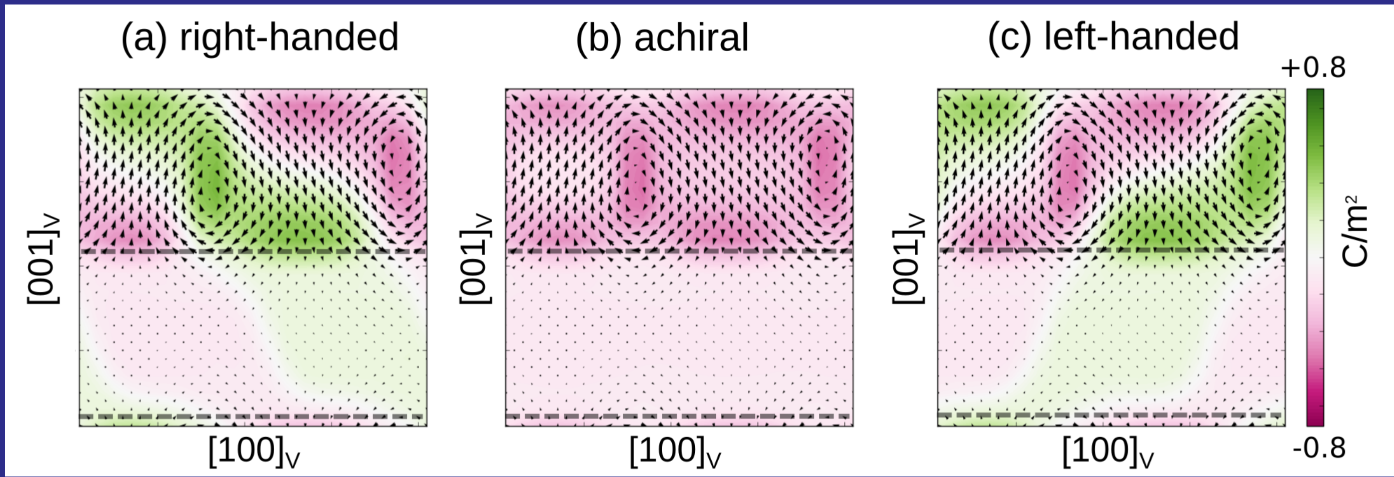

Domain walls of a mixed Ising-Bloch-Néel character

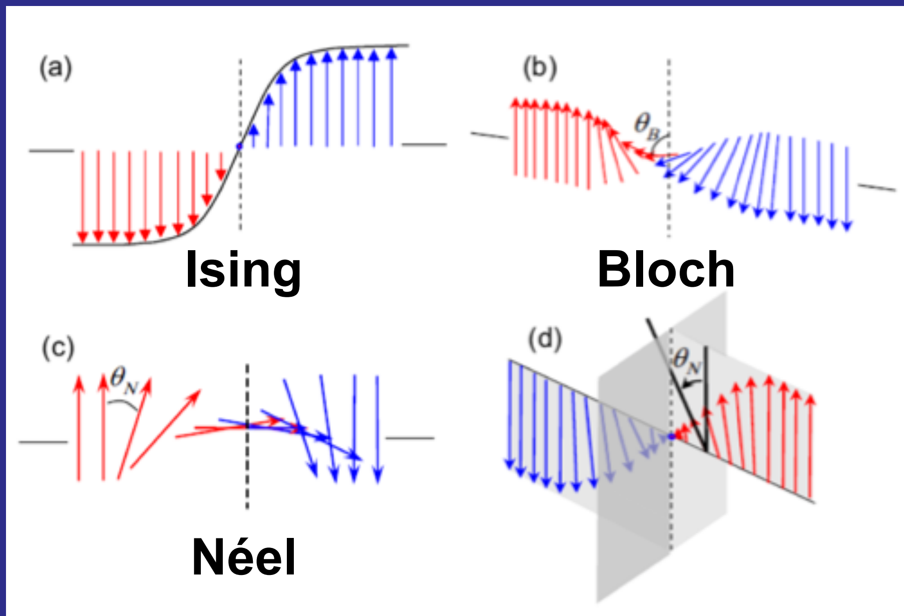

D. Lee *et al.*
Phys. Rev. B 80, 060102 (2009)

Chirality of simulated three-dimensional electrical polarization configuration

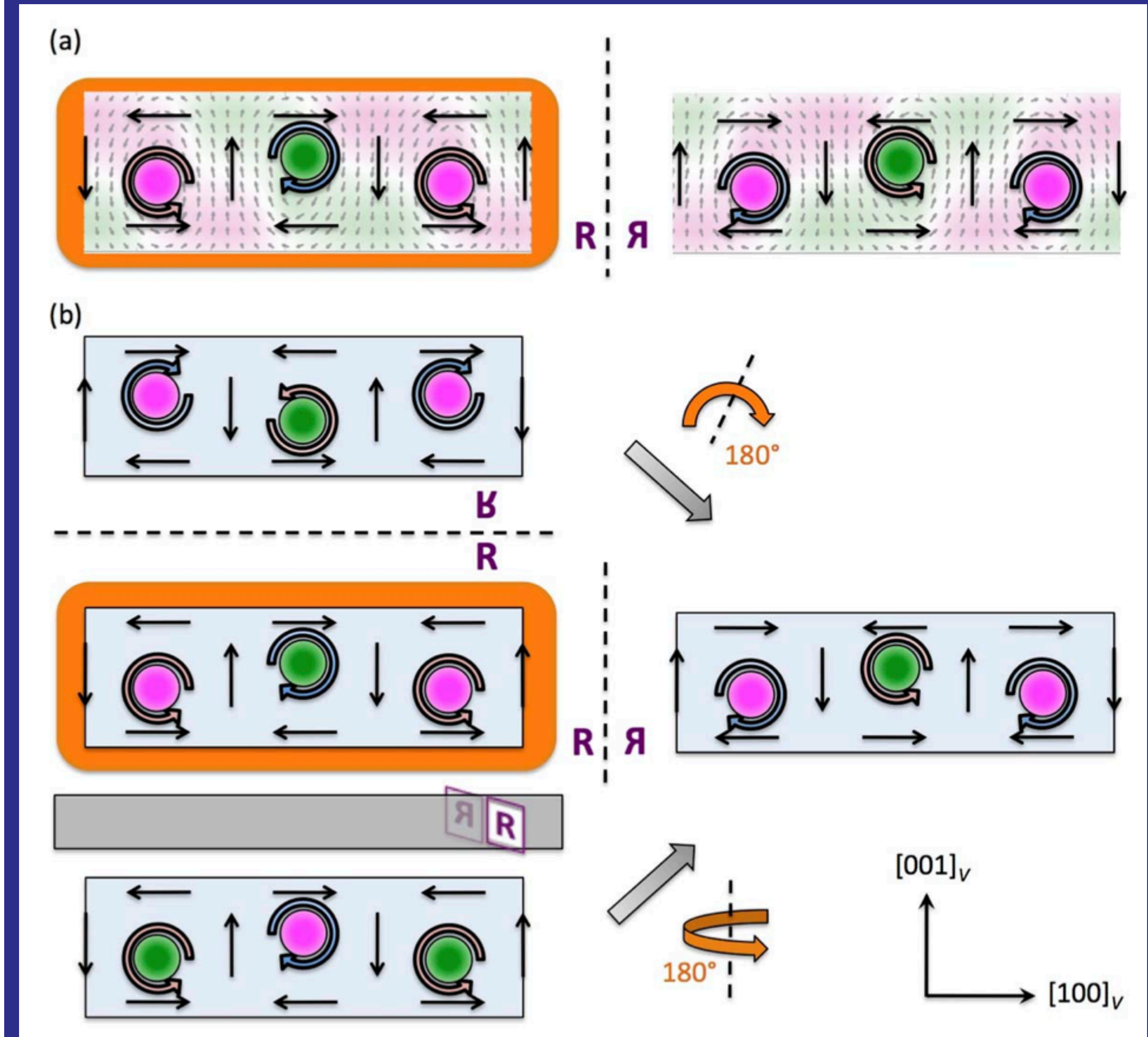

Three orthogonal reflections of the original vortex supercell

The reflected images all map onto one another
BUT
cannot be mapped onto the original structure by any combinations of rotations and/or translations

They are chiral enantiomers

P. Shafer, P. García-Fernández *et al*. submitted

Two of the structures are chiral enantiomers

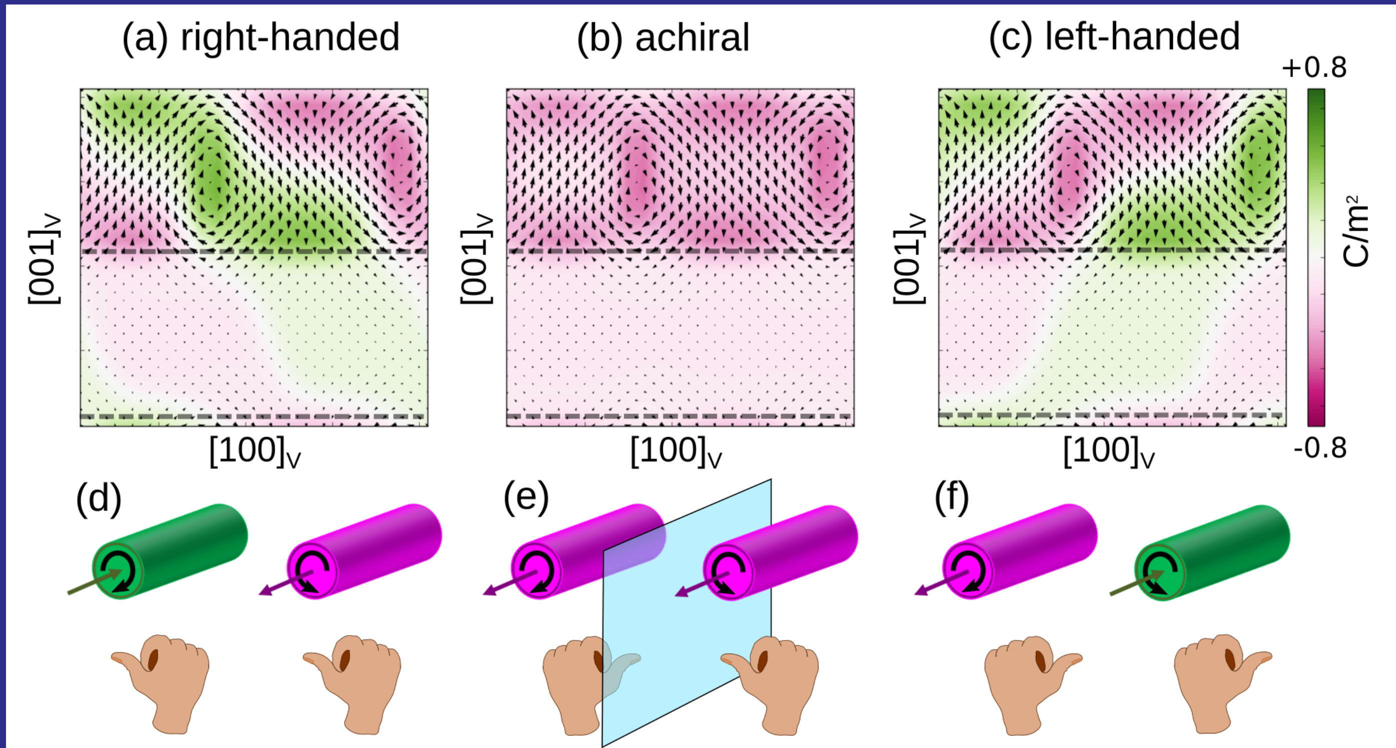

A handedness can be defined

P. Shafer, P. García-Fernández *et al*. submitted

The handedness of a given vortex can be characterized by the sign of the helicity

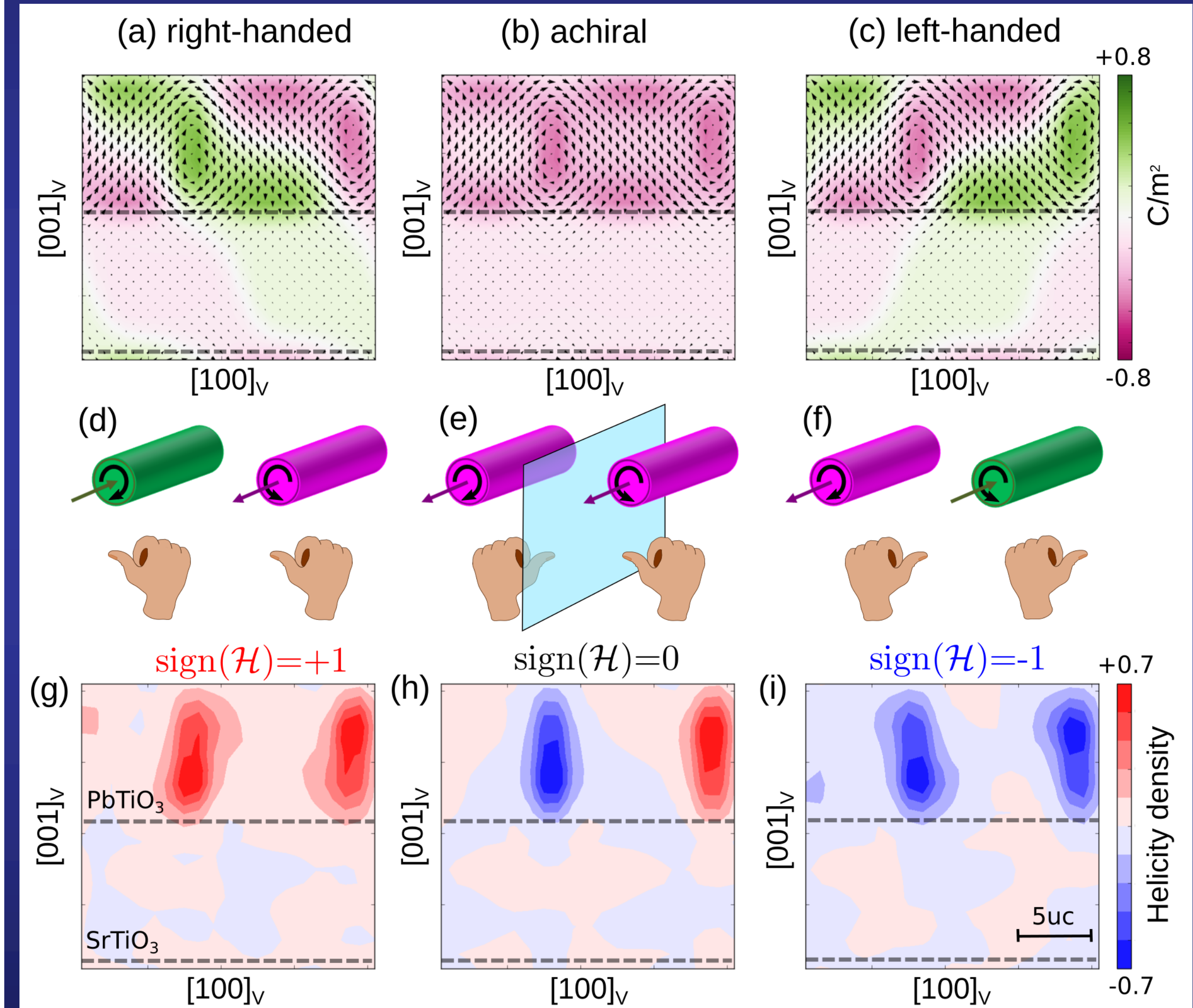

Helicity

$$\mathcal{H} = \int \vec{p} \cdot (\nabla \times \vec{p})\, d\vec{r}$$

Helicity density concentrated at vortex cores

P. Shafer, P. García-Fernández *et al*. submitted

Within the central $PbTiO_3$ layers of the chiral vortex arrays, the electric polarization forms a helical struc

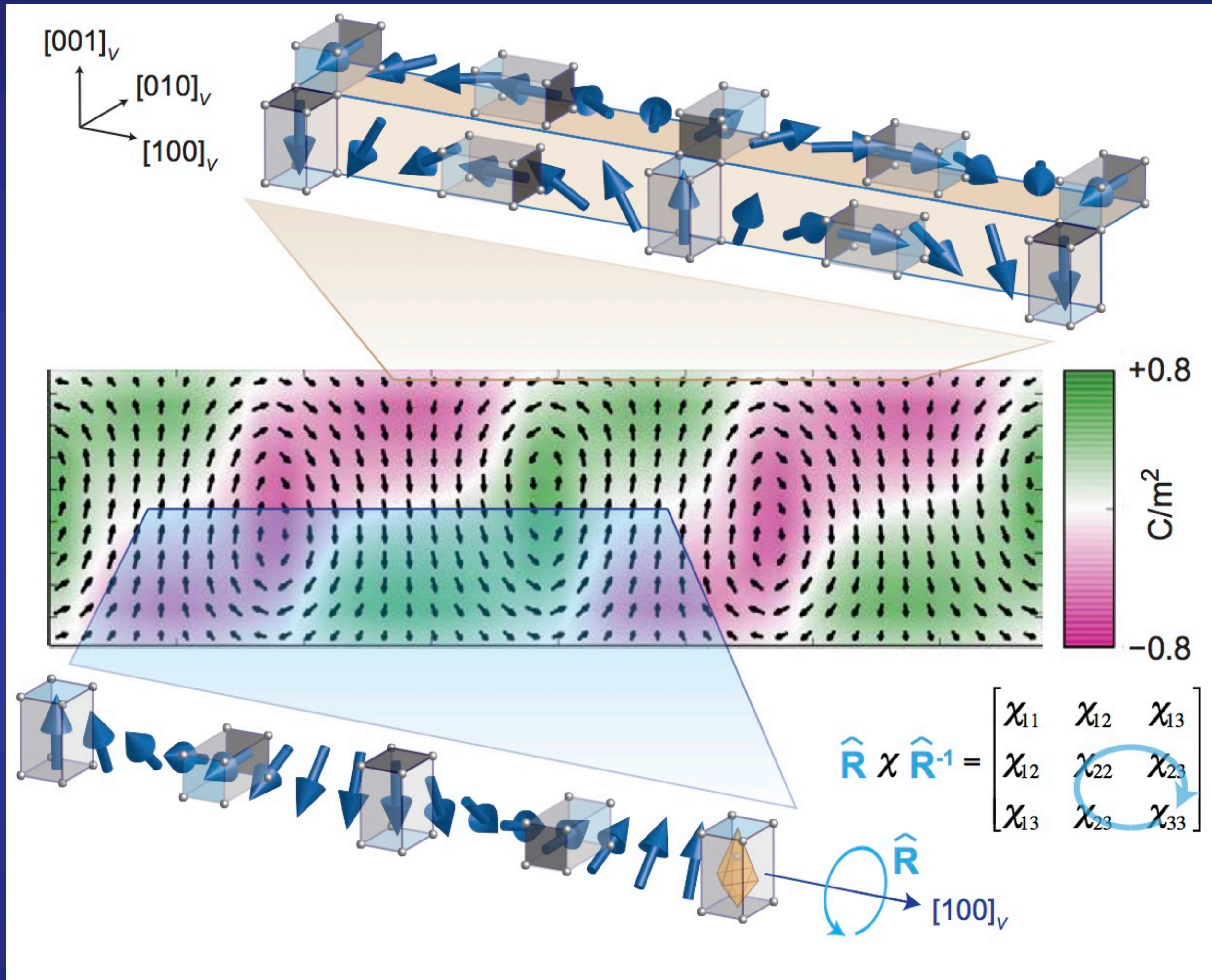

Each TiO_6 unit provides a a contribution to the x-ray scattering amplitude that varies with polarization orientation

P. Shafer, P. García-Fernández *et al*. submitted

The chiral helical structure imparts a chiral structure factor onto the scattering amplitude

Near resonant transitions, the x-rays are sensitive to the anisotropic electronic structure of the distorted TiO_6 octahedra

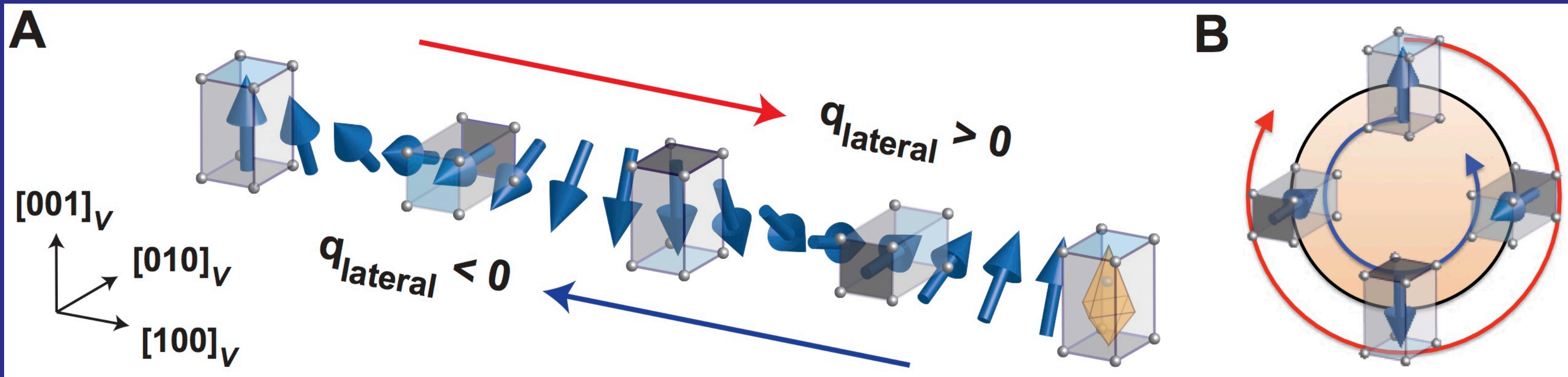

Mirrored diffraction vectors detect opposite rotational patterns in chiral textures

A helical rotation of the electric polarization can produce resonant soft x-ray diffraction peaks with anti-symmetric XCD

Mirrored diffraction vectors detect opposite rotational patterns in chiral textures

Helical arrangement of the electric polarization and associated anisotropic octahedral distortion

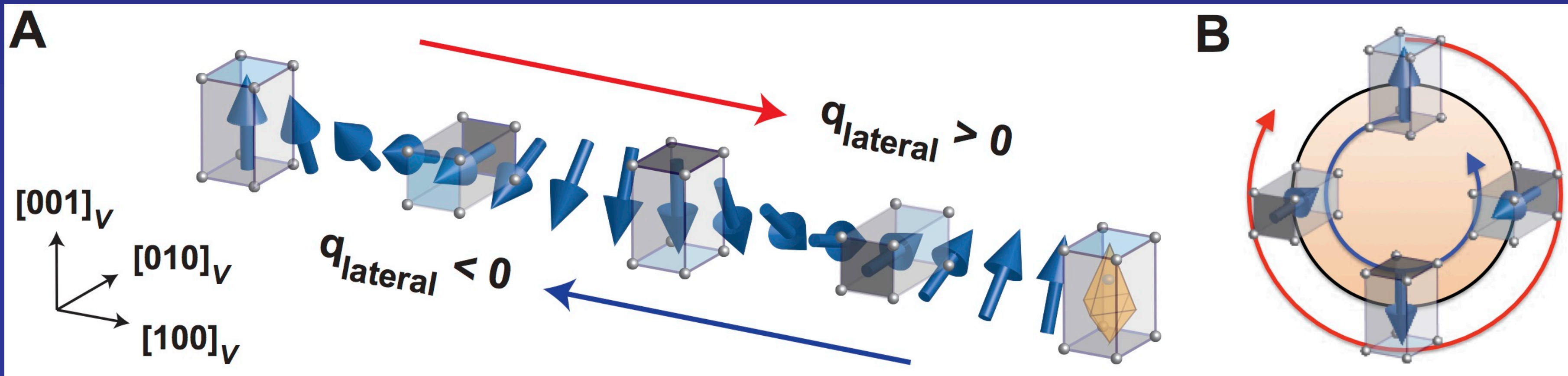

Continuous rotation of the local ferroelectric polarization
Continuous tilts of the Ti t_{2g}-like orbitals relative to polarized x-ray beam

$q_{\mathrm{lateral}} > 0$ **senses a clockwise helical rotation of the polarization**

$q_{\mathrm{lateral}} < 0$ **senses a counterclockwise helical rotation of the polarization**

Anti-symmetric XCD in these diffraction spots is a result of the chiral texture being detected with opposite rotational sense

P. Shafer, P. García-Fernández *et al*. submitted

Evidence of quirality measured in polar vortex arrays by resonant soft x-ray diffraction

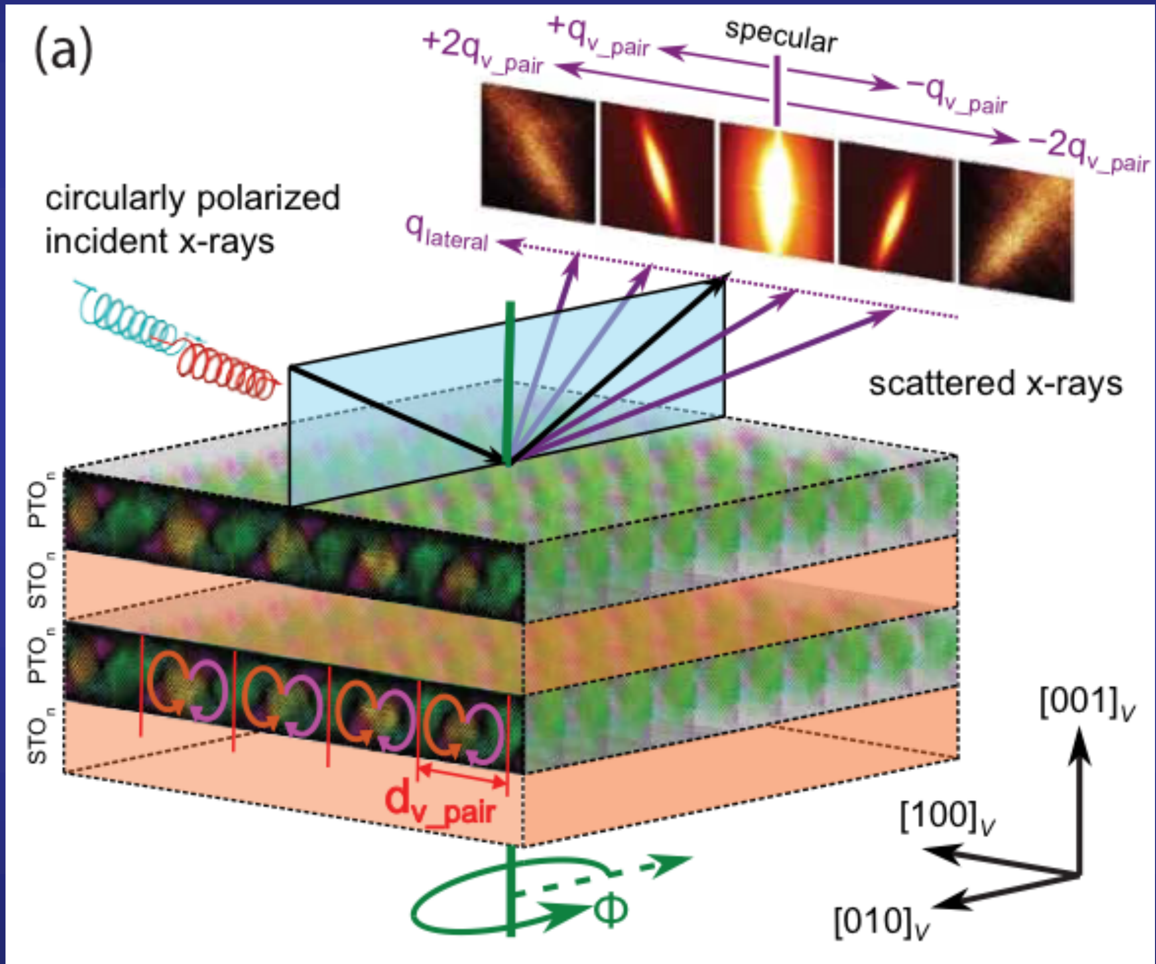

P. Shafer, P. García-Fernández *et al.* submitted

Soft x-ray wavelength: (1-3 nm)

Well matched to the periodicity of the lateral vortex modulations

Soft x-ray energy in the vicinity of resonant electronic transitions:

$Ti_{2p} \longrightarrow Ti_{3d\,(t2g)}$

Directly probe the anisotropic electronic structure of the TiO_6 octahedra

+

Enhancement of the scattering cross section

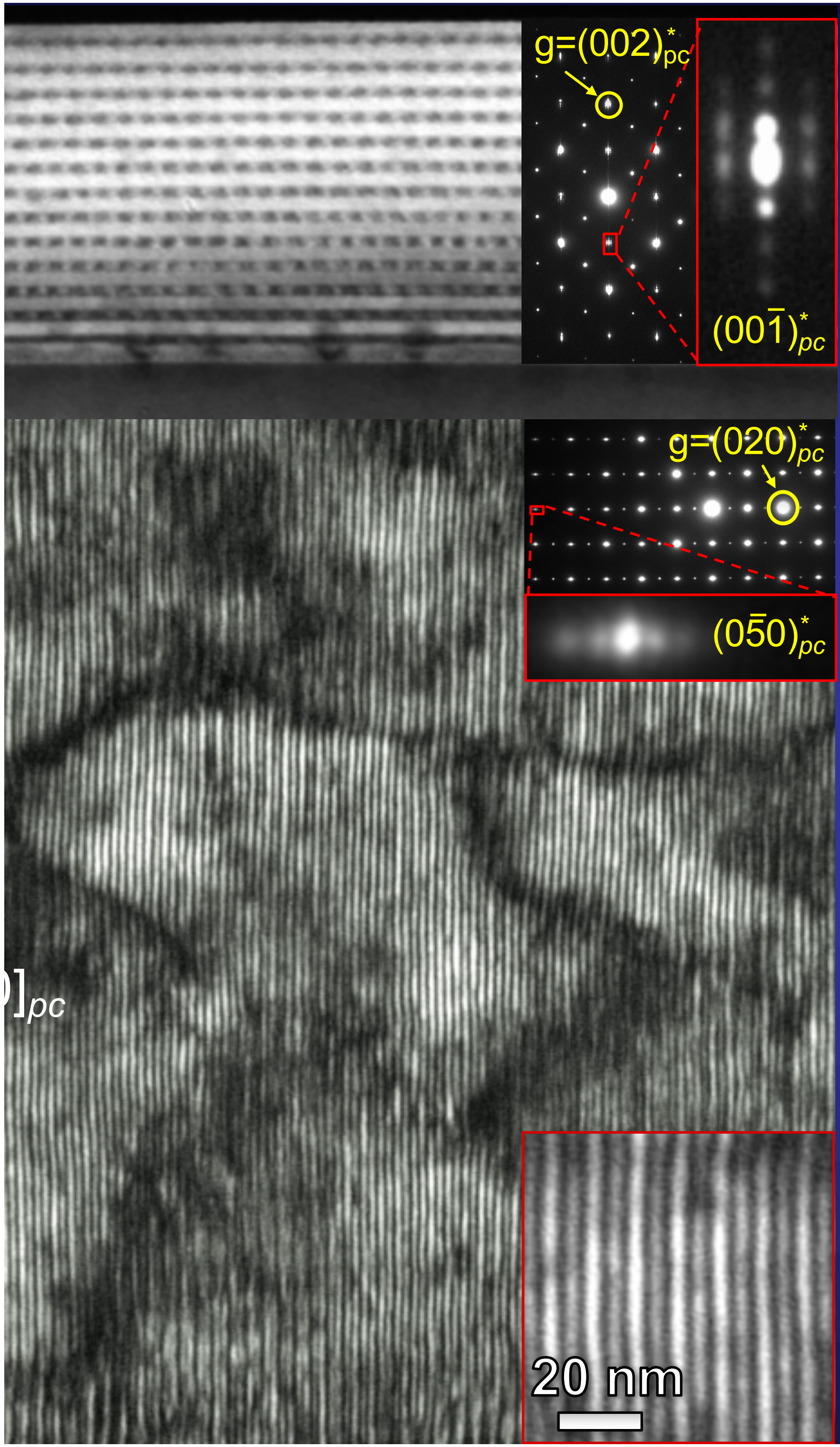

Synchrotron-based XRD reciprocal space maps have confirmed these lateral superlattice modulations as pairs of weak satellites that decorate the atomic Bragg peaks

$$\vec{q} = \vec{G} \pm (m\vec{q}_{\mathrm{v,pair}})$$

$\vec{q}_{\mathrm{v,pair}}$ **corresponds to the lateral period, directed along $[100]_V$**

m **is the order of the satellite**

Evidence of quirality measured in polar vortex arrays by resonant soft x-ray diffraction

Line cut through lateral satellite peaks

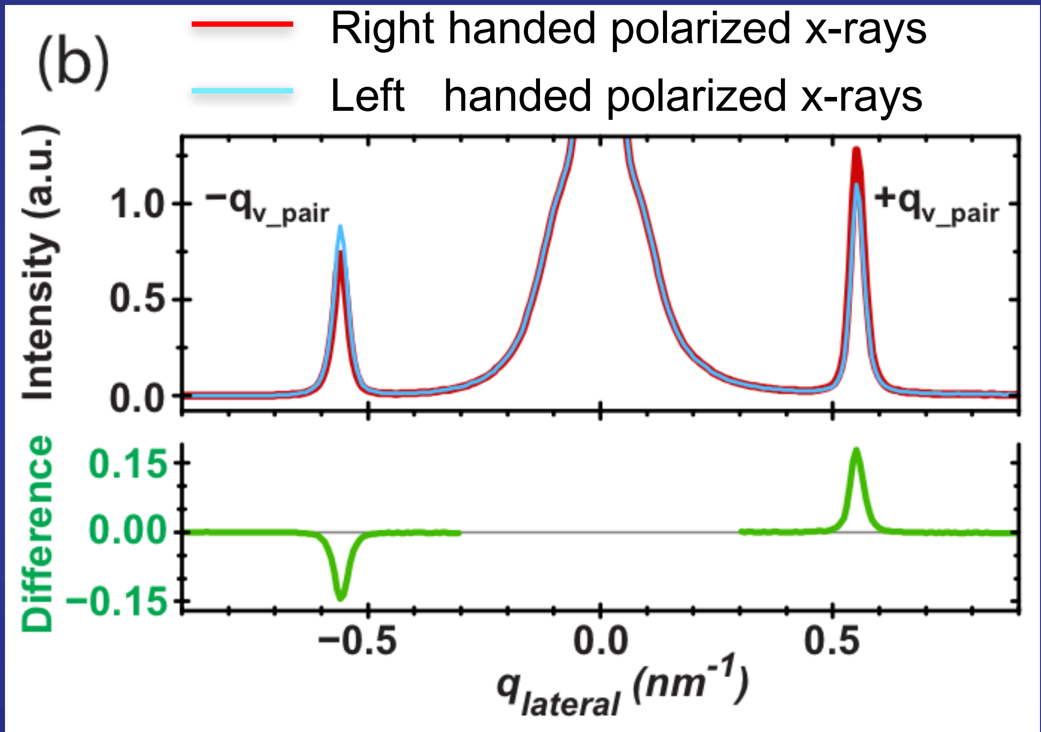

$$q_{\mathrm{v,pair}} = \frac{2\pi}{d_{\mathrm{v,pair}}}$$

Lateral period of the counter-rotated vortex pair
8 nm (n=10)
11.4 nm (n=16)

The intensity of the diffraction peak is markedly different for circularly polarized incoming x-rays with opposite left- and right-helicity, with differences on the order of ~20%.

P. Shafer, P. García-Fernández *et al*. submitted

Evidence of quirality measured in polar vortex arrays by resonant soft x-ray diffraction

Line cut through lateral satellite peaks

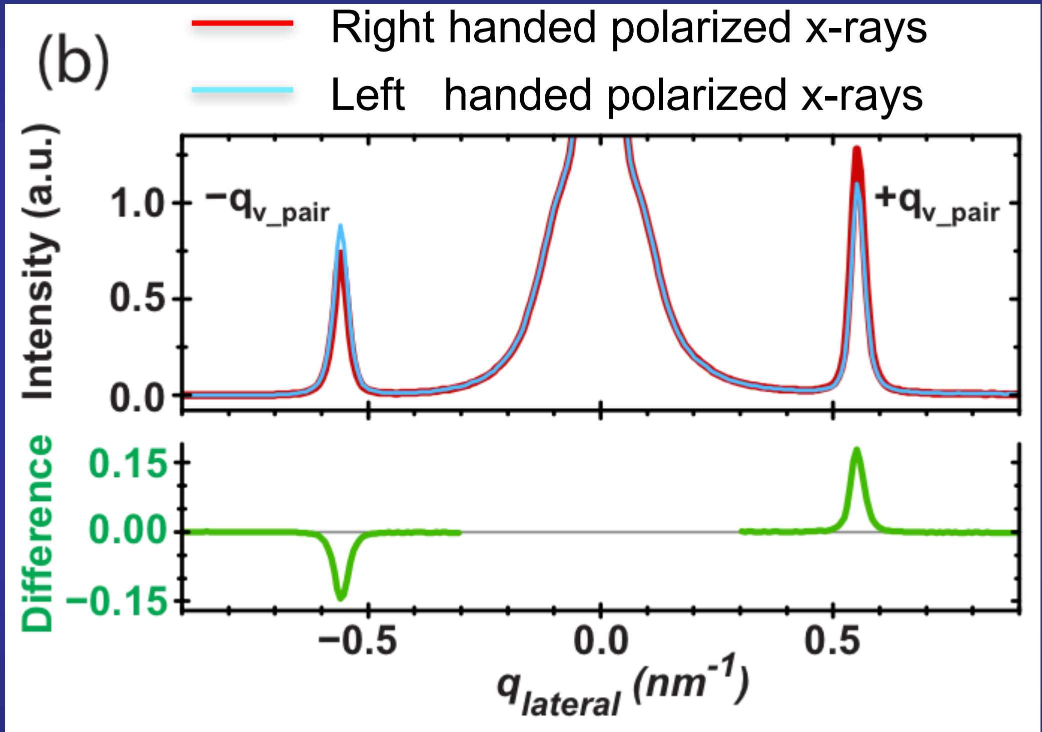

$$q_{\mathrm{v,pair}} = \frac{2\pi}{d_{\mathrm{v,pair}}}$$

Lateral period of the counter-rotated vortex pair
8 nm (n=10)
11.4 nm (n=16)

The intensity of the diffraction peak is markedly different for circularly polarized incoming x-rays with opposite left- and right-helicity, with differences on the order of ~20%.

P. Shafer, P. García-Fernández *et al*. submitted

Take home message

Chirality can be induced by the complex interactions in artificial superlattices constructed from two non-chiral objects

Chirality manifests as an alternating in-plane component of electric polarization, that couples to the swirling cores of a vortex structure

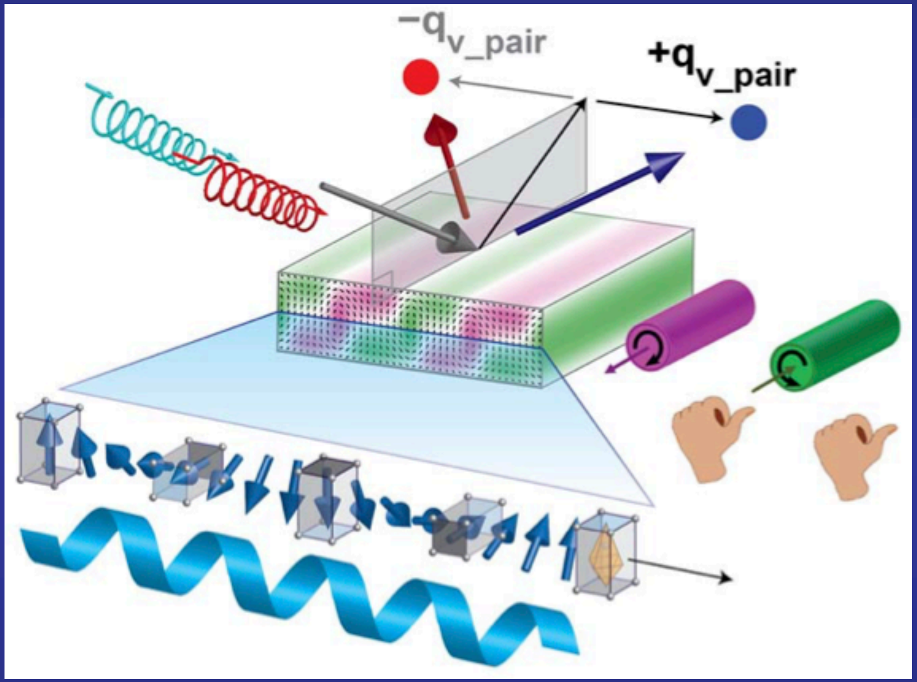

Second-principles simulations in very good agreement with resonant soft x-ray diffraction patterns

P. Shafer, P. García-Fernández *et al*. submitted

Take home message

Chirality can be induced by the complex interactions in artificial superlattices constructed from two non-chiral objects

Chirality manifests as an alternating in-plane component of electric polarization, that couples to the swirling cores of a vortex structure

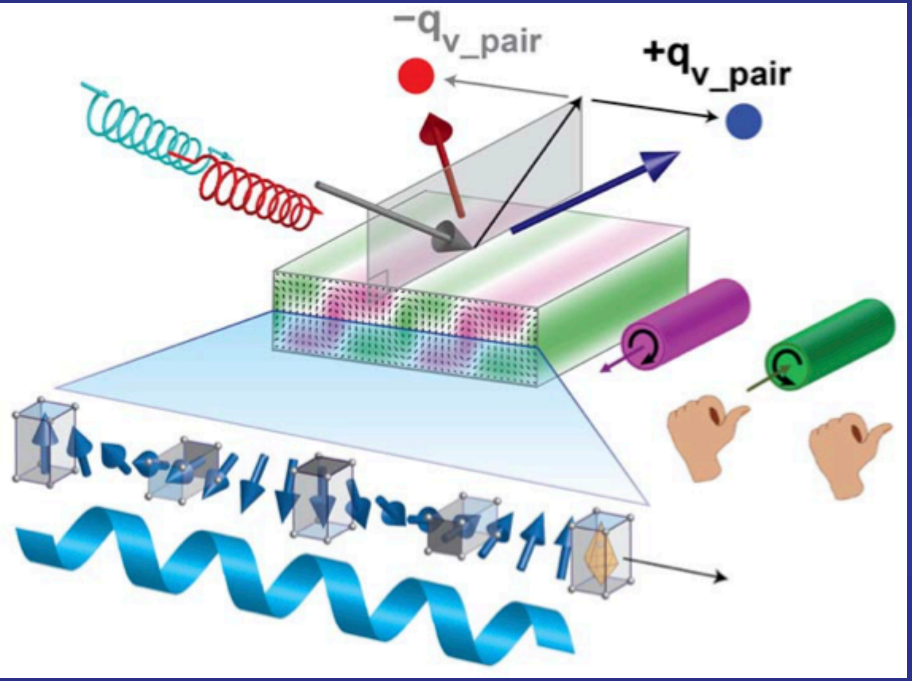

Second-principles simulations in very good agreement with resonant soft x-ray diffraction patterns

P. Shafer, P. García-Fernández *et al*. submitted

Emergent topological properties at $PbTiO_3/SrTiO_3$ superlattices

Emerging chirality in polar vortex superlattices

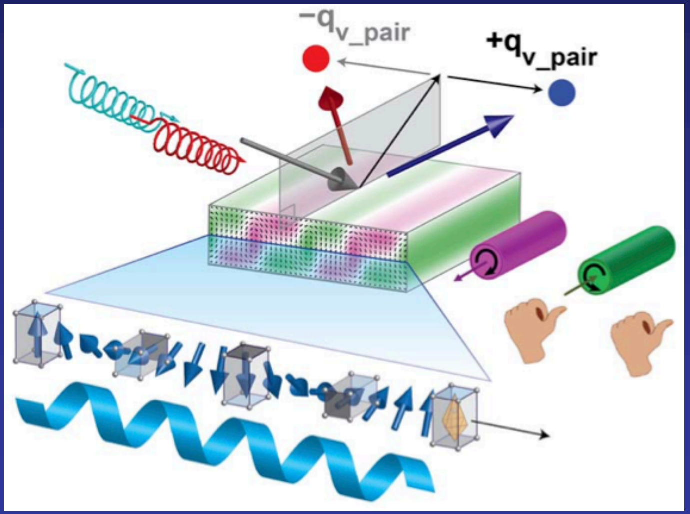

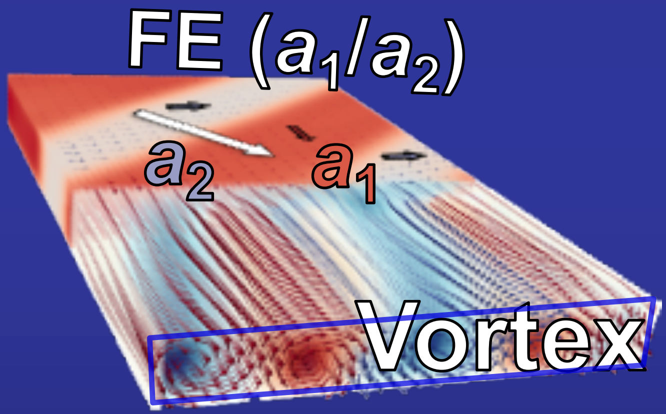

Coexistence of phases

Bubble skyrmions

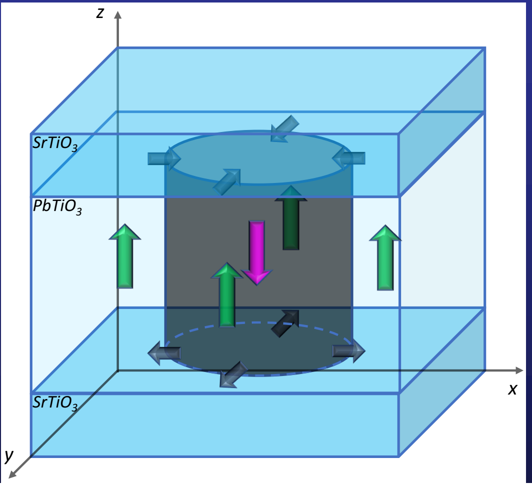

Phase Evolution vs. superlattice periodicity

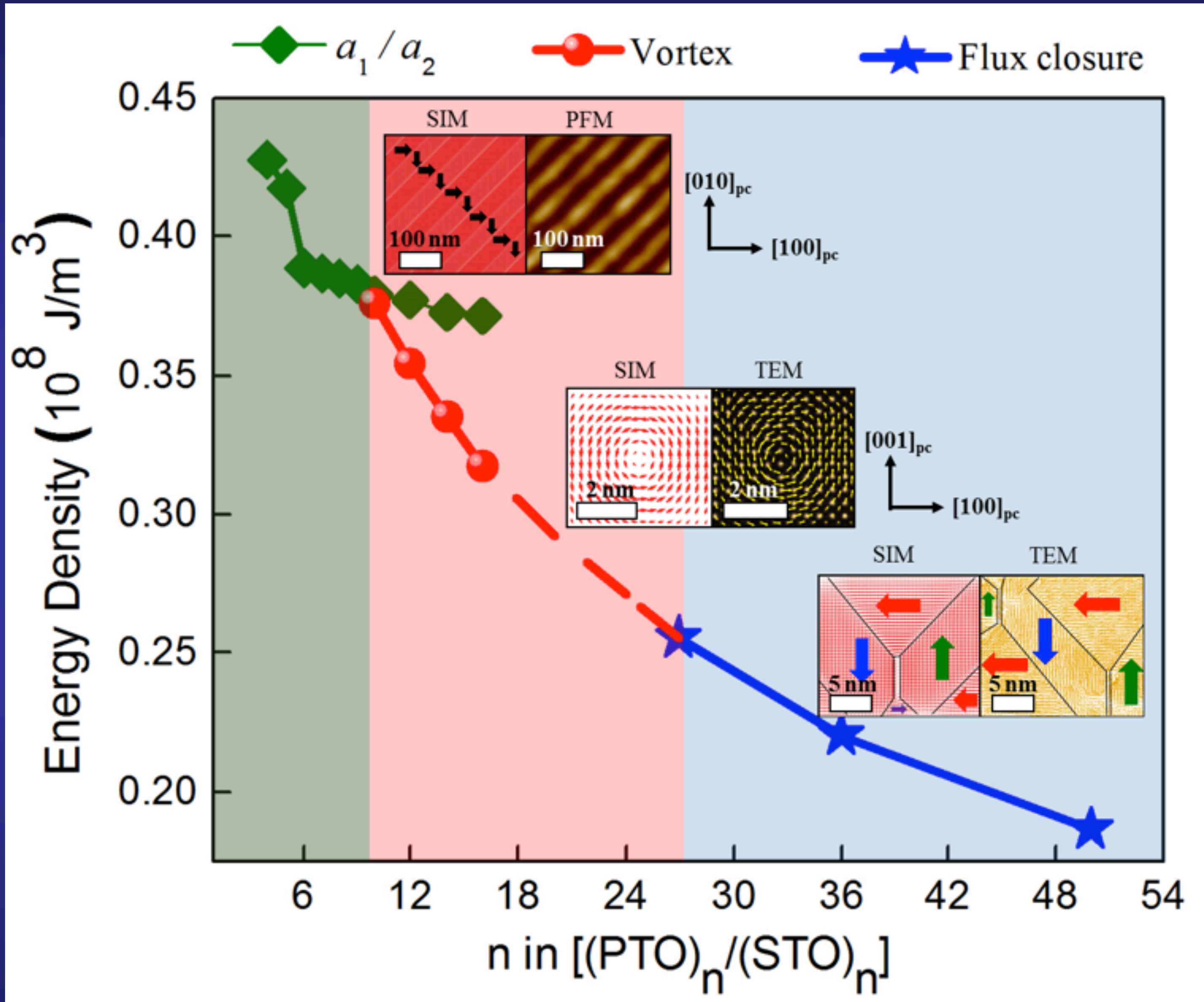

A. Damodaran *et al*. Nat. Mater. 16, 1003 (2017)

Structural evolution of ferroelectric and vortex phases with superlattice periodicity

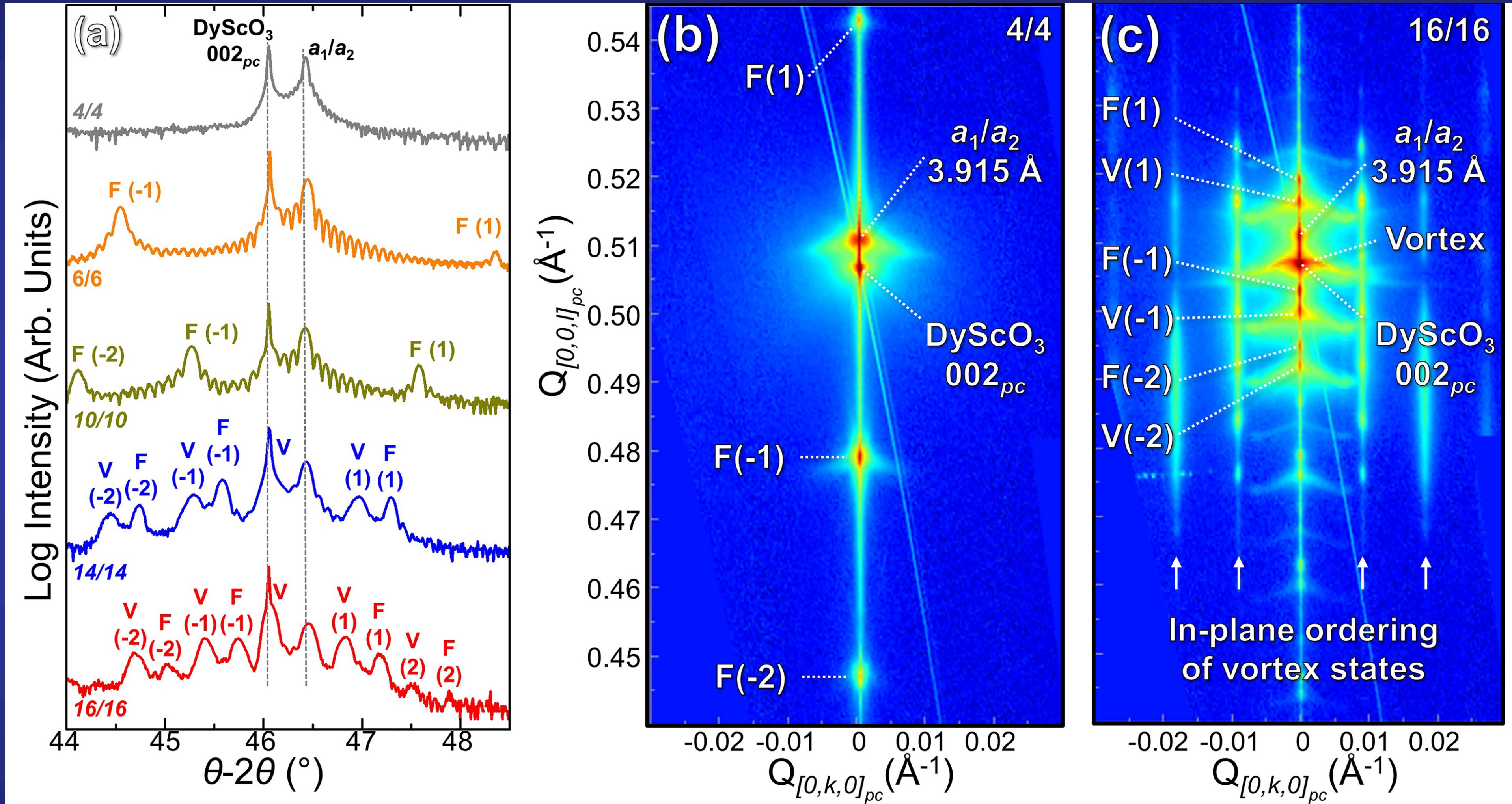

Phase competition, order parameter coexistence and emergent order parameter in the same $PbTiO_3/SrTiO_3$ superlattice system

A. Damodaran *et al*. Nat. Mater. 16, 1003 (2017)

At room temperature, the coexisting vortex and ferroelectric phases spontaneously assemble in a mesoscale

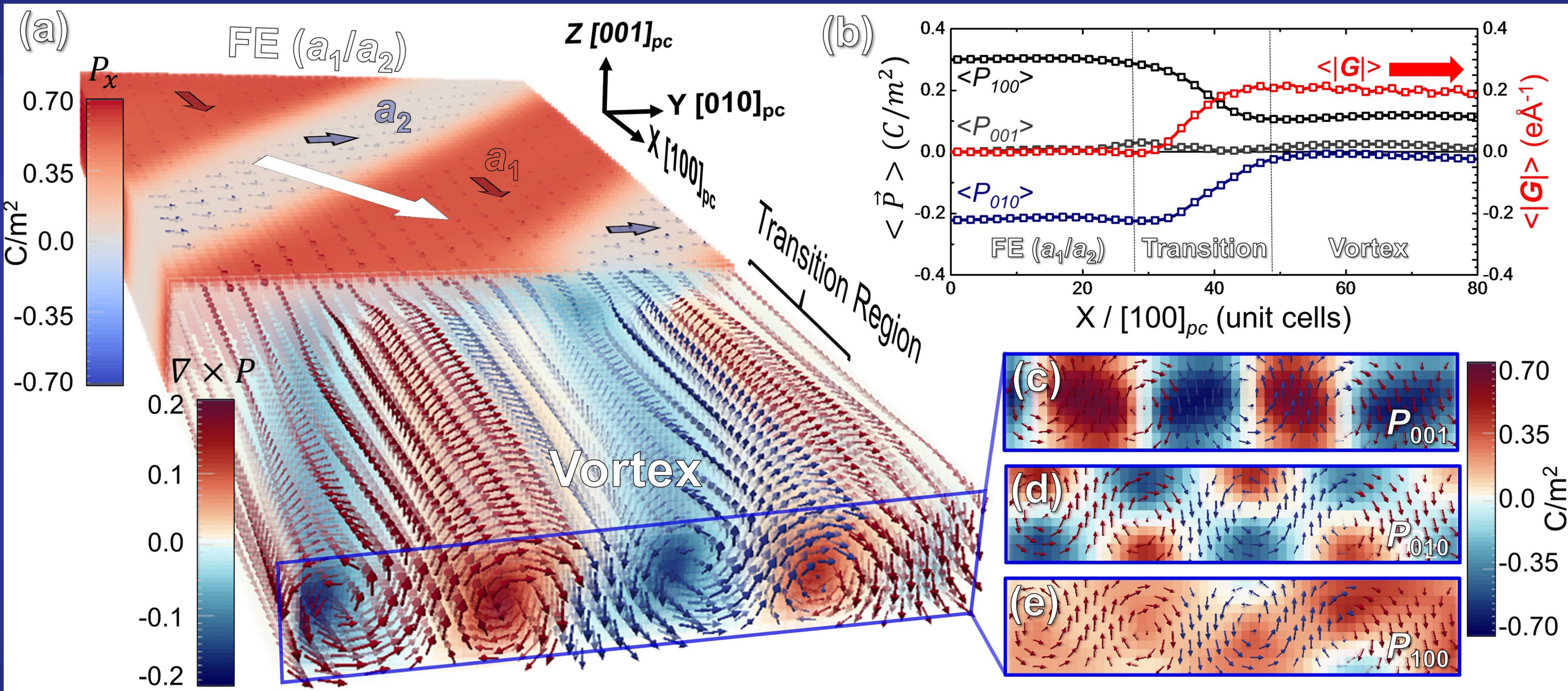

A. Damodaran *et al.* Nat. Mater. 16, 1003 (2017)

The application of an electric field results in the deterministic interconversion between the vortex and the FE phase

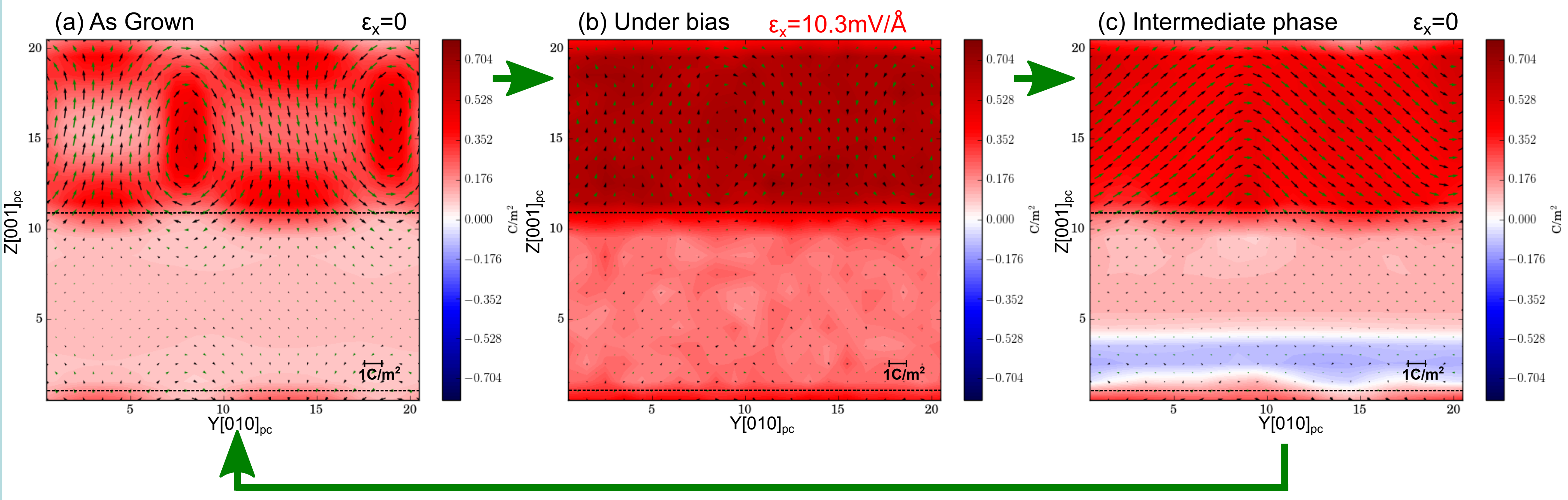

As grown: clockwise and anticlockwise vortices

Collapse of the local dipoles to point parallel to the field, forming a unique domain along x

Sinusoidal domain structure in the yz plane nucleates, the first Fourier component of the vortex phase

Orders of magnitude changes in piezoelectric and nonlinear optical properties
A similar effect to colossal magnetorresistance

A. Damodaran *et al*. Nat. Mater. 16, 1003 (2017)

Take home message

Ferroelectric a_1/a_2 domains coexist with vortex structures

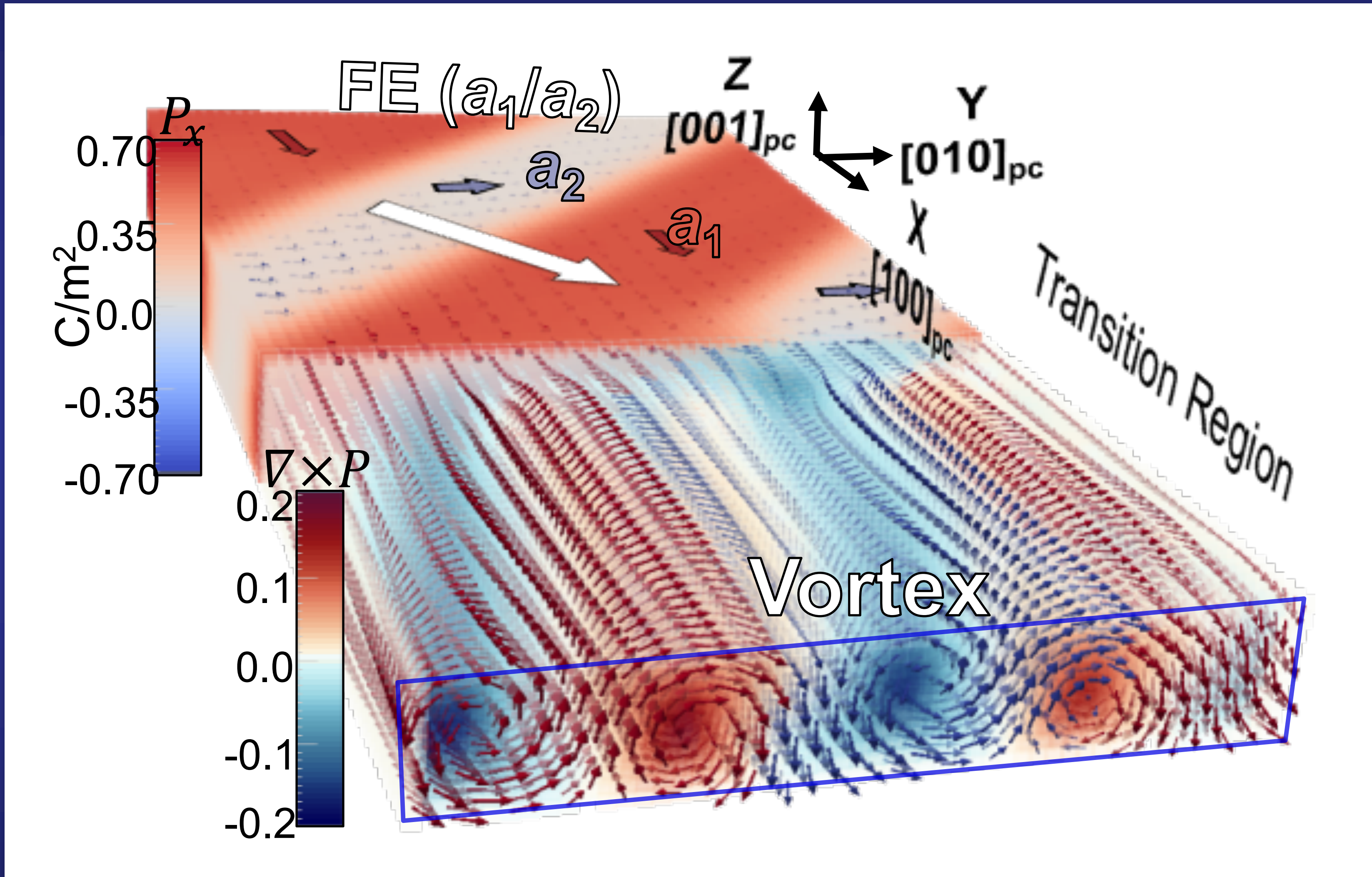

Reversible phase transitions can be induced

A. Damodaran *et al*. Nat. Mater. 16, 1003 (2017)

Emergent topological properties at $PbTiO_3/SrTiO_3$ superlattices

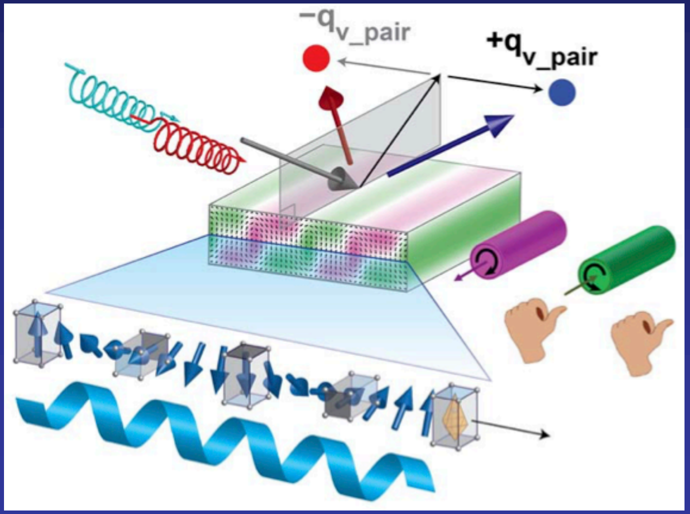

Emerging chirality in polar vortex superlattices

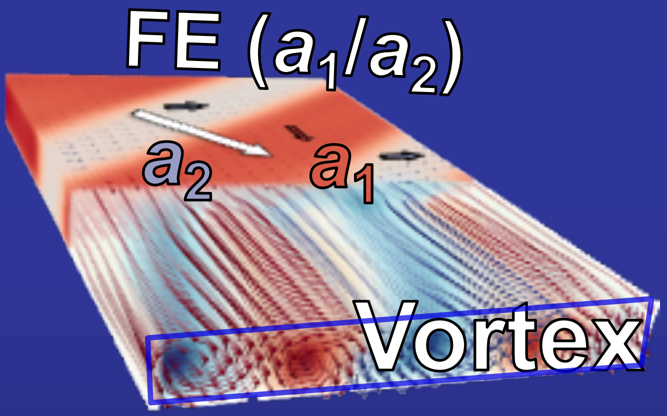

Coexistence of phases

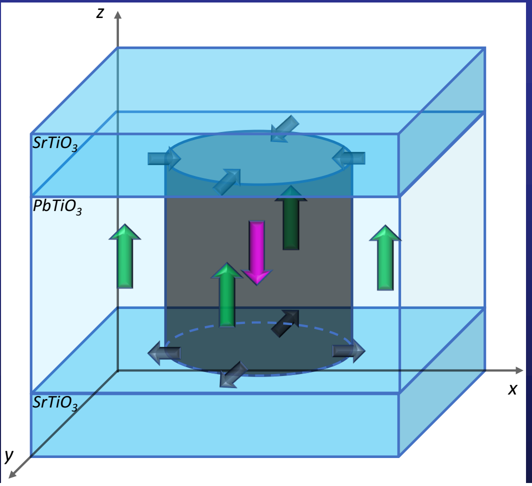

Bubble skyrmions

“Bubble domains” in $Pb(Zr_{0.2}Ti_{0.8})O_3/SrTiO_3/Pb(Zr_{0.2}Ti_{0.8})O_3$

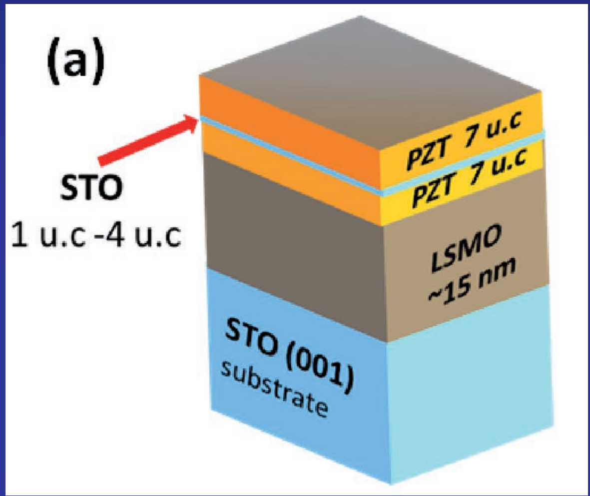

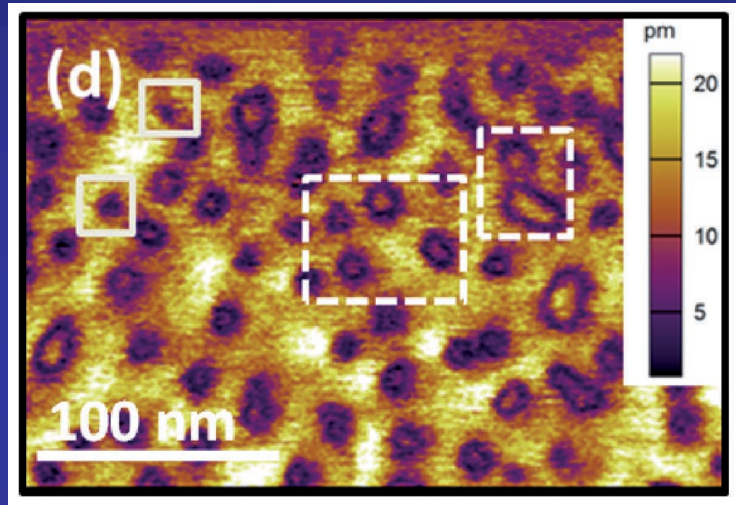

Laterally confined spheroids of sub 10 nm-size with local dipoles self-aligned in a direction opposite to the macroscopic polarization of a surrounding ferroelectric matrix

Q. Zhang *et al*. Adv. Mater. 1702375 (2017)

"Bubble domains" in $PbTiO_3/SrTiO_3$ superlattices

Experimental challenge:

Image with atomic resolution

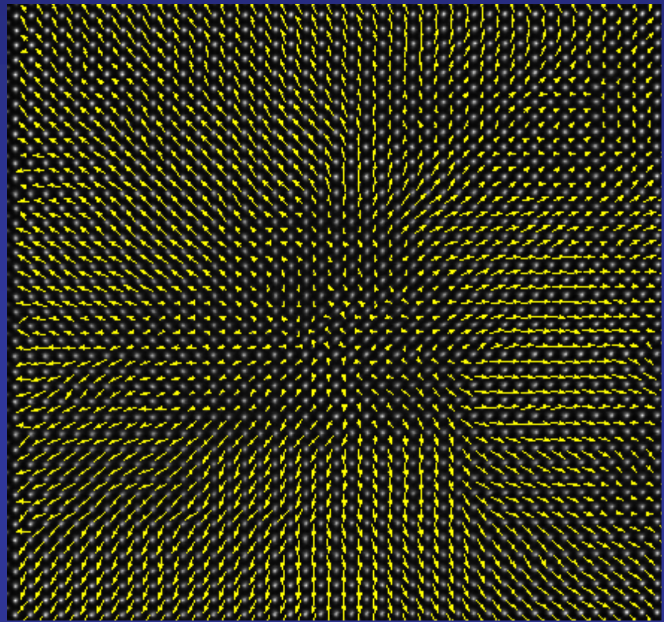

From Ramesh's group
(see next talk)

Theoretical challenge:

Modern chiral skyrmions can be topologically identical to classical magnetic bubble domains,

Can ferroelectric bubble domains can be considered a precursor to electrical skyrmions?

Bubble structures at $PbTiO_3/SrTiO_3$ superlattices

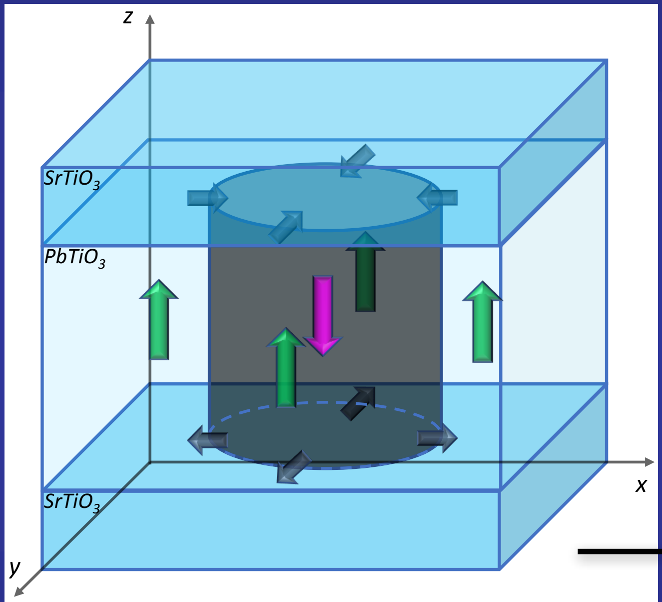

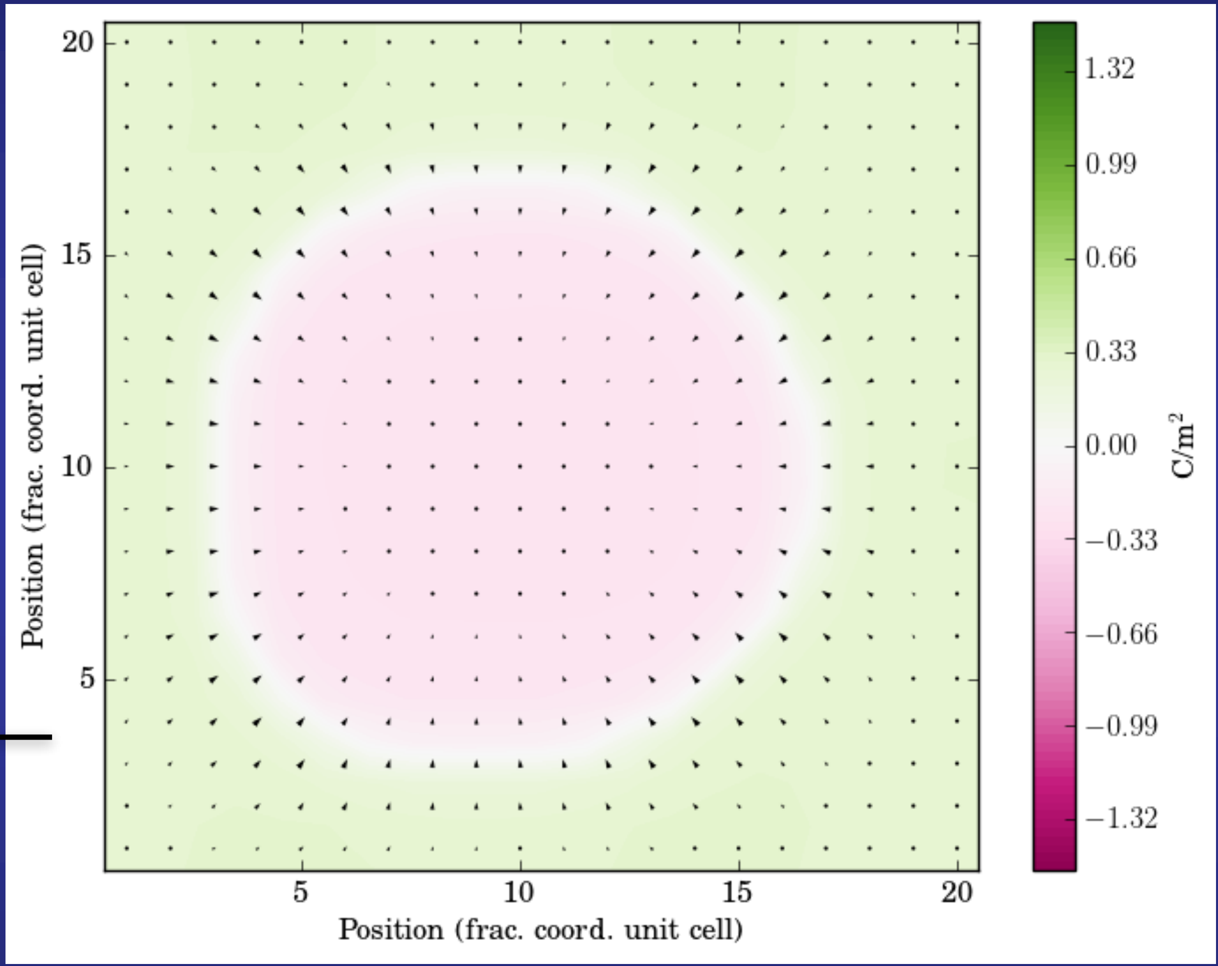

In-plane lattice constant $a = 3.901$ Å

Bubble structures at $PbTiO_3/SrTiO_3$ superlattices

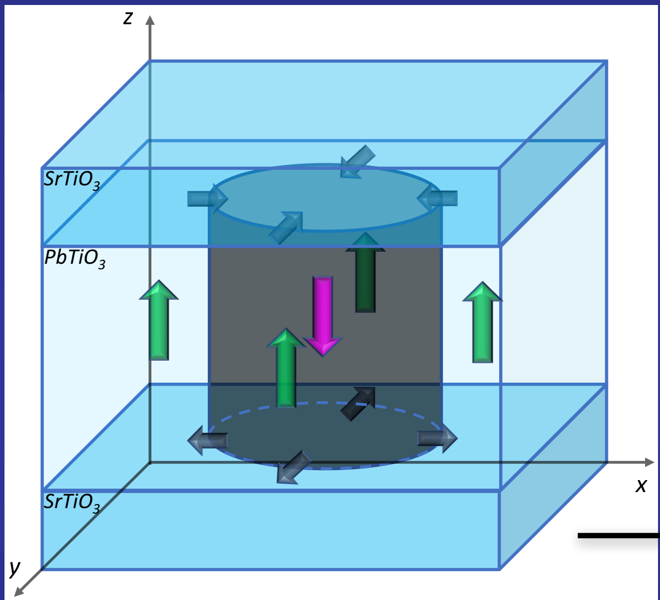

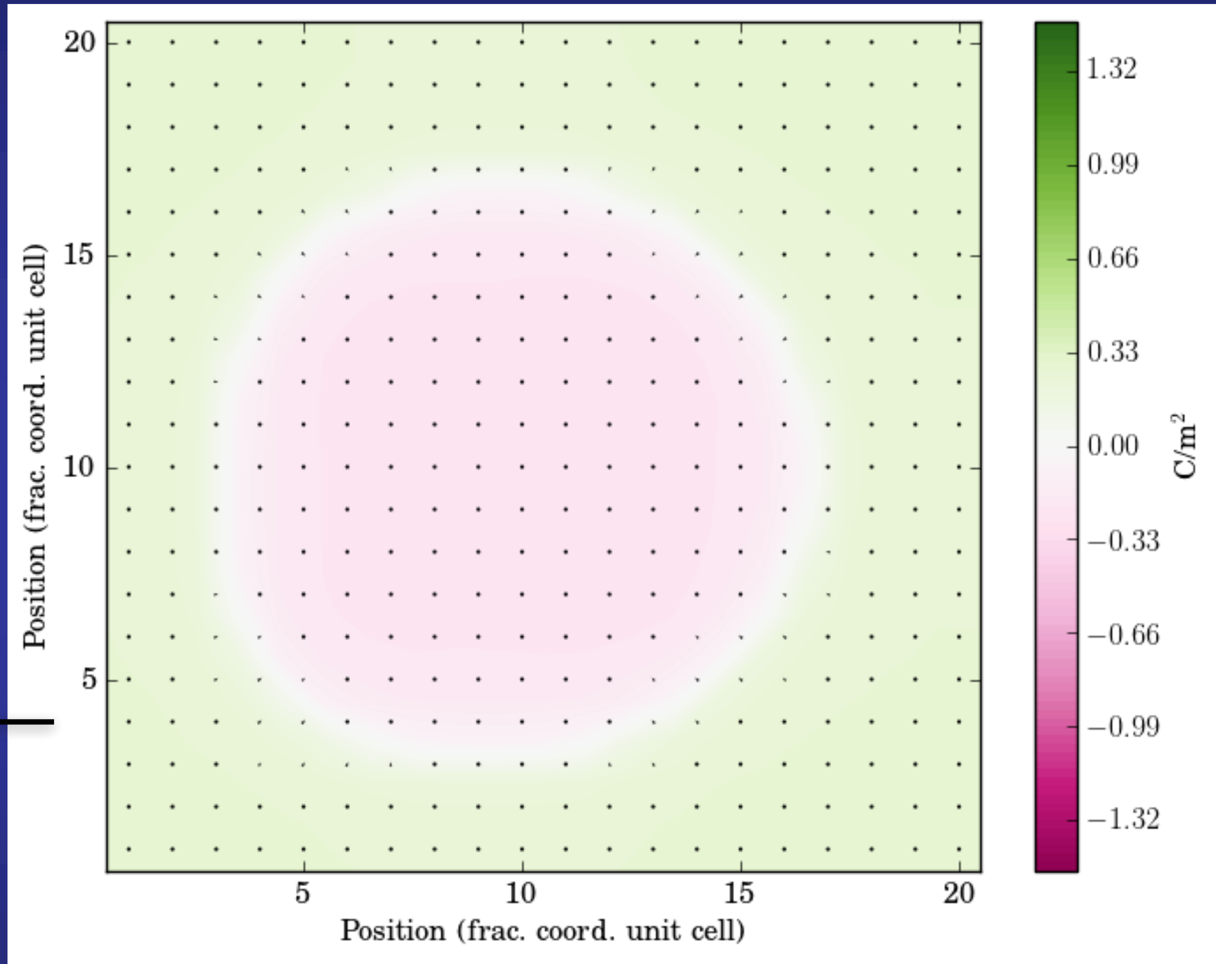

In-plane lattice constant $a = 3.901$ Å

Bubble structures at $PbTiO_3/SrTiO_3$ superlattices

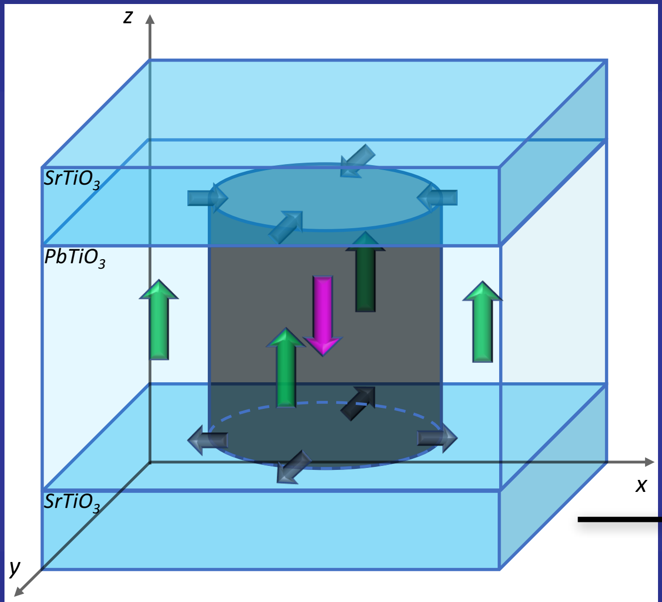

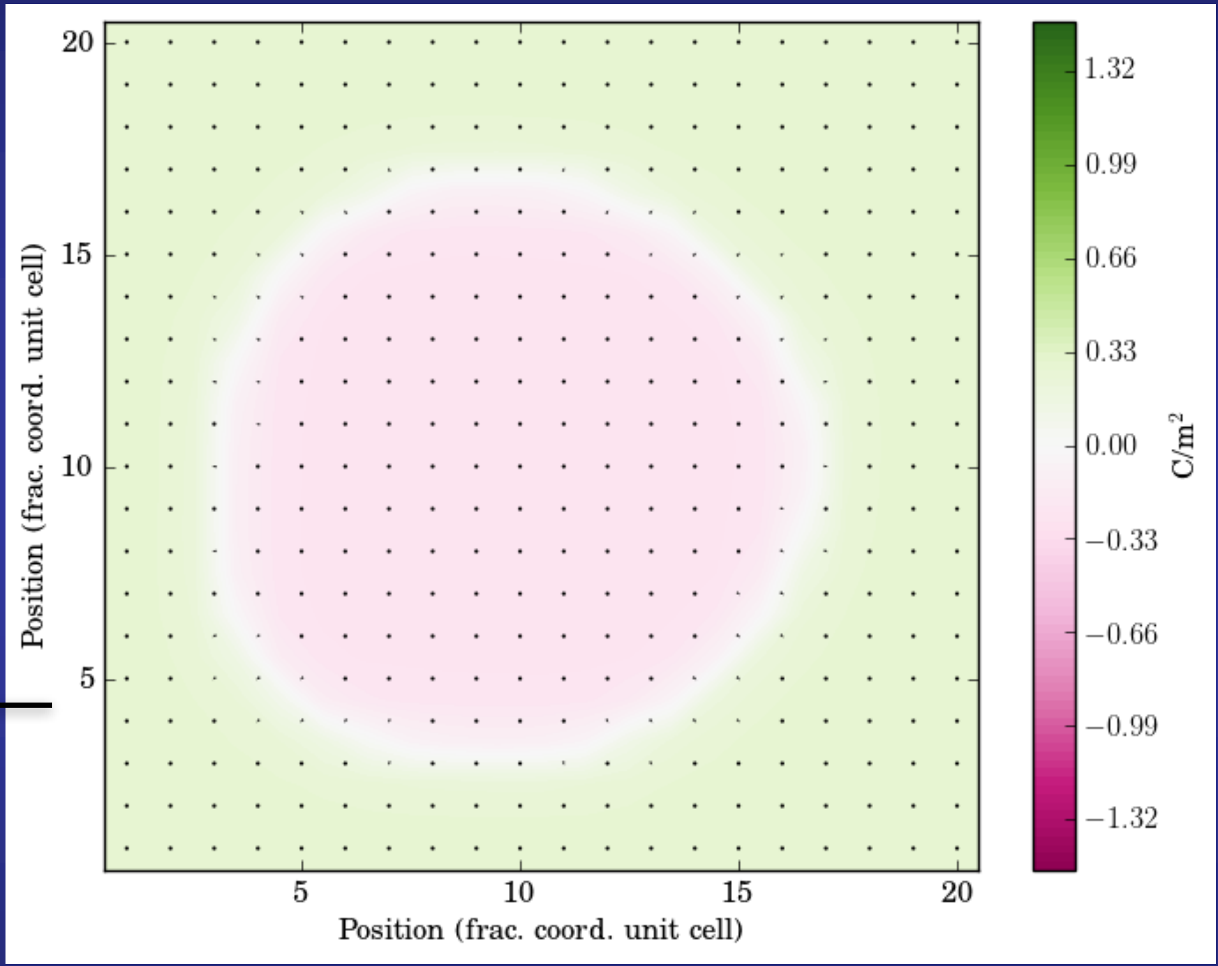

In-plane lattice constant $a = 3.901$ Å

Bubble structures at $PbTiO_3/SrTiO_3$ superlattices

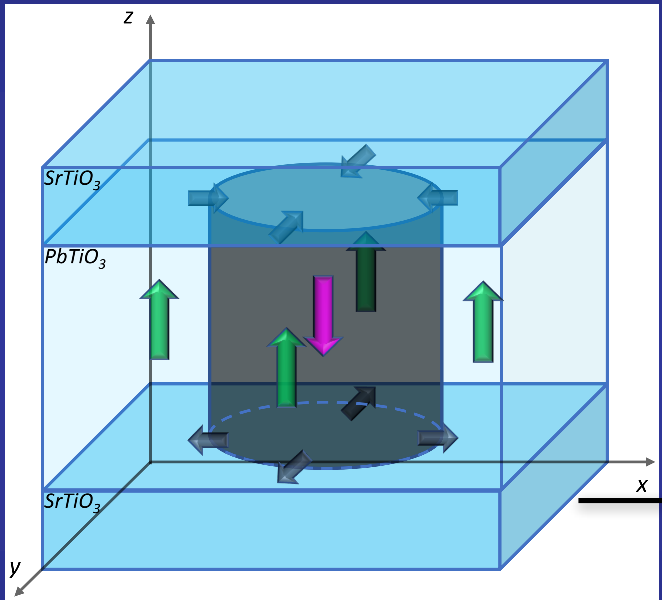

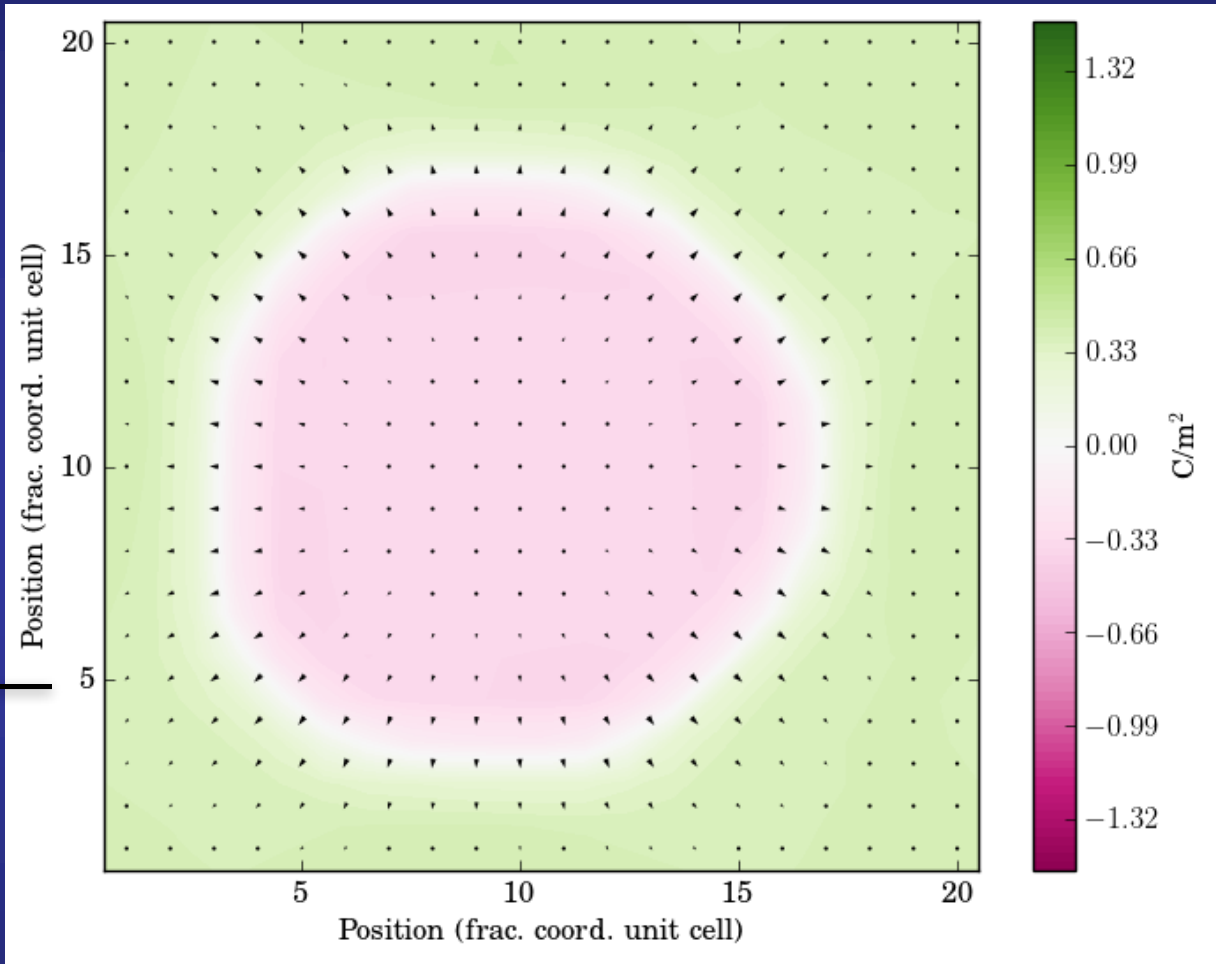

In-plane lattice constant $a = 3.901$ Å

Bubble structures at $PbTiO_3/SrTiO_3$ superlattices

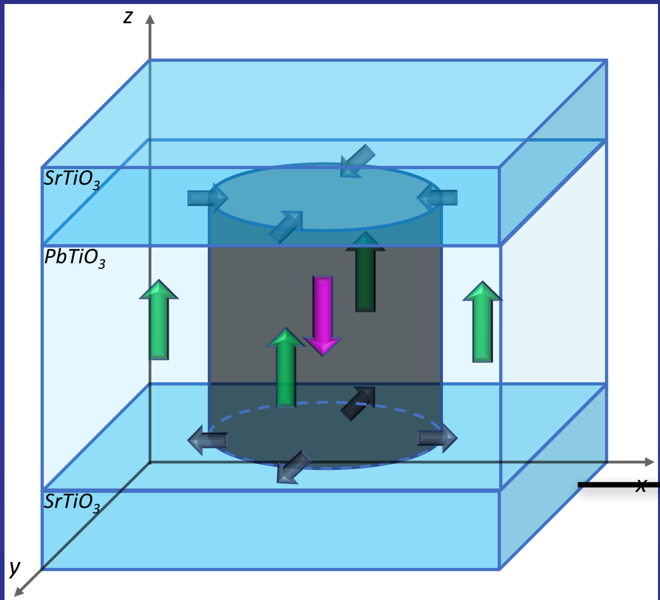

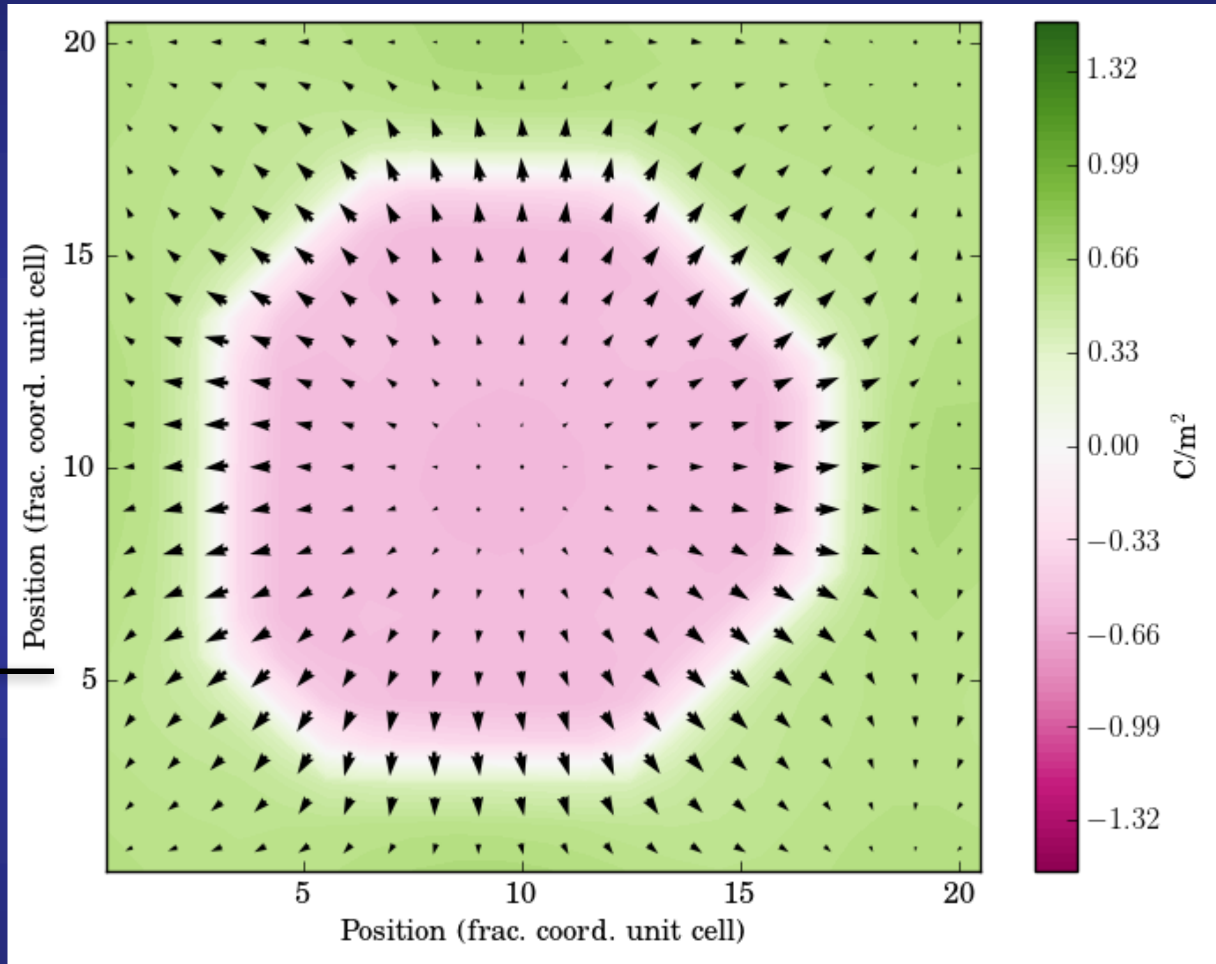

Bottom interface

In-plane lattice constant $a = 3.901$ Å

Bubble structures at $PbTiO_3/SrTiO_3$ superlattices

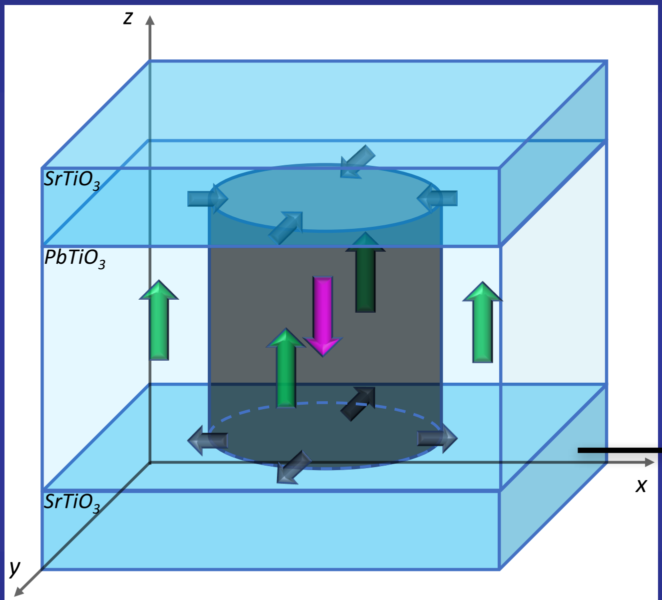

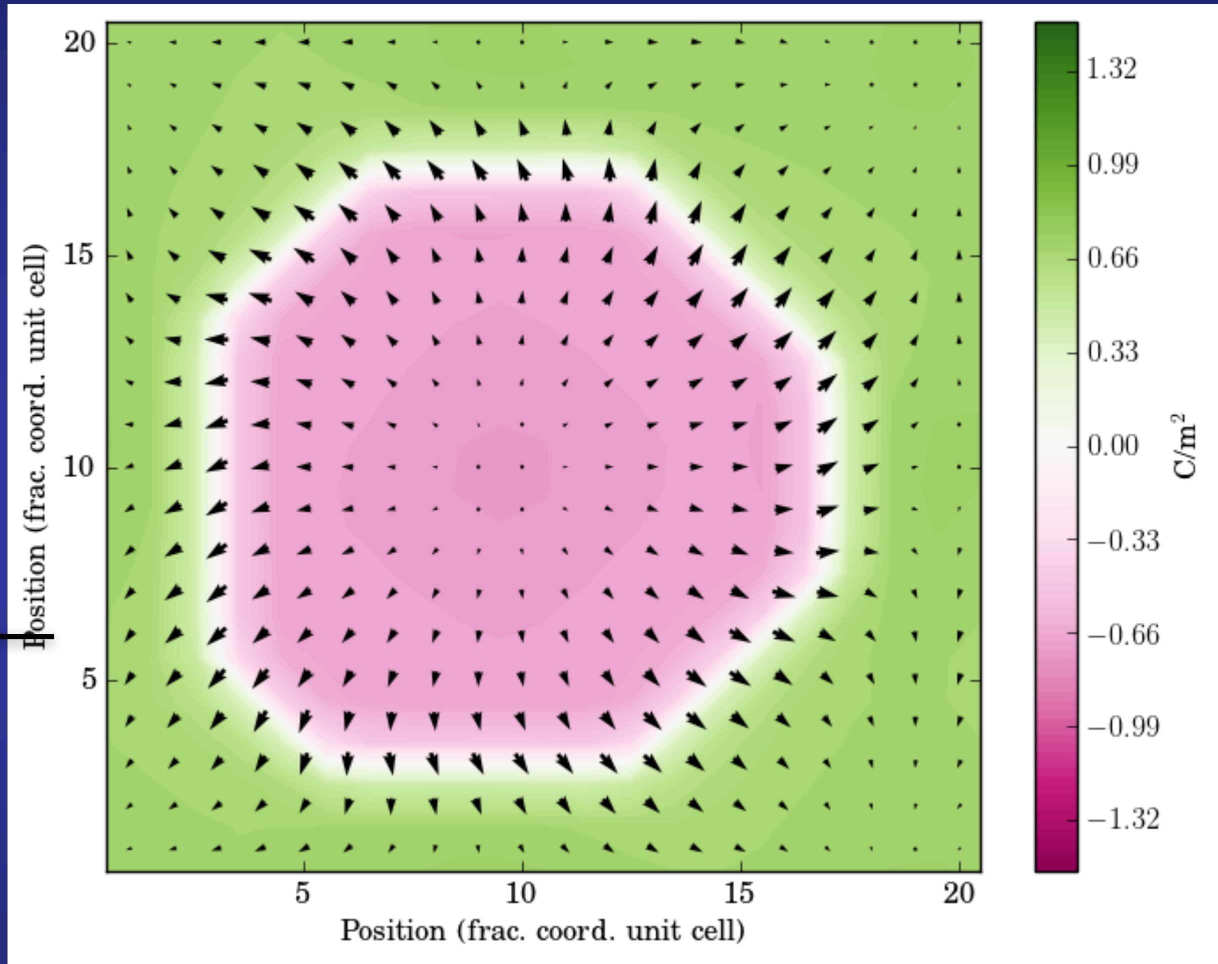

In-plane lattice constant $a = 3.901$ Å

Bubble structures at $PbTiO_3/SrTiO_3$ superlattices

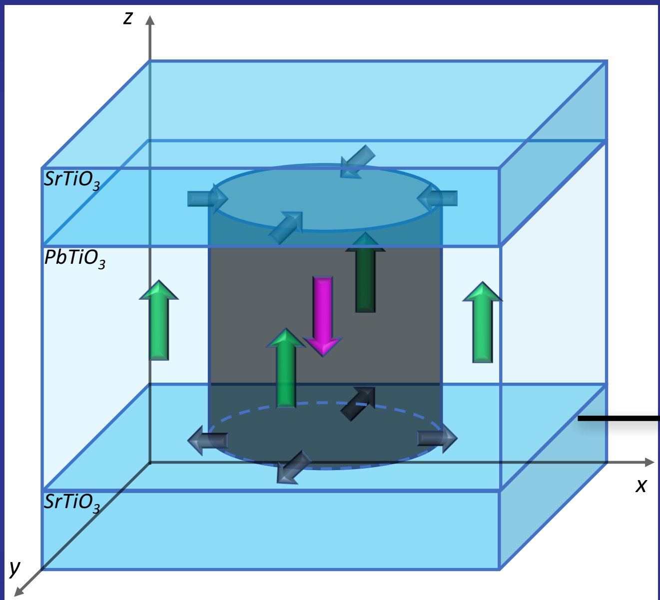

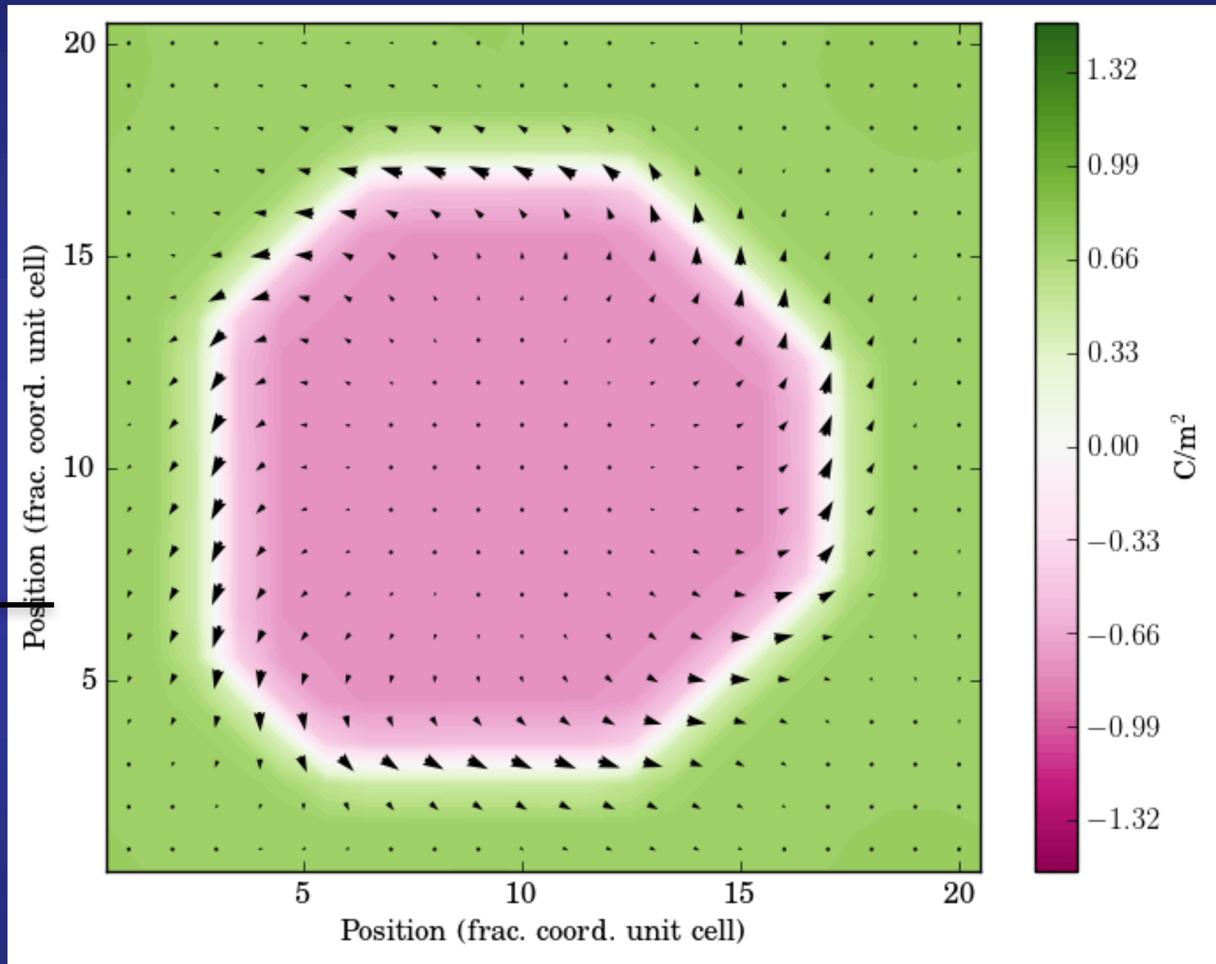

In-plane lattice constant $a = 3.901$ Å

Bubble structures at $PbTiO_3/SrTiO_3$ superlattices

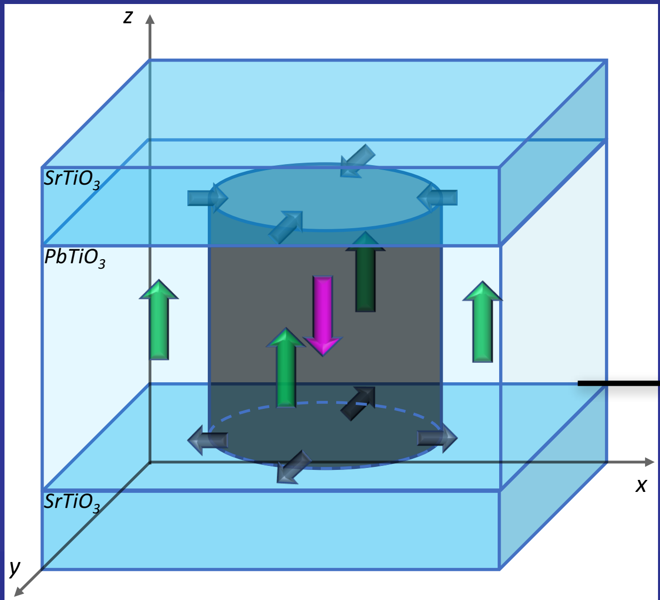

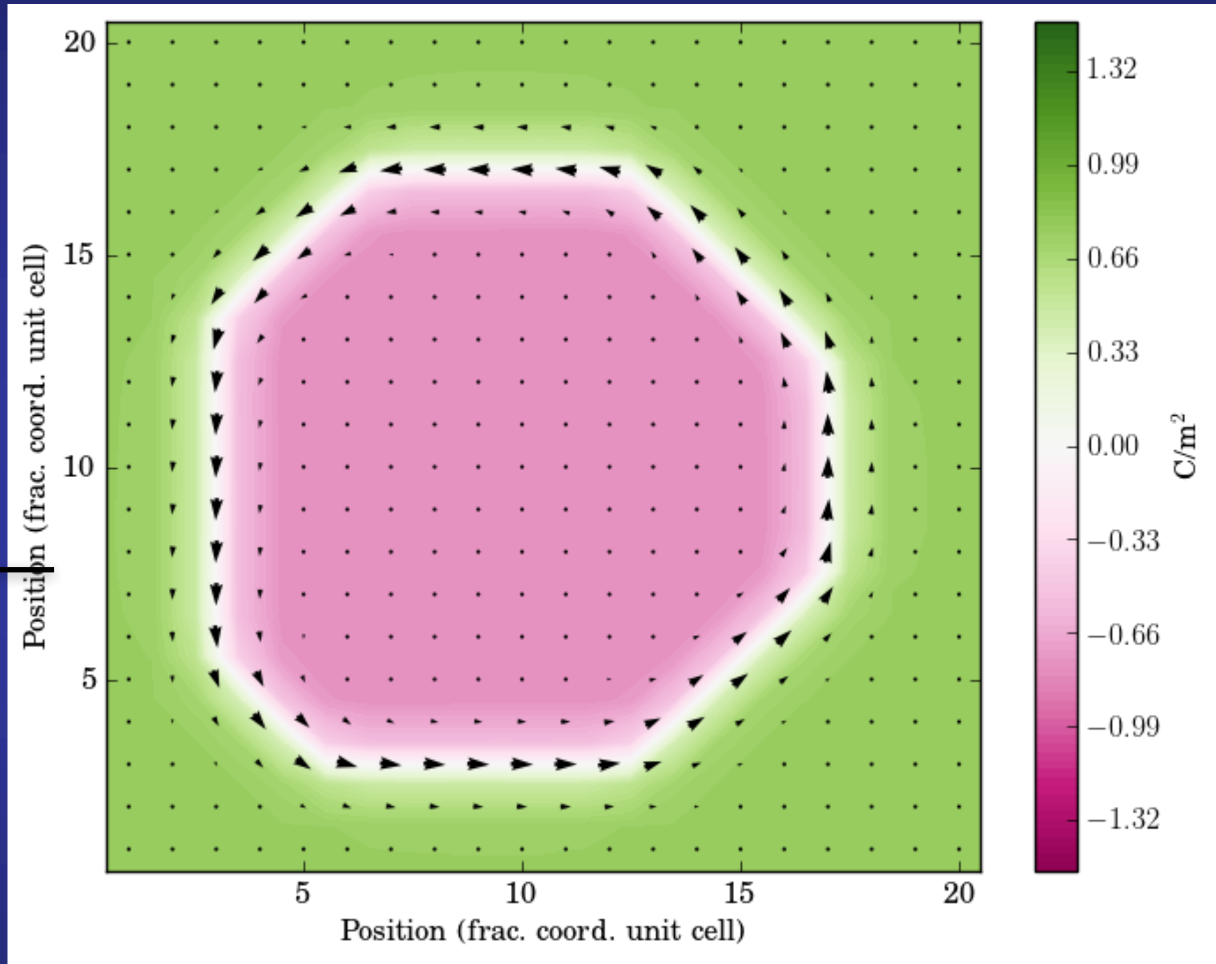

In-plane lattice constant $a = 3.901$ Å

Bubble structures at $PbTiO_3/SrTiO_3$ superlattices

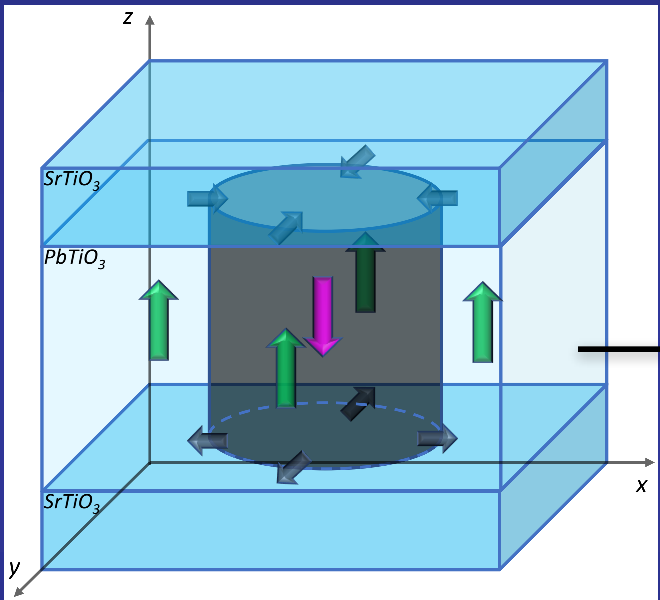

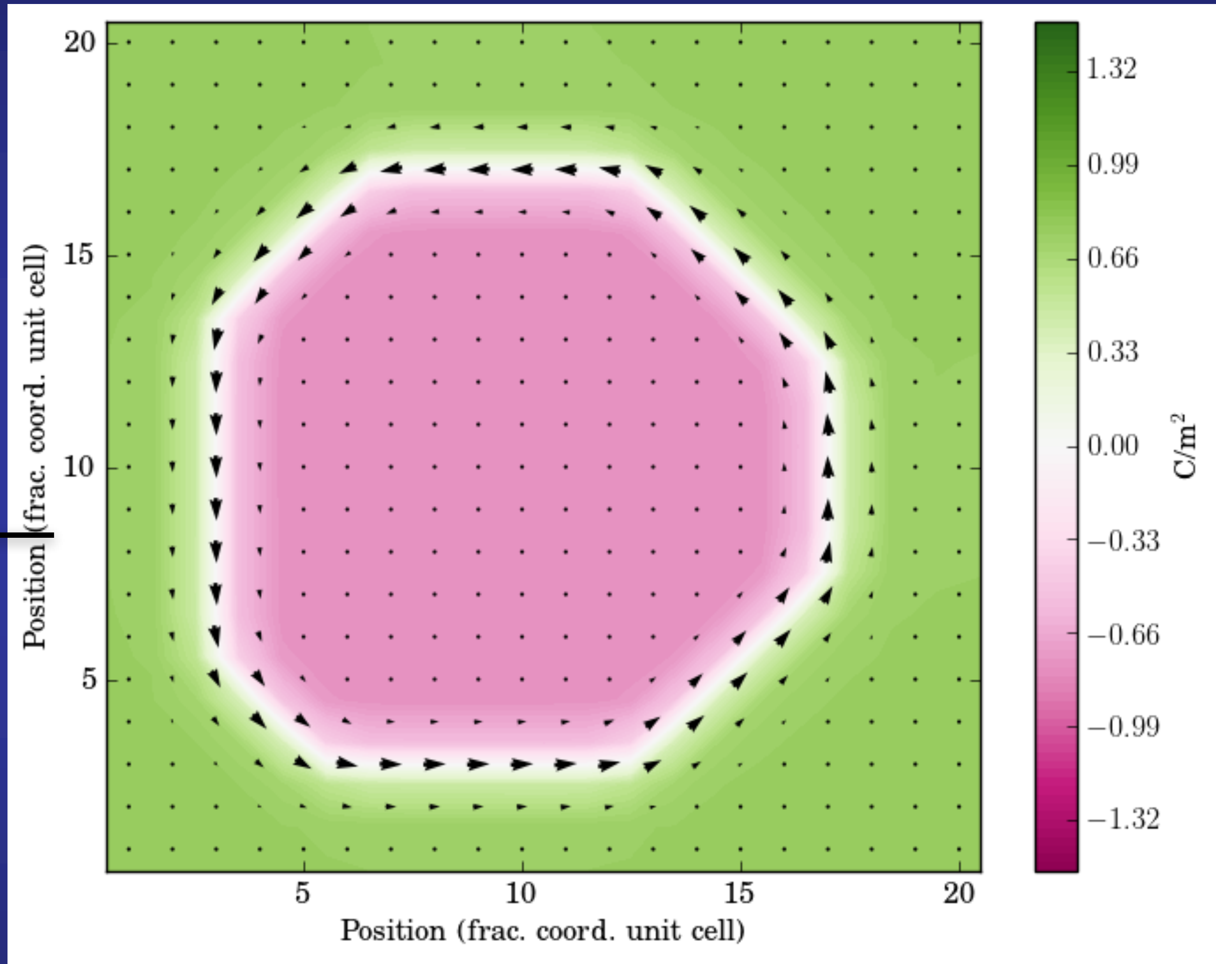

In-plane lattice constant $a = 3.901$ Å

Bubble structures at $PbTiO_3/SrTiO_3$ superlattices

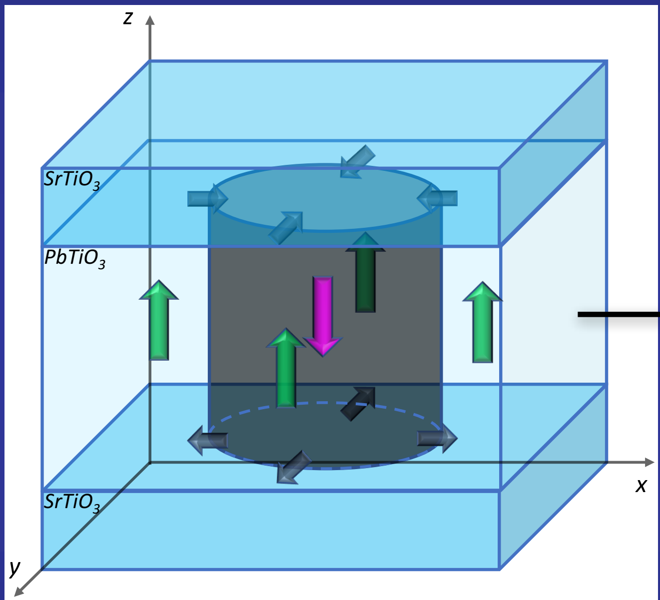

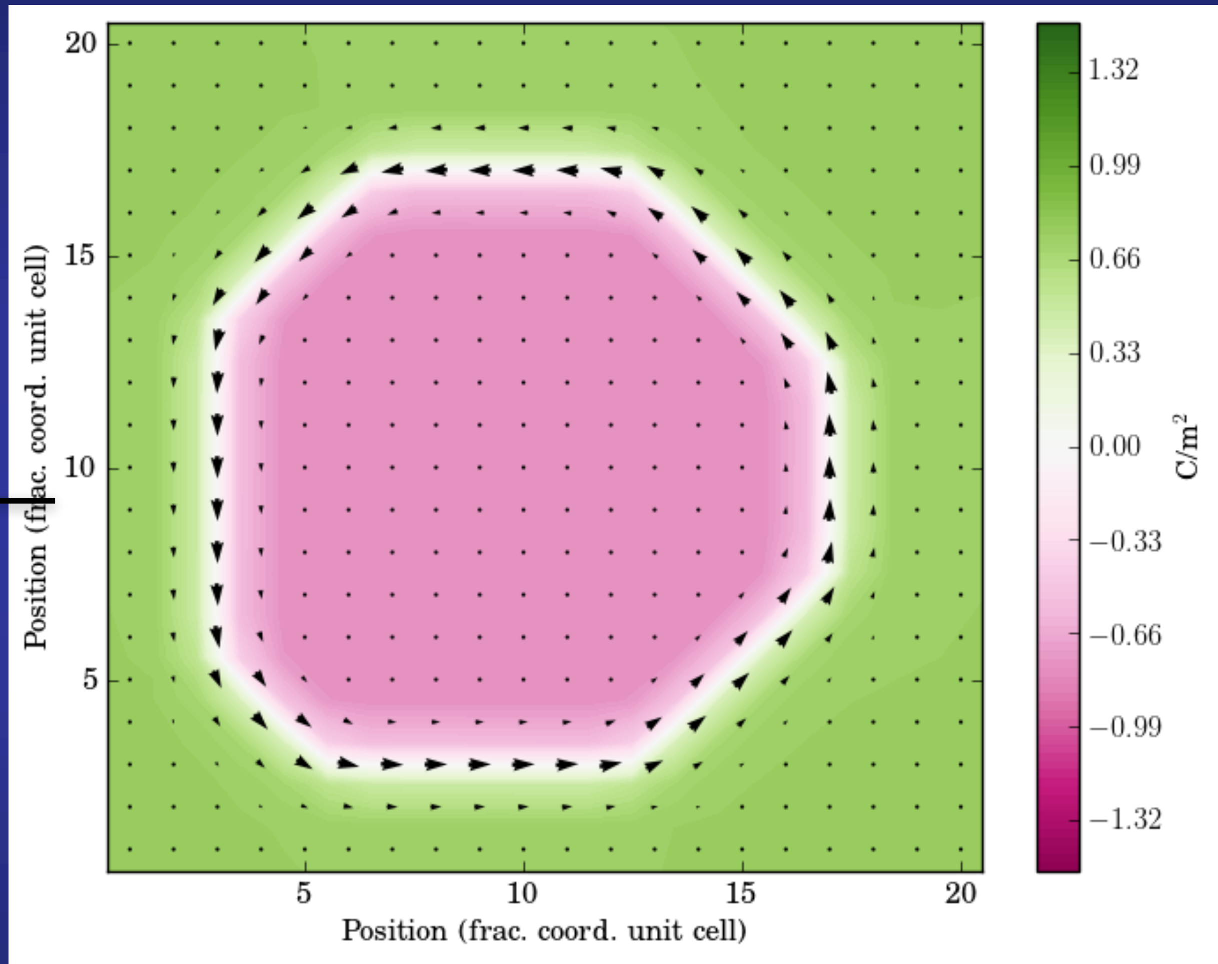

In-plane lattice constant $a = 3.901$ Å

Bubble structures at $PbTiO_3/SrTiO_3$ superlattices

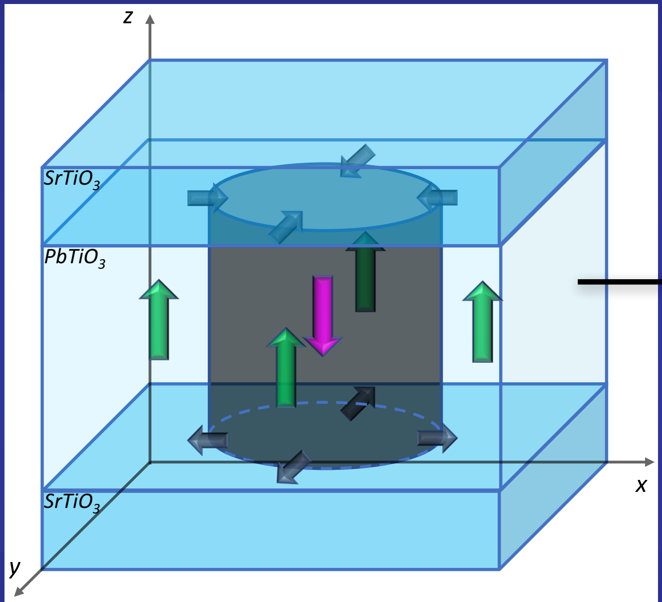

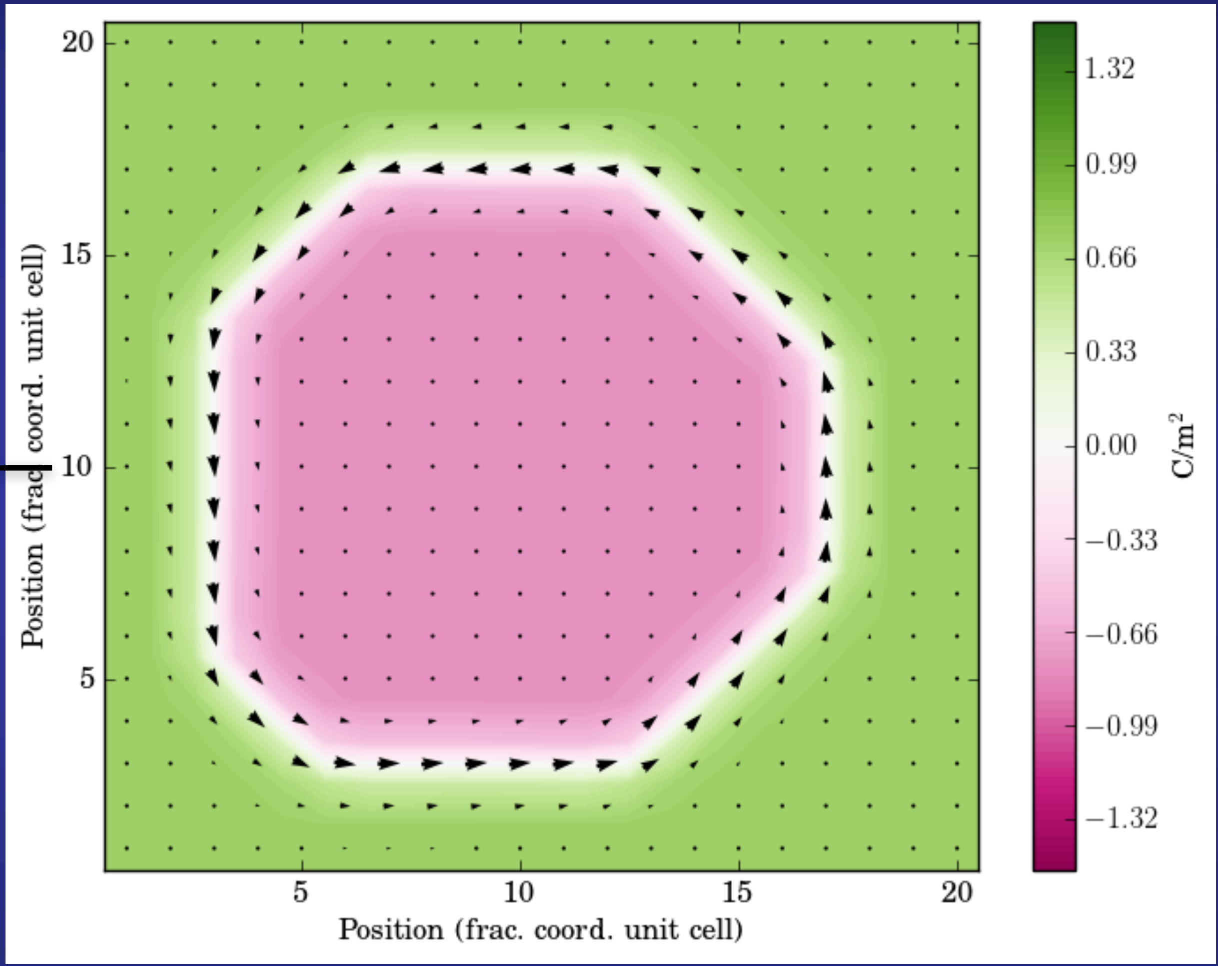

In-plane lattice constant $a = 3.901$ Å

Bubble structures at $PbTiO_3/SrTiO_3$ superlattices

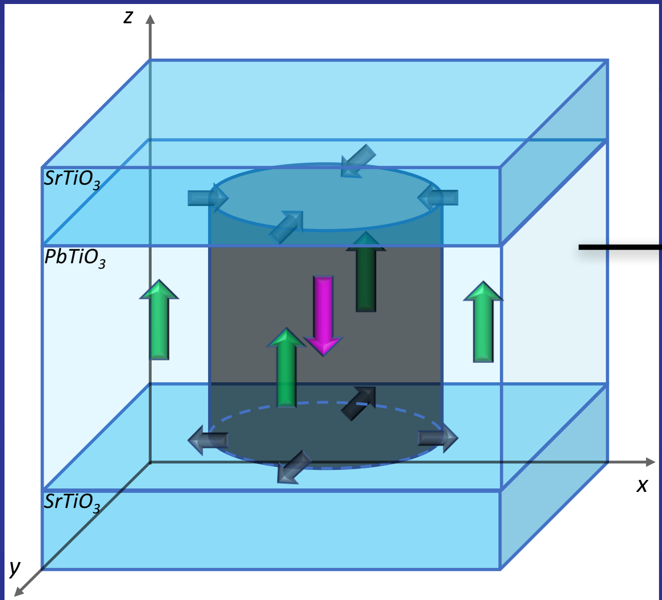

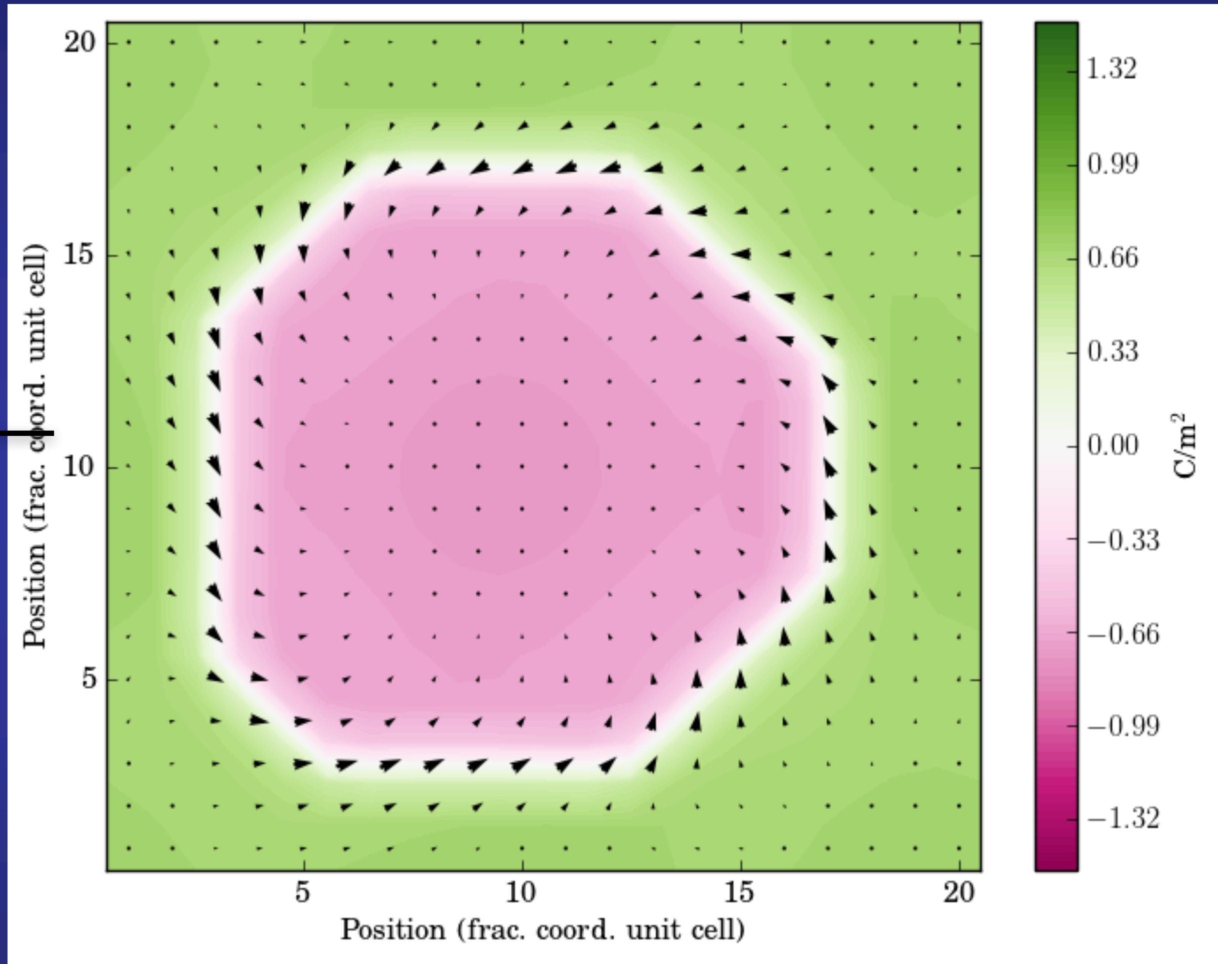

In-plane lattice constant $a = 3.901$ Å

Bubble structures at $PbTiO_3/SrTiO_3$ superlattices

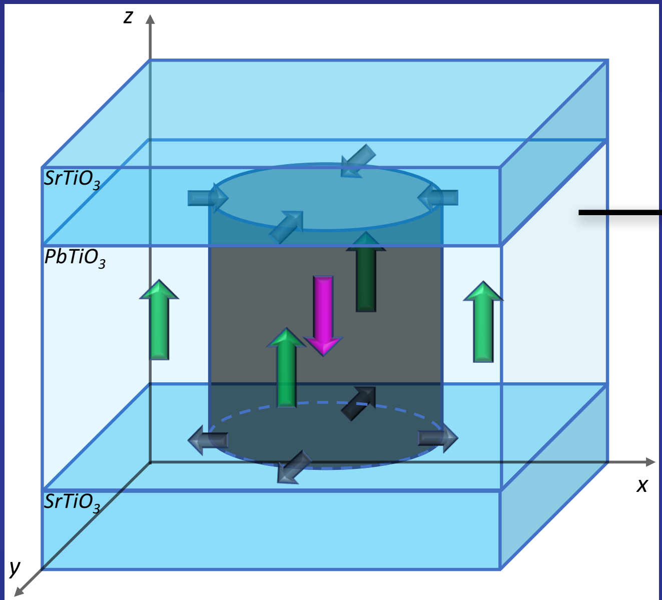

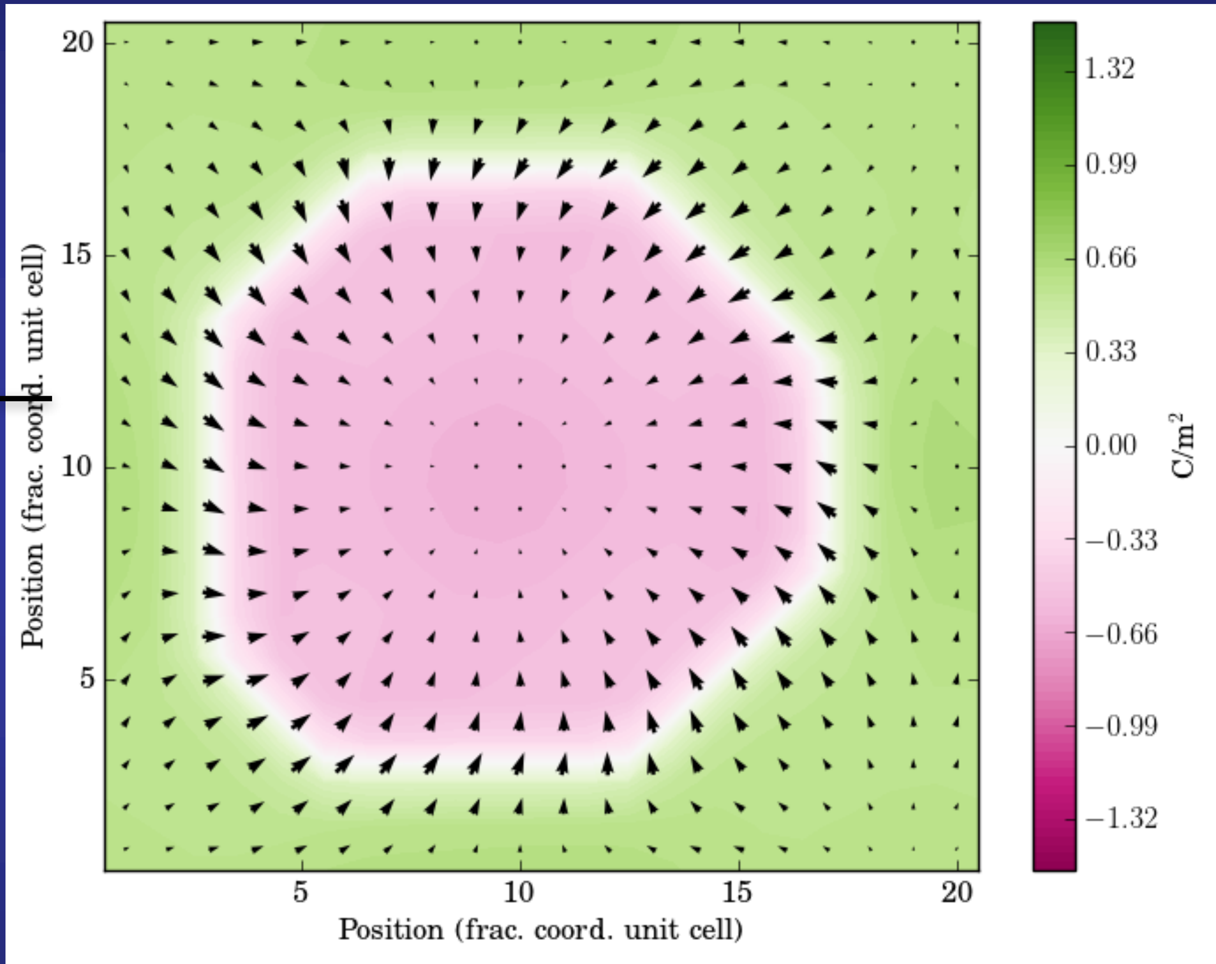

In-plane lattice constant $a = 3.901$ Å

Bubble structures at $PbTiO_3/SrTiO_3$ superlattices

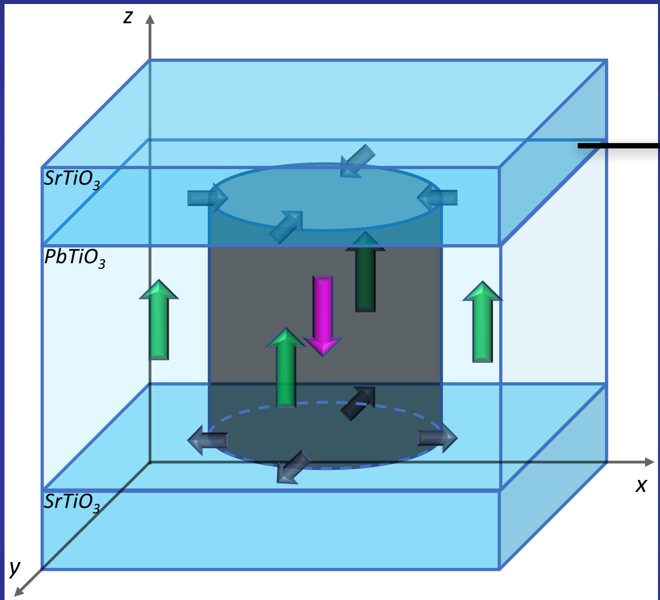

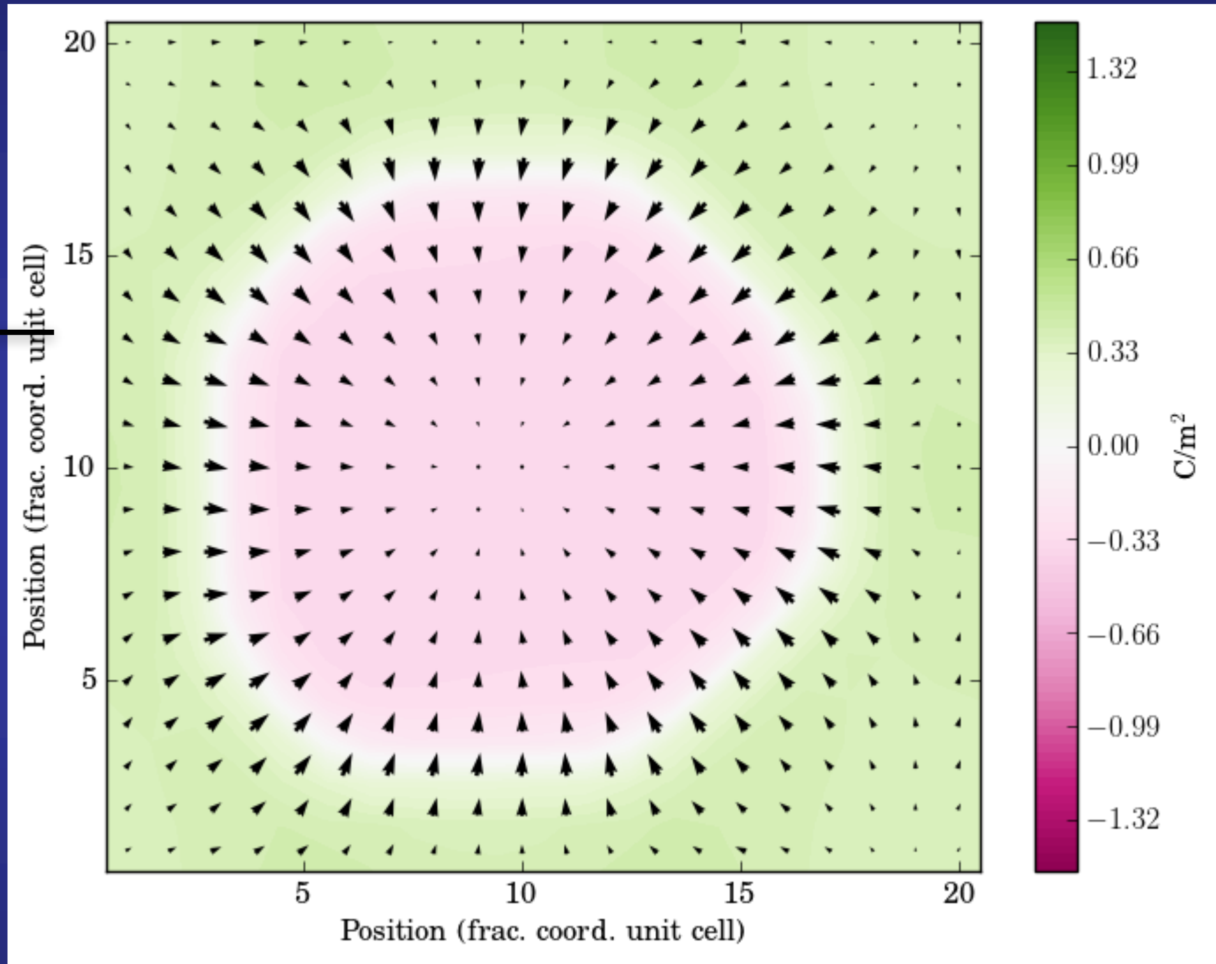

Top interface

In-plane lattice constant $a = 3.901$ Å

Bubble structures at $PbTiO_3/SrTiO_3$ superlattices

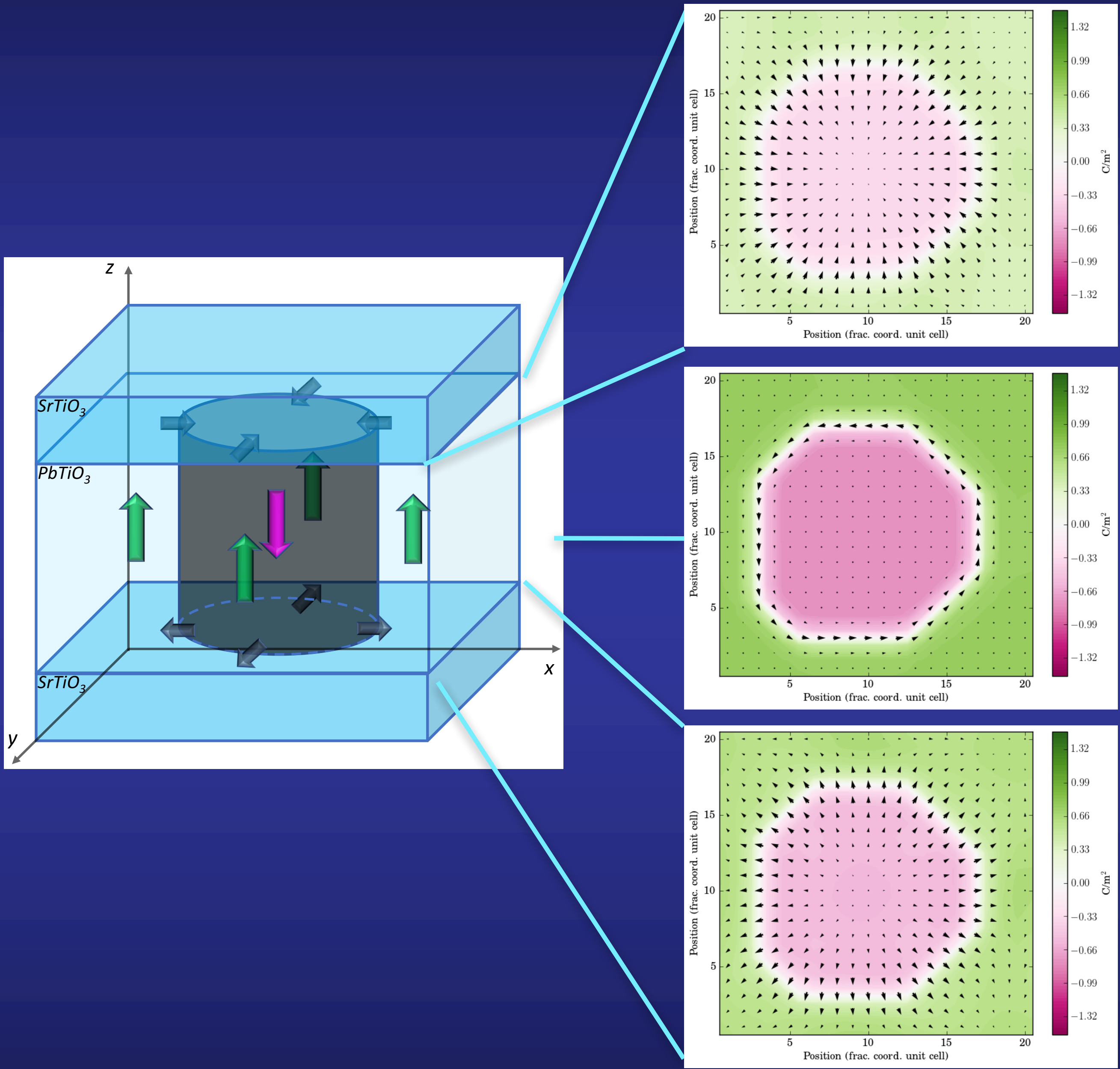

Hedgehog skyrmions both at the top and bottom interfaces

At the central plane, we find skymion like local pattern of dipoles

In-plane lattice constant $a = 3.901$ Å

Bubble structures at $PbTiO_3/SrTiO_3$ superlattices

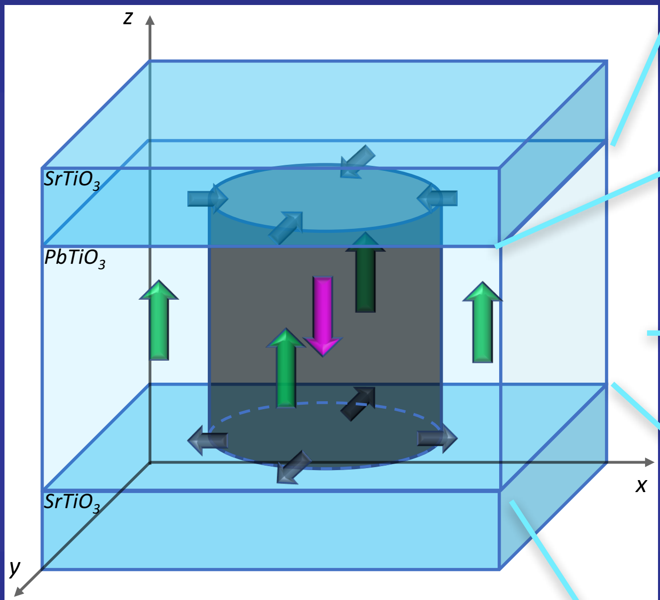

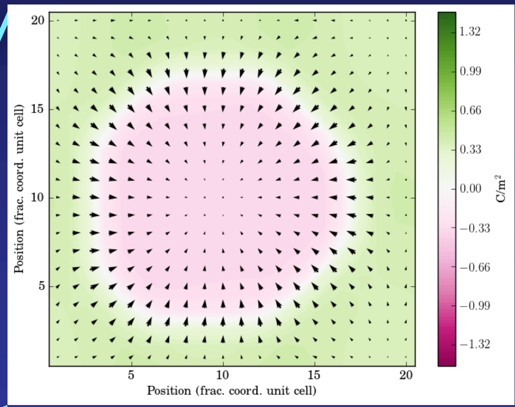

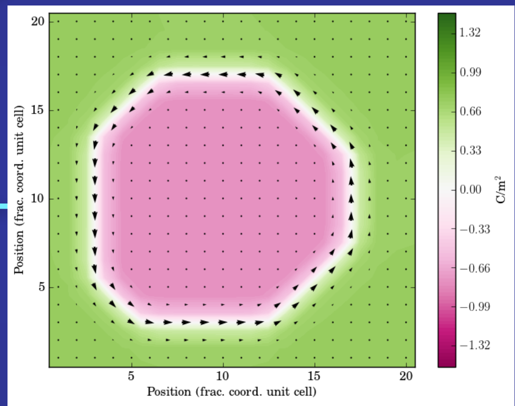

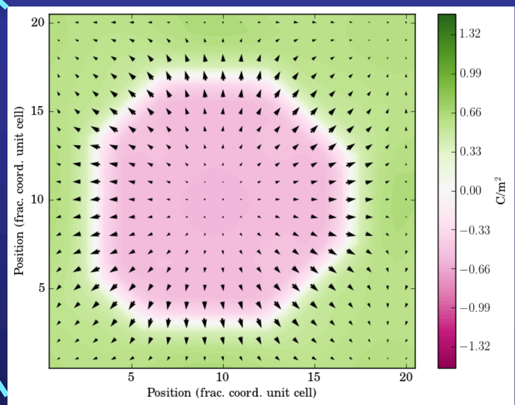

All of them are topologically equivalent

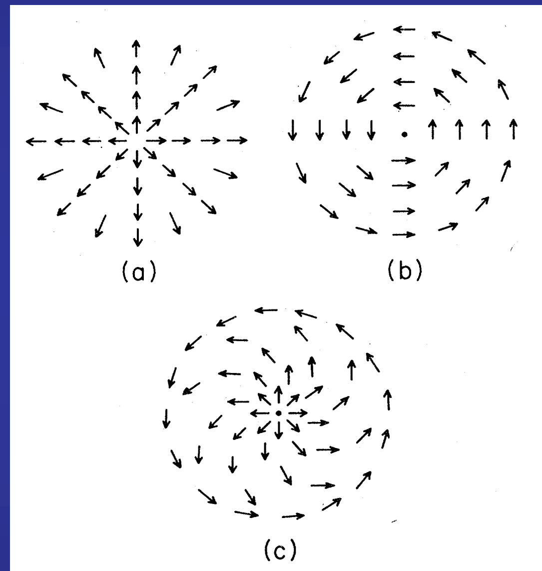

N. D. Mermin
Rev. Mod. Phys. 51, 591 (1979)

In-plane lattice constant $a = 3.901$ Å

Similar structures found in other Condensed Matter Problems

PRL **118,** 016401 (2017) PHYSICAL REVIEW LETTERS week ending 6 JANUARY 2017

Pseudospin Vortex Ring with a Nodal Line in Three Dimensions

Lih-King Lim[1,2] and Roderich Moessner[2]

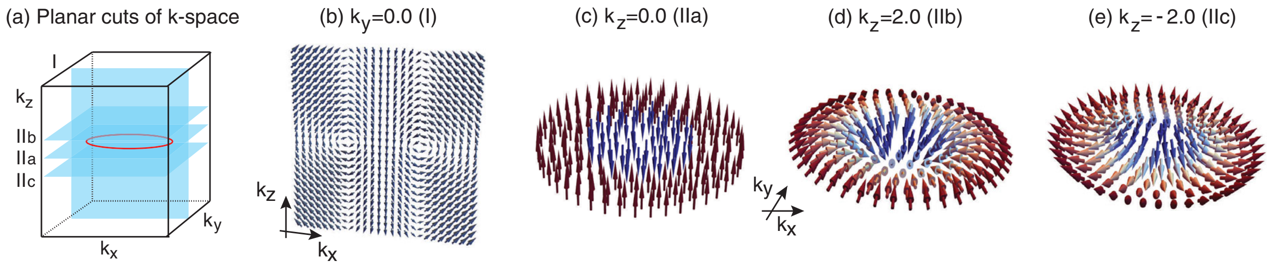

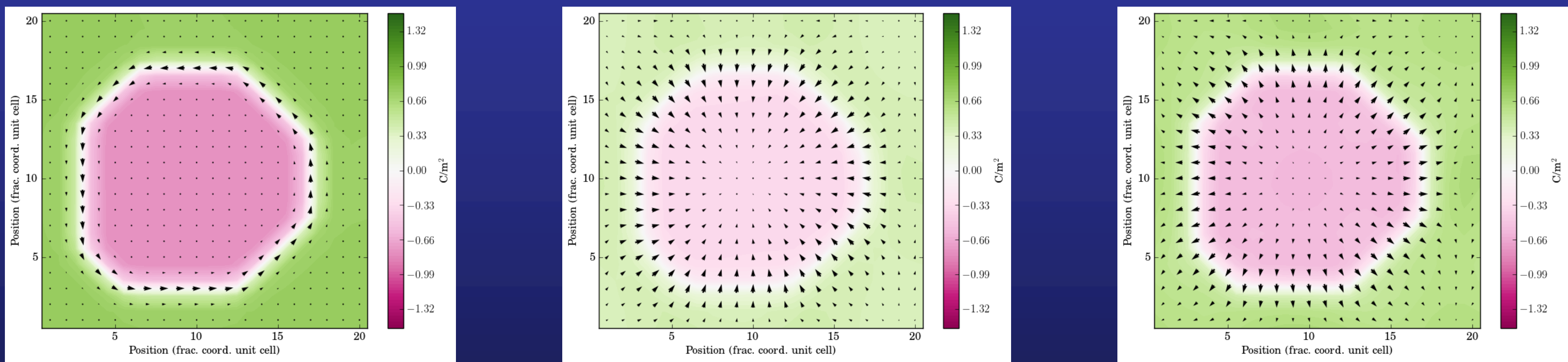

In-plane lattice constant $a = 3.901$ Å

Bubble structures at $PbTiO_3/SrTiO_3$ superlattices

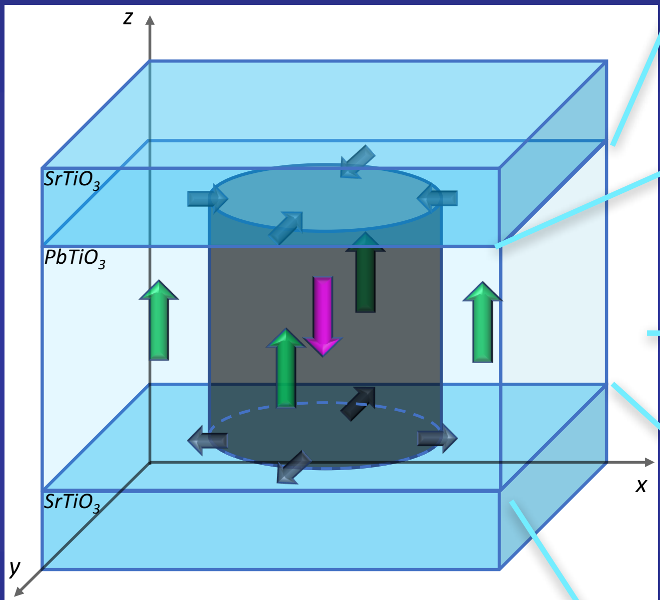

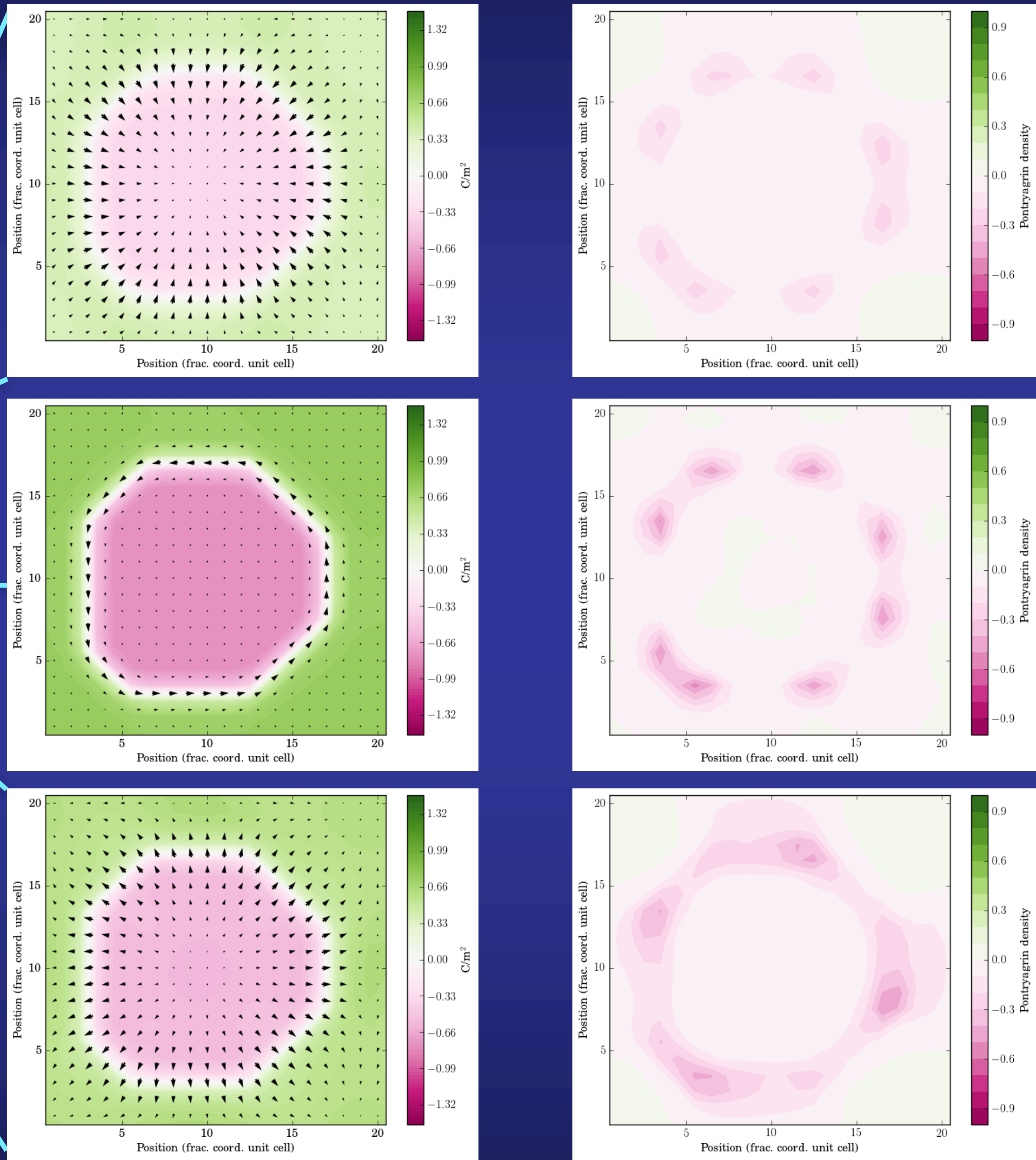

Skyrmion number

$$N_{\rm sk} = \frac{1}{4\pi}\int\int d^2\vec{r}\ \vec{p}\cdot\left(\frac{\partial\vec{p}}{\partial x}\times\frac{\partial\vec{p}}{\partial z}\right)$$

Pontyagrin density

$$N_{\rm sk} = 1$$

Take home message

Ferroelectric bubble domains can be considered a precursor to electrical skyrmions

All layers along [001] plane do have a well defined skyrmion number of +1

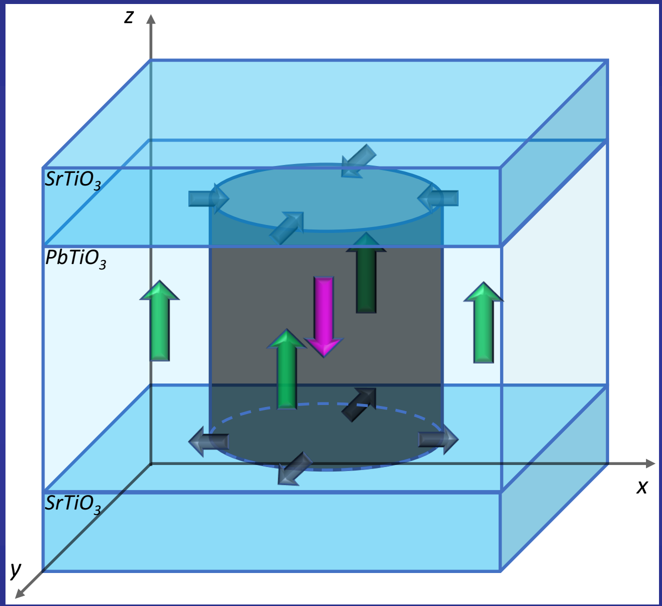

Top and bottom interfaces show hedgehog like structures
Central planes show planar skyrmions

From the “Workshop description”

The main goal of the workshop is to refine attendees’ picture of the state of the art regarding ferroelectric domain walls properties and applications, focusing on what are the open problems, and what are the opportunities for development of approaches to solve them

SCALE UP
An implementation of SPDFT

SCALE-UP:
Second-principles Computational Approach for Lattice and Electrons
https://www.secondprinciples.unican.es

IOP PUBLISHING JOURNAL OF PHYSICS: CONDENSED MATTER
J. Phys.: Condens. Matter **25** (2013) 305401 (25pp) doi:10.1088/0953-8984/25/30/305401

First-principles model potentials for lattice-dynamical studies: general methodology and example of application to ferroic perovskite oxides

Jacek C Wojdeł[1], Patrick Hermet[2,3], Mathias P Ljungberg[1], Philippe Ghosez[2] and Jorge Íñiguez[1]

PHYSICAL REVIEW B **93**, 195137 (2016)

Second-principles method for materials simulations including electron and lattice degrees of freedom

Pablo García-Fernández,[1] Jacek C. Wojdeł,[2] Jorge Íñiguez,[2,3] and Javier Junquera[1]

Vortices.. A Fundamental Aspect of Nature

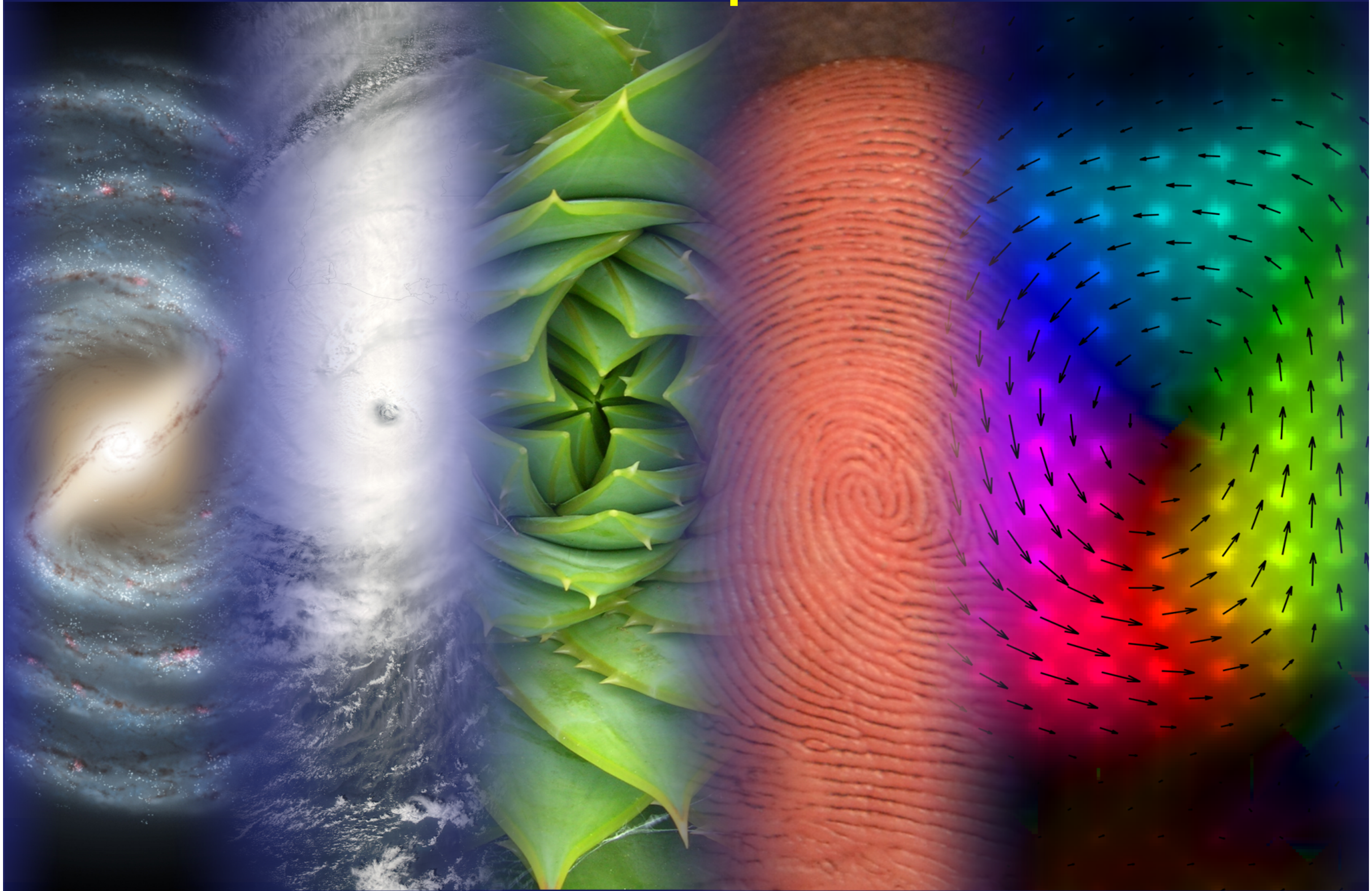

Supplementary information

Vortex structure stable up to 85 K

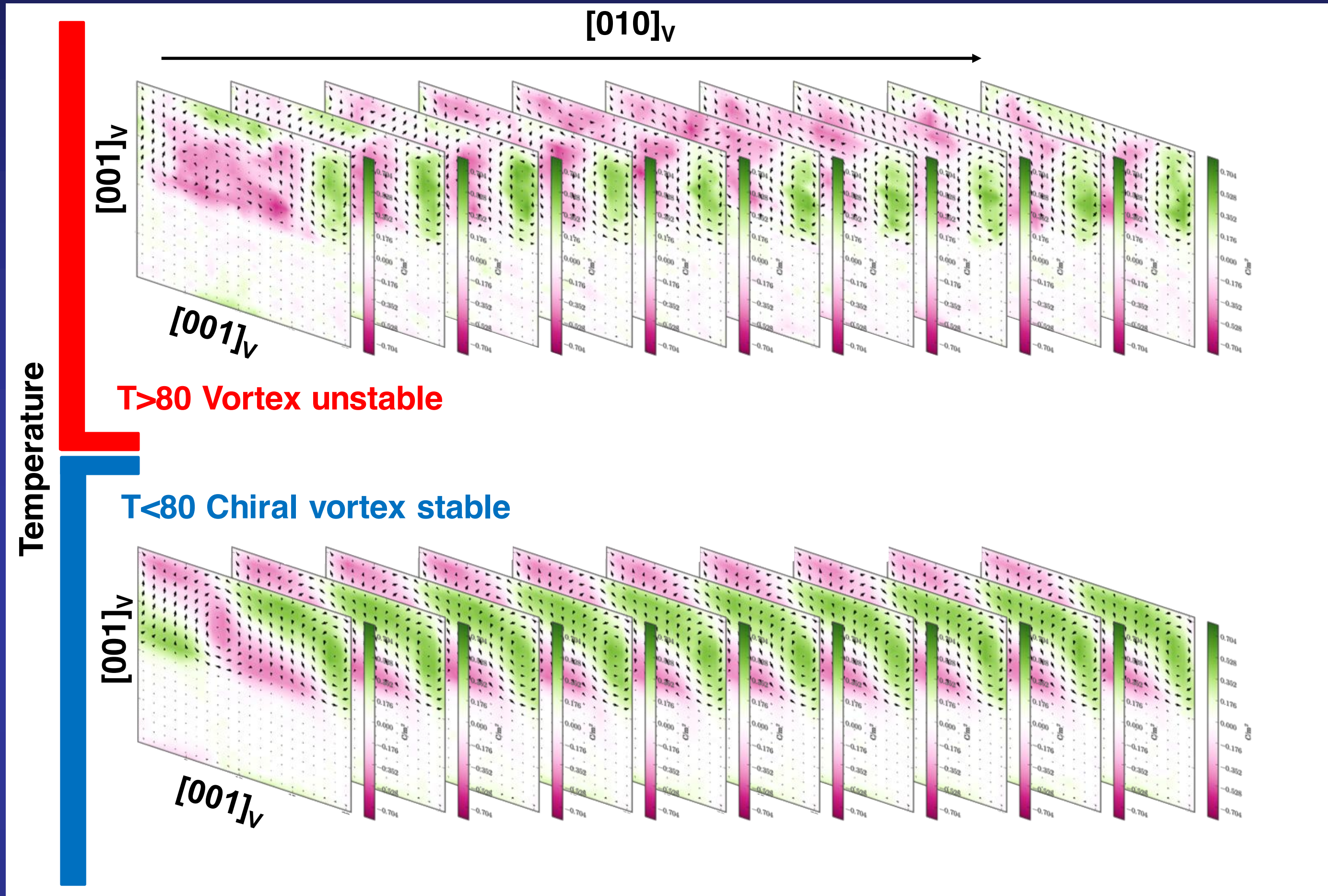

At high temperature, thermal fluctuations allow local flipping of some dipoles
The domain wall changes their shape from one plane to the next

The actual transition temperature might be significantly higher than this theoretical value, as an accurate determination of the transition point is known to be especially challenging to second-principles methods

P. Shafer, P. García-Fernández *et al*. submitted

Potential detection of the axial component in planar view HR-STEM or dark field transmission electron microscopy

Variations in the strength and orientation of the axial polarization as a function of depth act to dilute the signal below detection limits

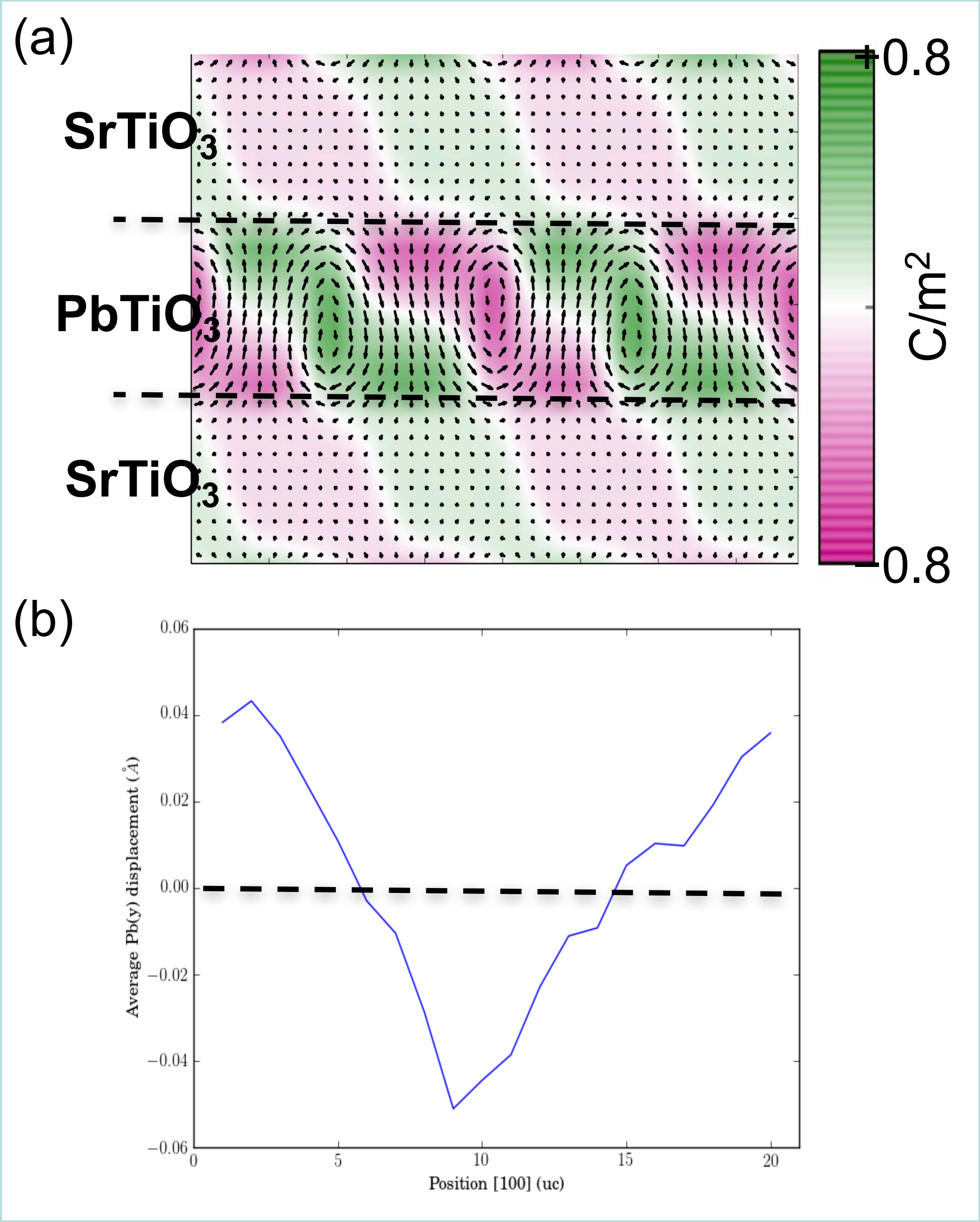

Nanoscale vortex modulation in $PbTiO_3/SrTiO_3$ superlattices and particularly depth-dependence challenges nearly every advanced characterization technique in detecting the alternating axial polarization

Anisotropic tensor susceptibility (ATS) scattering

Near resonant transitions, the x-rays are sensitive to the anisotropic electronic structure of the distorted TiO_6 octahedra

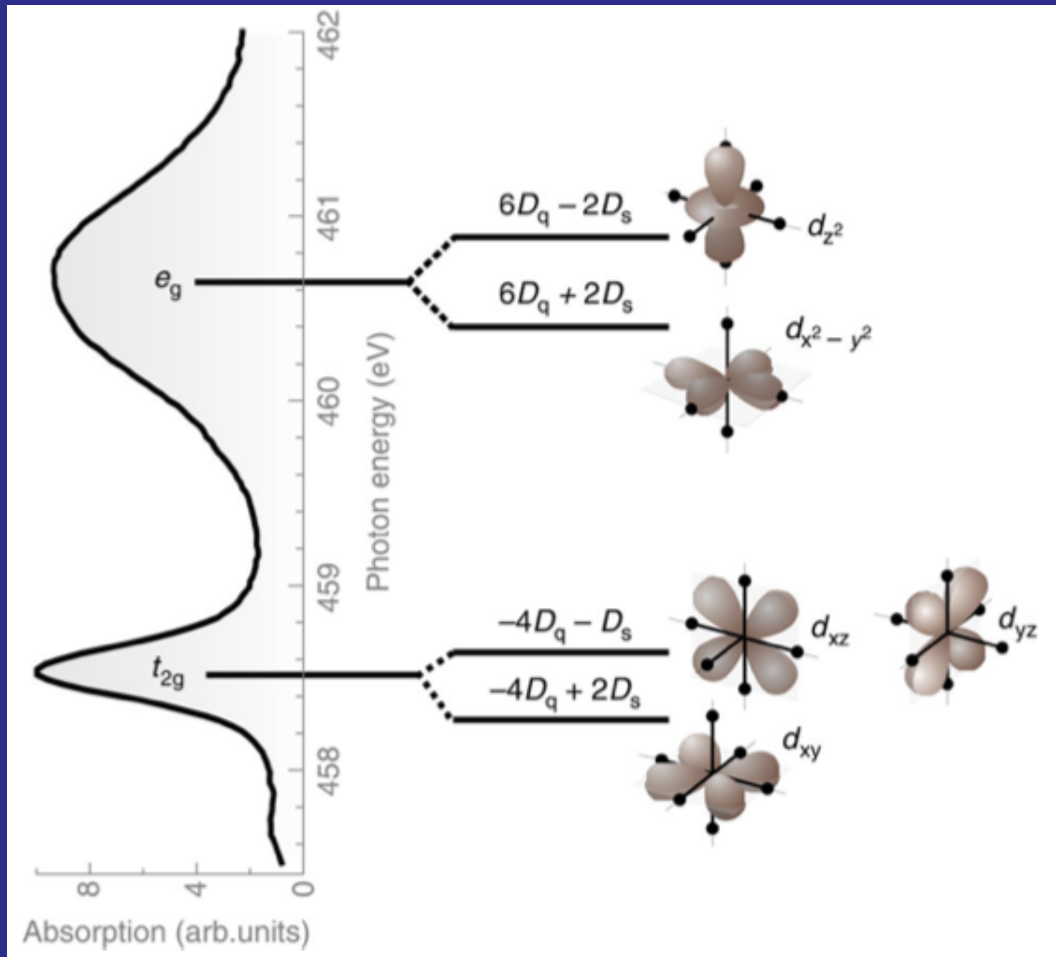

The anisotropic dielectric response of each TiO_6 unit to resonant soft x-rays provides a contribution to the x-ray scattering amplitude that varies with polarization orientation

Anisotropic tensor susceptibility (ATS) scattering

Near resonant transitions, the x-rays are sensitive to the anisotropic electronic structure of the distorted TiO_6 octahedra

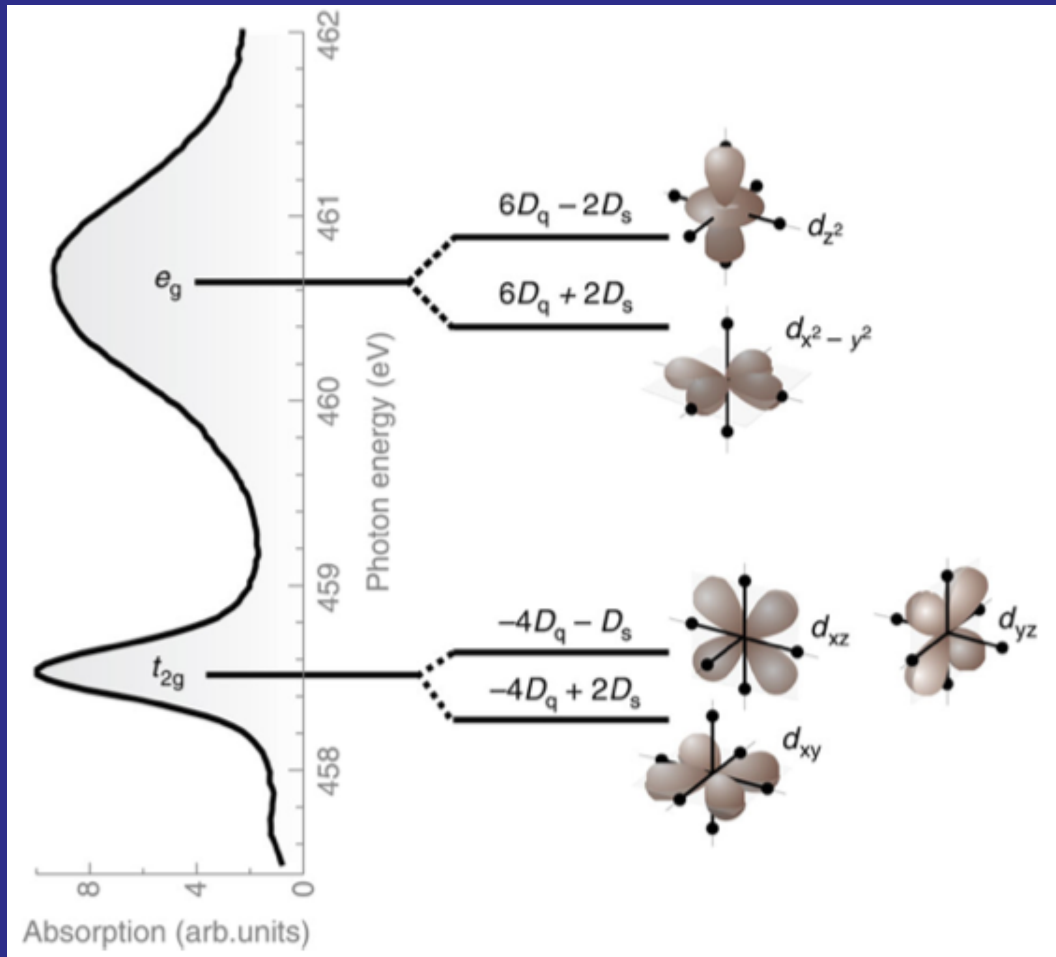

The chiral helical structure imparts a chiral structure factor onto the scattering amplitude

The chiral electric polarization texture of the vortex arrays generates a coherent superposition of chiral structure factors

Evolution of the interlayer coupling with thickness in $(PbTiO_3)_n/(SrTiO_3)_n$

For larger $SrTiO_3$ thickness, electrostatic coupling decreases

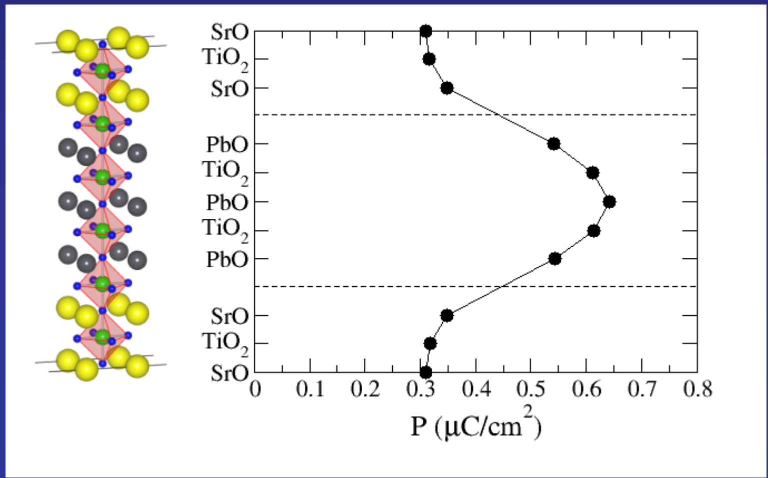

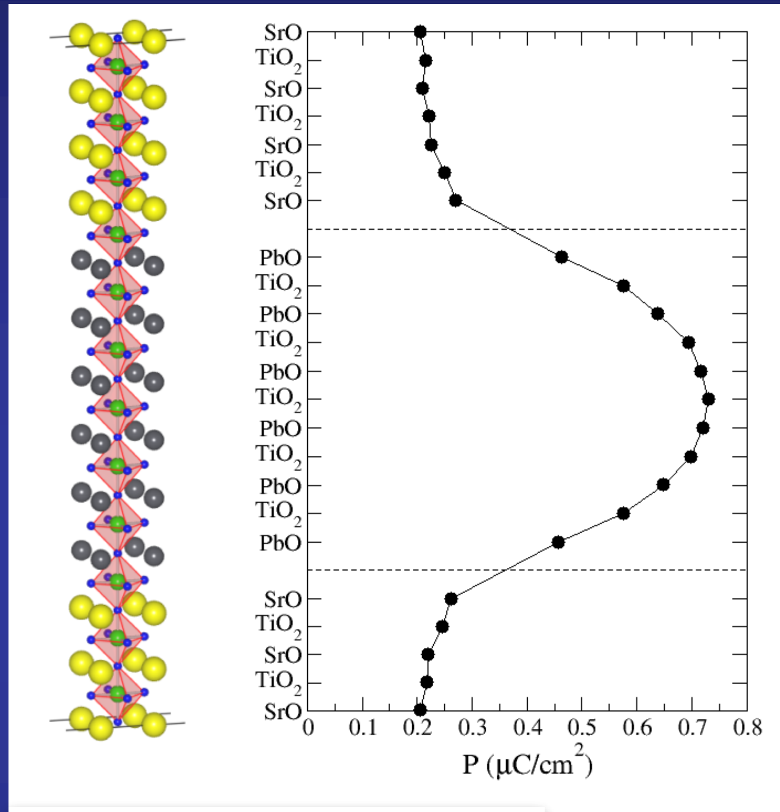

$SrTiO_3$ polarization reduces in ~30% from (3/3) to (6/6)

Progressive electrostatic decoupling

(P. Zubko et al. Nano Letters 12, 2846 (2012)

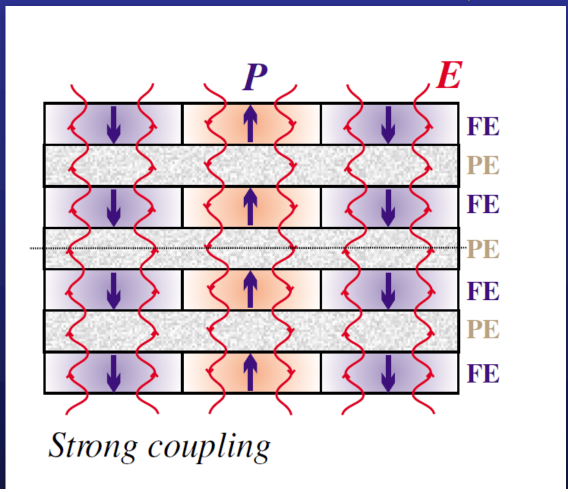

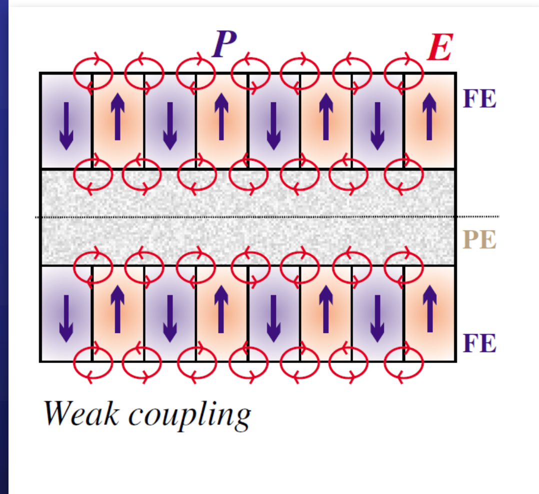

$PbTiO_3/SrTiO_3$ 6/6 superlattices ($DyScO_3$ substrate)

Parallel

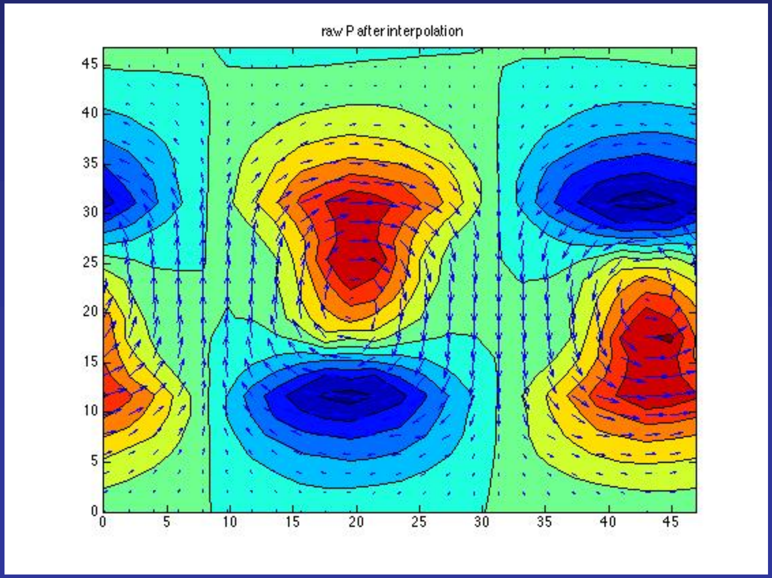

Antiparallel

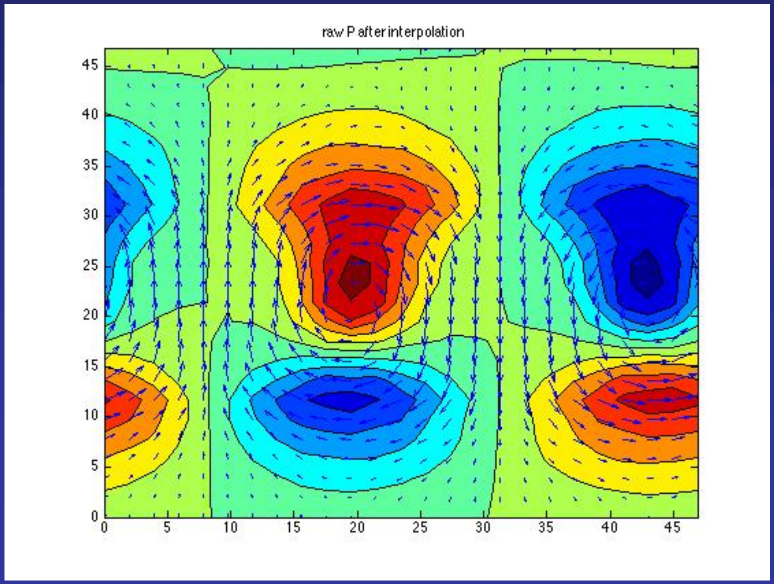

Offset

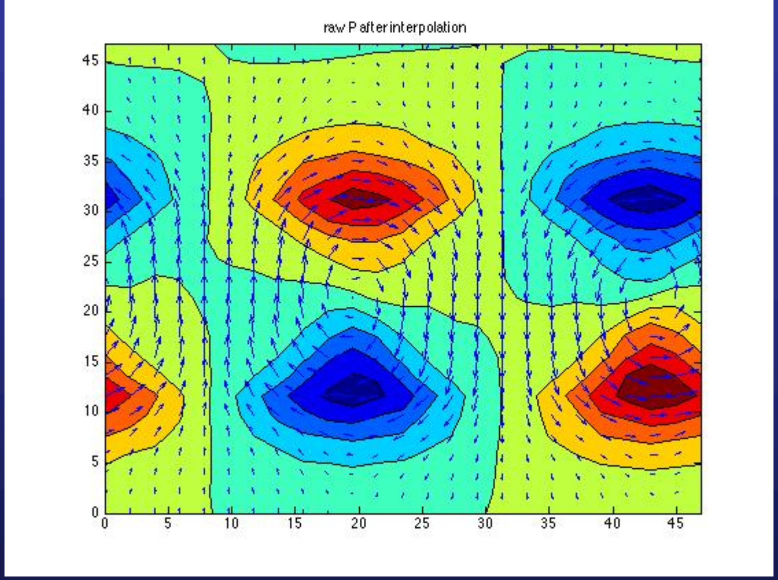

"No-py"

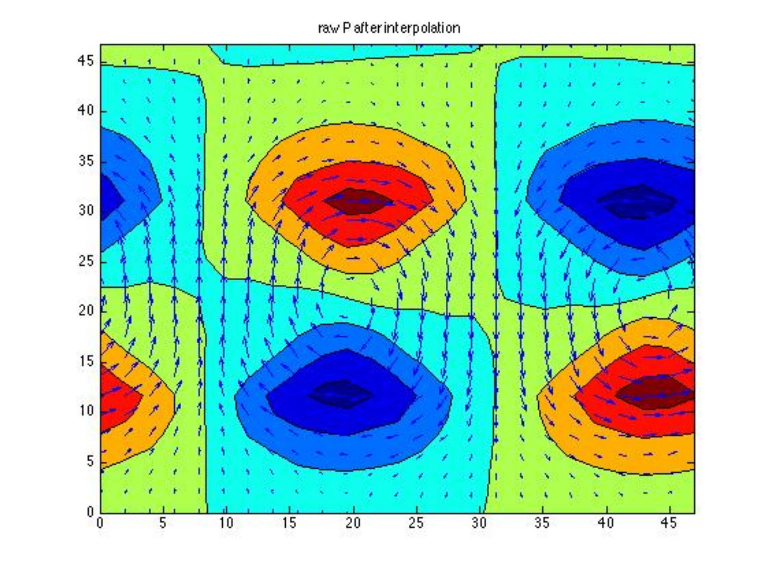

Different screening mechanisms of the depolarizing field

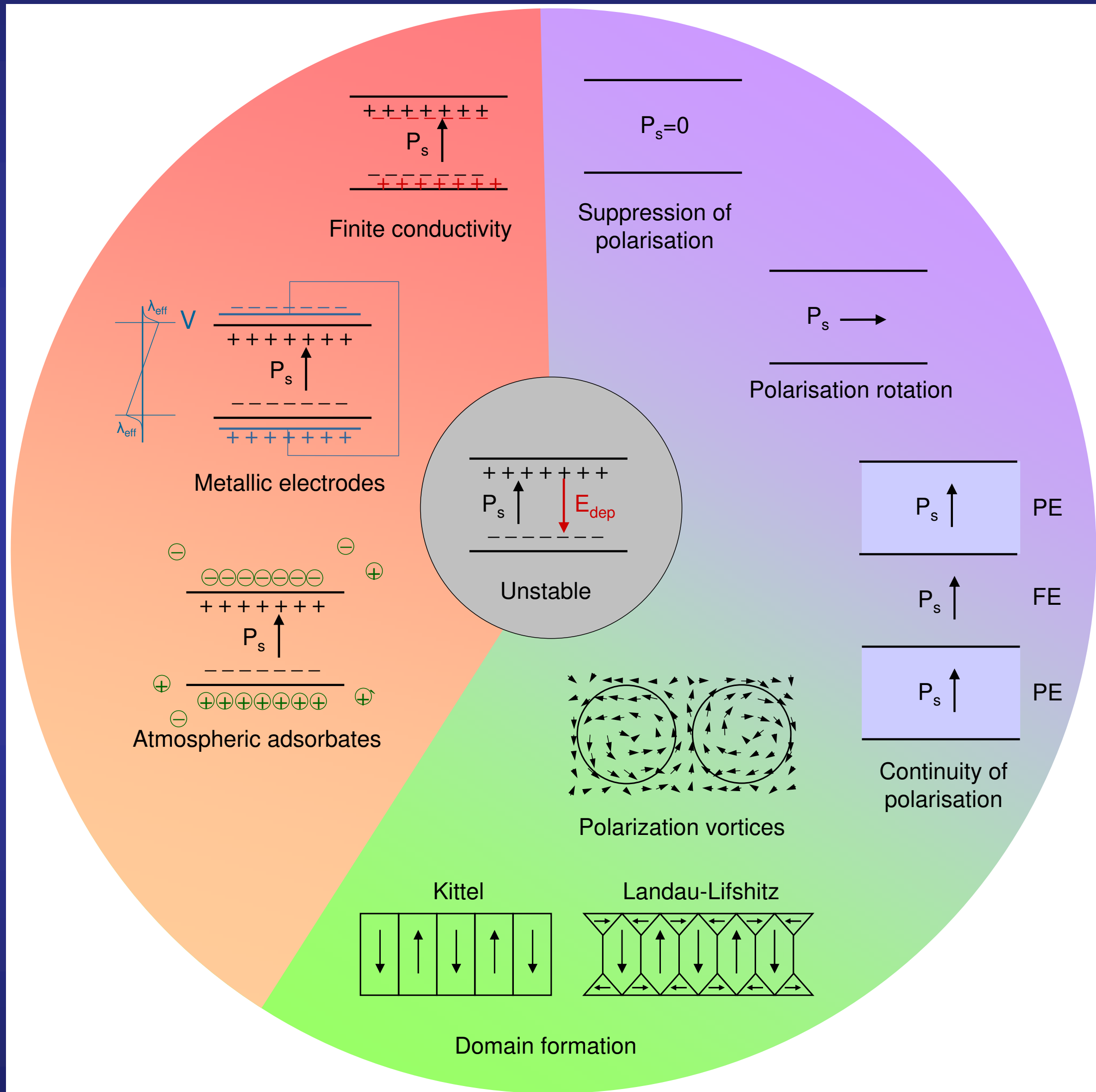

C. Lichtensteiger, P. Zubko, M. Stengel, P. Aguado-Puente, J.-M. Triscone, Ph. Ghosez and J. Junquera. Chapter 12 in Oxide Ultrathin Films, Science and Technology, Wiley (2011).

Definition of chirality and optical activity

A system is said to be chiral when it cannot be transformed into its mirror image with rotations and translations alone

In 2D:

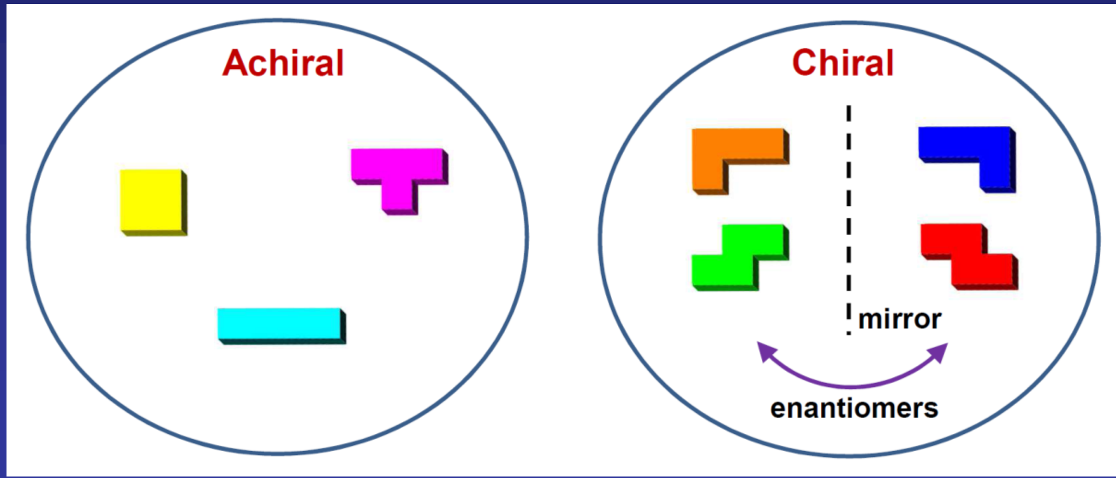

χειρ = hand

In 3D:

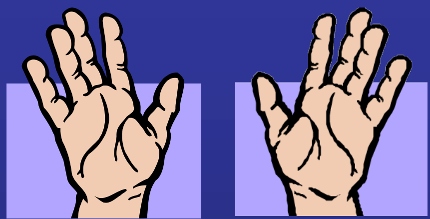

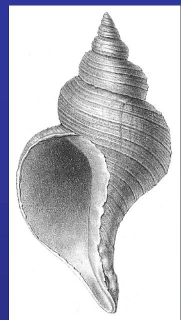

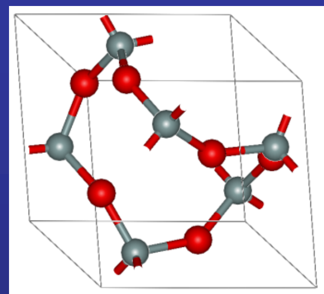

α-quartz

A handedness can be defined using the right-hand rule.

Compounds with chiral symmetry are optically active: polarization direction of linearly-polarized light rotates when light travels through the material.

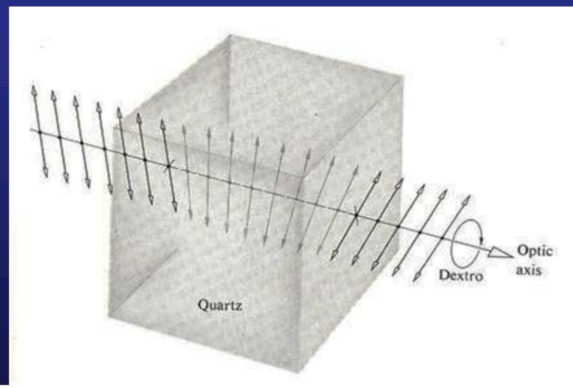

Chirality of the observed structures

Case without out-of-plane component of the poralization

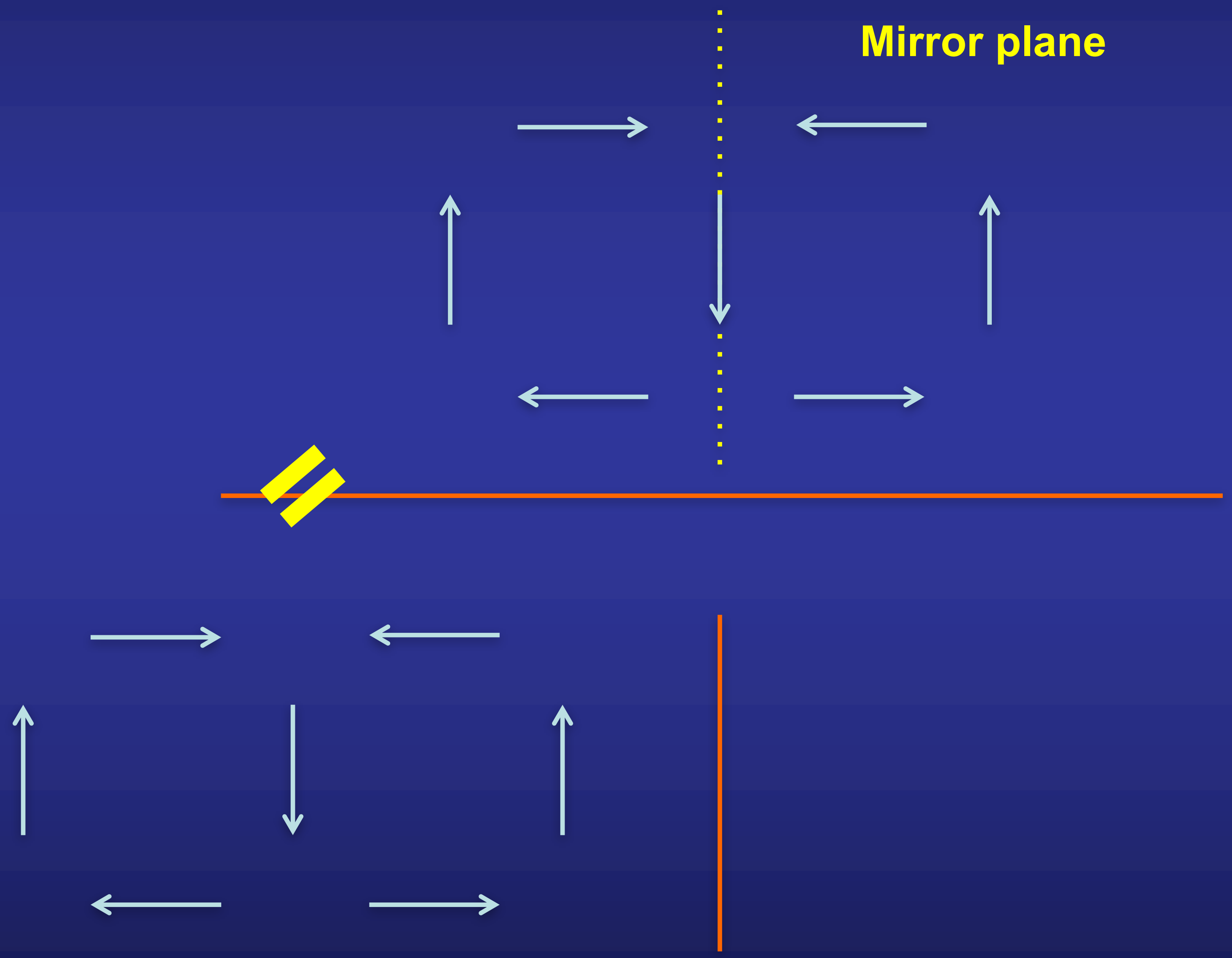

Chiral dipole arrangements could open the door to switchable optical activity

If toroidal moment can coexist with a polarization parallel to the toroidal axis in ferroelectric nanostructures, switchable chirality and optical activity could be accomplished

Electro-optic device

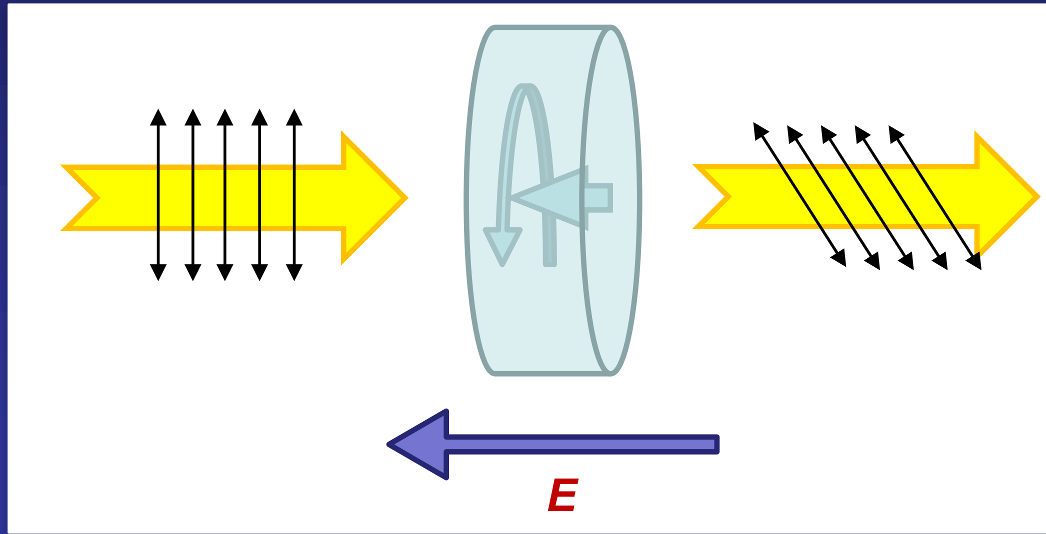

Four-fold stability → four “memory” states.

Positive/negative polarization
X
clockwise/anticlockwise vortex

This kind of dipole arrangements have been experimentally realized!

Enhanced conductivity in vortices in $BiFeO_3$

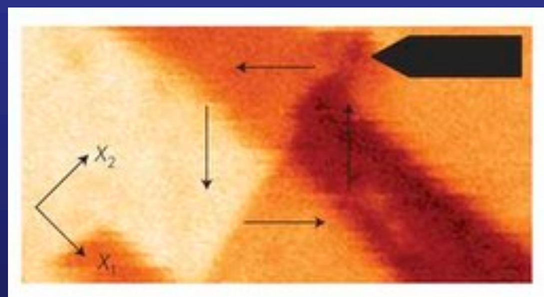

Balke, Nature Physics (2012)

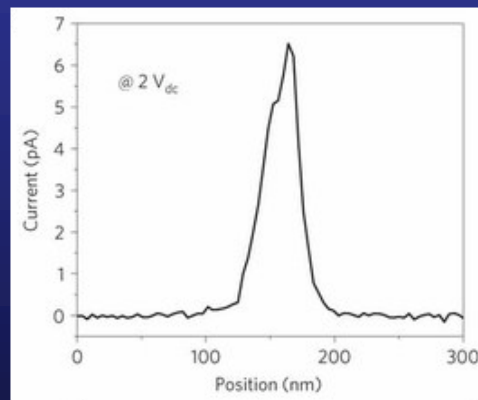

Evolution of the interlayer coupling with thickness in $(PbTiO_3)_n/(SrTiO_3)_n$

For larger $SrTiO_3$ thickness, electrostatic coupling decreases

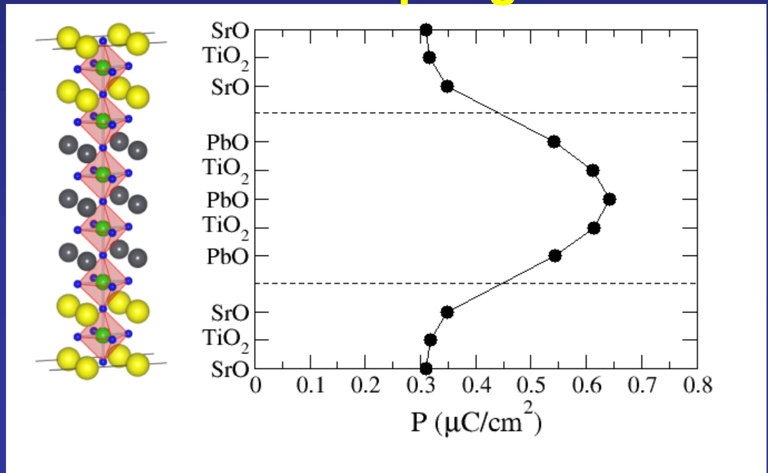

$SrTiO_3$ polarization reduces in ~30% from (3/3) to (6/6)

Progressive electrostatic decoupling

P. Zubko et al. Nano Letters 12, 2846 (2012)

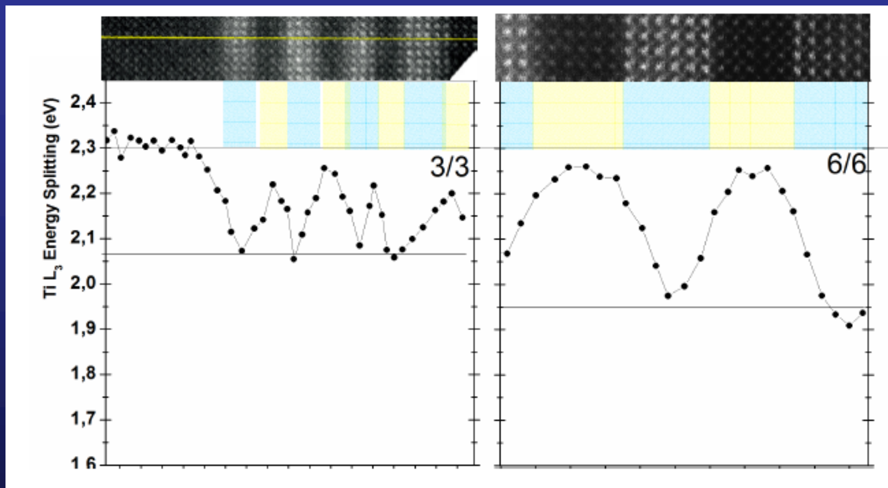

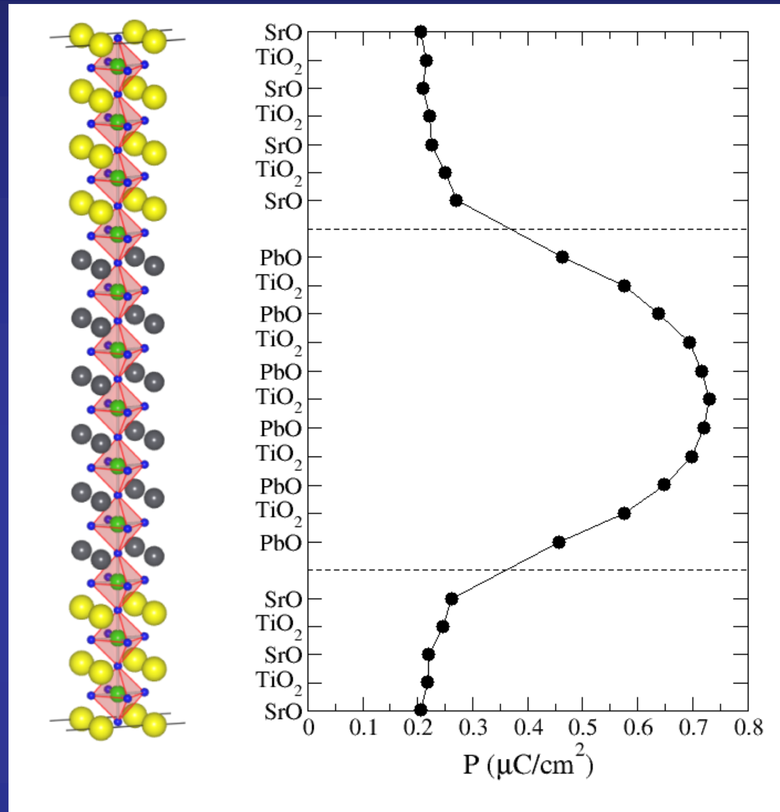

PTO polarization decreases upon upproaching the interface, in agreement with EELS measurements.

Mirrored diffraction vectors detect opposite rotational patterns in chiral textures

Helical arrangement of the electric polarization and associated anisotropic octahedral distortion

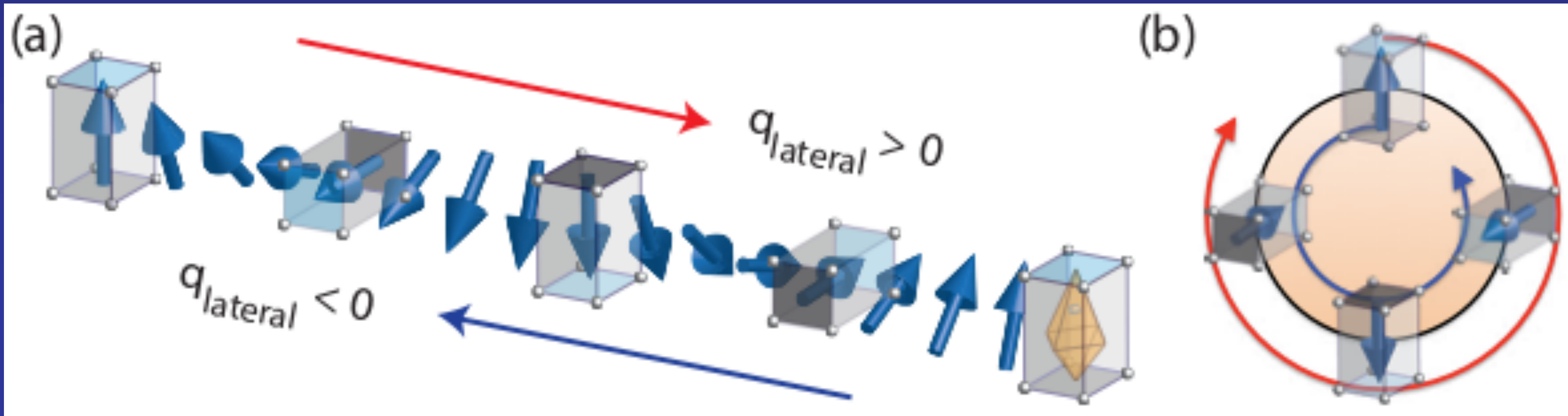

Continuous rotation of the local ferroelectric polarization
Continuous tilts of the Ti t_{2g}-like orbitals relative to polarized x-ray beam

$q_{\text{lateral}} > 0$ **senses a clockwise helical rotation of the polarization**

$q_{\text{lateral}} < 0$ **senses a counterclockwise helical rotation of the polarization**

Anti-symmetric XCD in these diffraction spots is a result of the chiral texture being detected with opposite rotational sense

P. Shafer, P. García-Fernández *et al*. submitted